Spring 2010

MicroRNAs' role in brain development and disease

Sarah Kathryn Fineberg
University of Iowa

MICRORNAS' ROLE IN BRAIN DEVELOPMENT AND DISEASE

By

Sarah Kathryn Fineberg

An Abstract

Of a thesis submitted in partial fulfillment
of the requirements for the Doctor of
Philosophy degree in Molecular Physiology and Biophysics
in the Graduate College of
The University of Iowa

May 2010

Thesis Supervisor: Professor Beverly L. Davidson

ABSTRACT

microRNA (miRNA) function is required for normal animal development, in particular in stem cell and precursor populations. I hypothesize that miRNAs are similarly required for stem cell maintenance and appropriate fate commitment in the brain. To test the requirement for global microRNA production, I depleted the microRNA biosynthetic enzyme DICER in the developing mouse brain. I found that DICER loss in embryonic neural progenitor cells leads to embryonic lethality with microcephaly. By histological analysis, I found defects in both neural progenitor cell maintenance and cell differentiation. I also identified new candidate microRNAs for this phenotype by profiling miRNAs in DICER-depleted and control cells. Three microRNAs which are good candidates to modulate nervous differentiation are miR-23b, -182, and -34a. I describe the expression pattern and functional characterization of these candidates. In particular, miR-34a depletes neuron production after progenitor cell differentiation in culture, likely by modulating cell cycling and Notch pathway genes.

Abstract Approved: _____
Thesis Supervisor

_____
Title and Department

_____
Date

MICRORNAS' ROLE IN BRAIN DEVELOPMENT AND DISEASE

By

Sarah Kathryn Fineberg

A thesis submitted in partial fulfillment
of the requirements for the Doctor of
Philosophy degree in Molecular Physiology and Biophysics
in the Graduate College of
The University of Iowa

May 2010

Thesis Supervisor: Professor Beverly L. Davidson

Graduate College
The University of Iowa
Iowa City, Iowa

CERTIFICATE OF APPROVAL

PH.D. THESIS

This is to certify that the Ph.D. thesis of

Sarah Kathryn Fineberg

has been approved by the Examining Committee for the thesis requirement for the Doctor of Philosophy degree in Molecular Physiology and Biophysics at the May 2010 graduation.

Thesis Committee:

Beverly Davidson, Thesis Supervisor

Michael Anderson

Robert Cornell

Wayne Johnson

Andrew Russo

To the mentors who first helped me see the sparks in science, especially Yolanda Cruz and Taylor Allen.

ACKNOWLEDGMENTS

Thanks so very much to the friends who have made my Iowa City family during this process: Nancy and Devon, Cathy and Zola and Corinna and Christopher. Thanks to my labmates for all the technical talk, but more for helping me laugh about it. Thanks to the students who have helped me to better explanations of my own work, and motivation to see it done right. Thanks to Bev for having me, and showing me a great deal about cutting through to the exciting parts.

ABSTRACT

microRNA (miRNA) function is required for normal animal development, in particular in stem cell and precursor populations. I hypothesize that miRNAs are similarly required for stem cell maintenance and appropriate fate commitment in the brain. To test the requirement for global microRNA production, I depleted the microRNA biosynthetic enzyme DICER in the developing mouse brain. I found that DICER loss in embryonic neural progenitor cells leads to embryonic lethality with microcephaly. By histological analysis, I found defects in both neural progenitor cell maintenance and cell differentiation. I also identified new candidate microRNAs for this phenotype by profiling miRNAs in DICER-depleted and control cells. Three microRNAs which are good candidates to modulate nervous differentiation are miR-23b, -182, and -34a. I describe the expression pattern and functional characterization of these candidates. In particular, miR-34a depletes neuron production after progenitor cell differentiation in culture, likely by modulating cell cycling and Notch pathway genes.

TABLE OF CONTENTS

LIST OF TABLES

LIST OF FIGURES

CHAPTER ONE: INTRODUCTION

1.1. Vertebrate forebrain development.

Development of the central nervous system (CNS) in vertebrates has been studied in several different models with consistent results in terms of anatomy and biochemistry. Many similarities exist as well between vertebrate models and invertebrate models, however some key differences have been noted. Here, I review key features of CNS development with a focus on corticogenesis. This will provide background for my studies in model systems of neurogenesis.

1.1.1. Cell Types in the developing forebrain

Anatomical definition of the central nervous system begins at neurulation, with closure of the neural tube and definition of the cells bounding the central canal as a pseudostratified epithelium committed to the neural lineage. These neuroepithelial cells (NEs) proliferate to self-renew and also to generate a heterogenous population of neural progenitor cells (NPCs). Definition of the forebrain occurs shortly after neural tube closure when five vesicles emerge along the apical-basal axis: the telencephalon, diencephalon, mesencephalon, metencephalon, and rhombencephalon. The telencephalic vesicle swells dramatically compared to the more caudal vesicles during development, going on to generate forebrain structures including cerebral cortex and hippocampus. Experiments in chick have defined the relative contributions of cerebrospinal fluid (CSF) –generated mechanical pressure and cell divisions to increasing size of the cerebral cortex during development [1]. They found a 10% increase in CSF pressure at each developmental stage, and, after experimentally maintaining drained ventricles for twenty-four hours, they found a 50% decrease in NE number. The authors hypothesize mechanosensitive receptors on NE cells that, when activated, stimulate proliferation.

The differences among cortical NPCs have been described at the morphological, biochemical, and functional levels (reviewed in Corbin *et al.* [2]). NEs begin as a single-

cell thick tube, and they contact the apical and basal surfaces of the neural tube. As cell migration and differentiation thicken the dorsal wall of the cerebral lateral ventricles, NE progeny, called radial glial cells, maintain contact with the apical (ventricular) surface and the basal (pial) surface. The long processes required for this continued cortex-spanning contact form a scaffold which is required for newborn neuron migration [3]. Radial glial cells are remarkable also for the choreographed apical to basal translocation of the nucleus within the cell during the cell cycle [4, 5]. During the quiescent and synthesis phases of the cycle, the nucleus migrates basally, toward the pial surface, but then moves back to the ventricle to complete cell division. The periventricular region which contains the mitotic nuclei of radial glial cells is termed the ventricular zone (VZ). In mice, a variety of (mostly cytoskeletal protein) markers have been described for the identification of radial glial cells. These include nestin (NES), intermediate filament-associated protein RC2 (RC2), and vimentin (VIM). Stem/progenitor cells in the developing brain were originally defined and studied using tracing studies. Proliferative cells were marked in whole animals by uptake of nucleic acid analogs (tritiated thymidine, following the method established by Sidman in 1959 [4], or, later, bromo-deoxyuridine (BrdU) [6]) and followed by serial sacrifice or slice cultures. More recently, infection of proliferative regions with low titer retroviral vectors has allowed researchers to follow single cells [7]. In this way, researchers discovered the location and morphology of NPCs, including radial glial cells. Using these systems with carefully timed BrdU exposure and analysis, cell cycle time was predicted by modeling and confirmed *in vivo* [8]. However, continued investigations into cellular heterogeneity have recently revealed at least one new cell type in the VZ. There are bipolar shaped cells in the VZ which are not cortex spanning, but are proliferating (shown by BrdU uptake) [9]. These cells, termed short neural precursors, are suspected to be a more committed population than radial glial cells because they express the neuronal marker alpha-tubulin. Radial glial cells and short neural precursors likely both contribute to an

NPC population which is located just basal to the VZ, called the subventricular zone (SVZ). SVZ-located NPCs, called intermediate progenitor cells, are thought to mostly undergo symmetric neuron-generating divisions [10]. Intermediate progenitor cells can be identified both by location in the SVZ and by the protein marker TBR2. It was first thought that intermediate progenitor cells would only contribute late-born neurons to the developing cortex, but more recent work has found that derivatives of TBR2+ cells are found throughout the mature cortex [11]. Corbin *et al.* [2] have argued in a recent review that there is a much greater degree of heterogeneity among VZ cells than is suggested by this simple conception of neuroepithelial, radial glial, short neural precursor, and intermediate progenitor cells as steps along a commitment pathway. One compelling set of data they review [12] shows differential regulation of the Notch pathway in the VZ in patterns that do not correspond to these already-defined cell type categories.

1.1.2. Radial Glial Cells are required as a physical scaffold in addition to their role as NPCs

The long cortex spanning process of the radial glial cell that extends from the cell soma to the basal surface of the developing cortex has been shown to function as a structural support upon which newborn neurons migrate to their final destination. Newborn neurons have been visualized in close approximation to radial glial cell processes (reviewed in Marin *et al.*) [13]. In a ferret model of disrupted cortical migration, it was further demonstrated that radial glial cells both support and depend on support from newborn neurons: maintenance of radial glial cell morphology requires signals from normal developing cortex [14]. Two factors have been identified as secreted molecules in the cortex that play a role in maintaining normal radial glial cell morphology. Neuregulin (NRG1) and reelin (RELN) can each rescue the disorganization of radial glial cell morphology that occurs after toxin-mediated disruption in ferret brain [3].

1.1.3. The Notch Pathway in neurogenesis

The Notch pathway is a well-conserved intracellular signaling mechanism, with key components conserved from fly to human. Signaling is activated when a ligand (Delta family or Jagged family member) on the surface of one cell binds to the transmembrane NOTCH1 protein on an adjacent cell. Following ligand binding, the intracellular domain of Notch (NICD) is released to interact with C promoting factor 1 (CBF1, also called recombination signal-binding protein for immunoglobulin kappa J region (RBPJ)) in the nucleus, permitting activation of target gene promoters. CBF1 is the mammalian homolog of the *Drosophila* gene *suppressor of hairless*. The best-known target genes are the transcription factors in the hairy/enhancer of split (HES) family, which block transcription of proneural targets including achaete-scute complex homolog 1 (*Ascl1*, also called *Mash1*) and neurogenic differentiation1 (*NeuroD1*). In the fly CNS, NOTCH is required for maintenance of the progenitor cell in an asymmetric division (reviewed in [15, 16]). Loss of NOTCH leads to a "neurogenic" phenotype, that is, excess production of neurons at the expense of progenitors. For example, *mind bomb* zebrafish lack function of mib1, an E3 ubiquitin ligase which helps to release the NICD, the effector of downstream Notch signaling [17]. Consistent with the idea that NOTCH supports progenitor fate, the *mind bomb* animals have sheets of contiguous neurons which are uninterrupted by the usual intervening non-neuronal cells [18]. Corbin *et al.* argue that the historical conception of the Notch pathway as a guardian of progenitor cells is an inappropriately limited one. They suggest that though NOTCH may function to help make a decision at a binary choice point, it could function in that role at a series of different choices (asymmetric divisions) over the course of neural development. For example, we have good data to suggest that NOTCH acts early, promoting progenitor cell fate in one cell at asymmetric progenitor divisions that make one progenitor cell and one neuron. However, this does not exclude a key role for NOTCH later, when that progenitor may choose to renew itself as a short neural precursor, or very late in

corticogenesis, when glial cells are made (NOTCH promotes glial fate) [19]. Furthermore, traditional read-outs of NOTCH activity may not tell the whole story. Mizutani *et al.* found that NOTCH is required in cells in which (the target of Notch pathway inhibition) MASH1 is present, suggesting that a non-canonical Notch pathway is at work [12].

1.1.4. The role of asymmetric division in cortical neurogenesis

When NPCs divide in the VZ, the mitotic spindle is generally oriented either horizontally (parallel to the ventricular surface) or vertically (perpendicular to the ventricular surface), and it has been hypothesized that this differential spindle orientation might be a mechanism of effecting symmetric vs. asymmetric divisions. In fact, spindle rotation has been observed in developing rat forebrain [20]. Though some data support this idea, the reports are conflicting (reviewed in [21]). However it is clear that regulation of spindle orientation is critical for maintenance of proliferating cells in the VZ. Loss of function mutants that result in random spindle orientation also deplete the NPC population [22]. In a recent review, Doe speculates that the key aspect of mitotic cleavage plane orientation may not be the orientation with respect to surrounding cells, but rather the orientation with respect to asymmetrically localized cytoplasmic components [21]. Indeed, in mammals as in flies, there is evidence of sub-cellular placement of signaling components, though some inter-organismal variation occurs. For example, mammalian NUMB is localized to the cell membrane, whereas in flies it is localized asymmetrically in the cytoplasm. The effect of loss of NUMB and NUMBL varies with stage of corticogenesis, but always strongly impacts the NPC population. The mechanism of action is likely multifactorial; NUMB has been shown to modulate signaling through the Notch, Shh, and p53 pathways. Another example of asymmetric protein localization in mammalian NPCs is apical localization of Par family members

during early corticogenesis. During this time of rapid proliferation, Par proteins interact with the Rho-GTPase CDC42 to maintain interkinetic nuclear migration [23].

1.1.5. Inside-out cortex formation

As neuronal differentiation proceeds, newborn neurons migrate away from the central fluid-filled ventricle, always moving past previously defined layers such that the first-born cells come to be located nearest the ventricle, and the latest born cells are found nearest the basal surface. This process is referred to as inside-out cortex formation. Differentiation of VZ/SVZ progenitors gives rise to both the Cajal-Retzius neurons that will reside on the basal (pial) surface of the brain, and projection neurons that make up layers II-VI. Cajal-retzius neurons regulate cortical neuron migration, likely acting through a mélange of attractive and migration-halting cues (reviewed in Soriano *et al.* [24]). Glutamatergic neurons in the cortex arise from these proliferative zones. GABAergic neurons and cortical interneurons are derived from regions of the ganglionic eminences, located medial and inferior to the ventricles.

1.1.6. Disorders of cortical neurogenesis

Disruption of cortical neurogenesis usually manifests grossly as microcephaly (decreased head size) or laminopathy (disorganization of layering, often recognized in human as a change in gyration) [25]. Usually, changes in NPC proliferation or commitment result in microcephalic phenotypes, while impairments in cell migration lead to laminopathies. However, these distinctions are not clearly separable.

It is important to note that loss of neurons in the mature brain can be a result of two, seemingly reciprocal, NPC defects. First, if NPCs fail to differentiate in a timely fashion to make viable neurons, then fewer neurons will be present in the adult brain. However, an increased propensity of NPCs to differentiate early in corticogenesis also results in small numbers of mature neurons. This is because the NPC population must self-renew and proliferate adequately to make neurons throughout the period of cortical

neurogenesis. If too many NPCs commit too quickly at the early stages of cortex formation, then the progenitor population becomes depleted, and neuron production tapers off prematurely. These two mechanisms are clearly demonstrated by mouse mutants in two opposing members of the Notch family. As discussed above, NOTCH1 functions in early NPC decisions to promote progenitor fate. Therefore, loss of NOTCH1 results in early overproduction of neurons with eventual microcephaly (reviewed in [26]). However, loss of the NOTCH1 antagonists NUMB and NUMBL also result in neuron loss, but through the opposite mechanism: asymmetric (differentiating) divisions are less likely than symmetric (self-renewing) divisions, so neuron production is diminished (reviewed in [27]).

1.2. microRNAs in vertebrate neural development

Mature miRNA levels within cells are managed by transcriptional regulation, enzymatic processing, and stability. Tight spatio-temporal control occurs resulting in the distinct expression patterns of many miRNAs [28,29], with levels changing quite dramatically in some contexts such as stem cell differentiation (reviewed in Gangaraju *et al.* [30]). The ability of miRNAs to alter coordinately and efficiently the expression program of many target mRNAs and their encoded proteins, combined with their tight control suggests that miRNAs may effect phenotypic transitions. Thus, miRNAs are reasonable candidates as inducers and enforcers of the changes in cellular state that occur during development.

Heimberg *et al.* [31] have posited that miRNAs may be largely responsible for increasing morphological complexity in the CNS. They assessed the evolution of miRNA families and that of new structural complexity (which they note is particularly evident in the CNS). Using bioinformatics and Northern blots they present evidence to argue that miRNAs contribute to an increase in “morphological complexity” in vertebrates vs. invertebrate chordates. They argue that the advent of new miRNA

families at a time separate from genome duplication, but coincident with increased "complexity", together with the tissue specific expression pattern of many new miRNAs, strongly suggests miRNAs causing the increase in complexity. While the authors of this study do present quite sweeping conclusions, the idea is intriguing that miRNAs may be even one of several key contributors to changes in cortical morphology in recent evolutionary time. Other recent work is shedding some light on miRNA birth events and on regulation of miRNA expression [32].

The nervous system provides an interesting case study for the hypothesis that miRNAs are key regulators of the changing expression programs during development. Many miRNAs are enriched in the nervous system [29, 33-36], and recent work is beginning to clarify their functions (reviewed by Gao *et al.* [37]). Over the last year, our understanding of miRNA contribution to nervous system development has greatly improved due to the publication of several studies which add up to a developmental series of Dicer depletions in nervous tissue. Together, the data support the hypothesis that miRNAs regulate cell differentiation and/or cell cycling in the developing nervous system.

1.2.1. miRNAs shift programs during neural differentiation

Changes in miRNA levels are observed as cellular commitment proceeds in the developing cortex, consistent with a role for miRNAs in cell fate regulation [35,38,39]. miRNAs which maintain the NPC pool fall with increasing commitment; other miRNAs which drive differentiation increase as cells differentiate. A few particular miRNAs have now been the focus of several studies in the neural development, especially miR-124, -125, and -9. These miRNAs are differentially expressed as neural development proceeds in culture and *in vivo*. Mature miRNA levels are regulated by transcriptional and post-transcriptional mechanisms (Figure 1). Pri-miRNA transcription occurs via RNA polymerase II or RNA polymerase III, upstream of either intergenic miRNAs or genes

hosting intronic miRNAs [40-43]. Intriguing recent reports also find that some intronic miRNAs are transcribed locally (from within the region of genomic DNA encoding the intron) from their own start sites [40, 44].

Mechanisms to control the rate and timing of miRNA processing are present at the DICER and DROSHA cleavage steps [45]. DICER levels rise during neural differentiation in cerebellar cultures [46]. In HeLa cell culture, DROSHA and DGCR8 regulate each other, with DROSHA protein decreasing *Dgcr8* mRNA, but DGCR8 protein stabilizing DROSHA protein [47].

Interaction of miRNA primary transcripts or precursor hairpins with regulatory proteins is a mechanism by which processing of an individual miRNA can be controlled. For example, pri-miR-let-7 processing is blocked by binding of lin-28 to the miR-let-7 loop [48, 49]. Another way to control processing of an individual miRNA is to alter the pri-miRNA sequence. ADAR (Adenosine Deaminase Acting on double stranded RNA) enzymes convert some adenosine (A) residues to inosine (I). A to I editing of pri-miRNAs has been demonstrated in human and mouse brain samples [50]. Because I is read as guanine (G) for base pairing, the functional consequence of the editing is alteration of the miRNA secondary structure and, hence, target selection. A to I changes in the pri-miRNAs -151 [50] and -142 [51] block processing to the mature form, likely due to changes in arrangement of the hairpin stem. Another sequence alteration that occurs at the pre-miRNA level blocks processing of the precursor to its mature form. Addition of a uridine tail to the pre-let-7 hairpin by lin-28 can decrease let-7 production [52].

miRNA function can also be controlled by subcellular localization. It has been established that local translation occurs in dendrites and that this has functional consequences in mature neurons (reviewed in Dahm *et al.* [53]). However, there is emerging data suggesting that mRNAs and translational machinery are also present in

developing axons [54]. Furthermore, local delivery of siRNA to axons mediates local silencing [55], confirming the presence of RNAi machinery as well.

1.2.2. miRNA levels vary in neurodevelopmental disorders.

1.2.2.1. Schizophrenia.

Analysis in human samples found that miRNAs are dysregulated in prefrontal cortex of schizophrenic and schizoaffective patients [56]. In another study, miRNAs levels were measured in brain samples from superior temporal gyrus from patients and healthy controls [57]. This brain region houses the auditory cortex, thought to be the anatomical substrate of auditory hallucinations in schizophrenia. Mature miR-181b was found to be increased in schizophrenia, and to repress two genes, GRIA2 and VSNL1, which are known to be decreased in the brains of schizophrenia patients.

1.2.2.2. Rett Syndrome.

Rett Syndrome is a neurodevelopmental disorder which becomes apparent in toddlers after timely achievement of early developmental milestones. It progresses with spastic movements, epilepsy, and loss of motor and communicative skills. The disease results from loss of function of the Methyl CPG binding protein 2 (MECP2) in human, but gain or loss of the protein in mouse both result in Rett-like symptoms. Klein *et al.* [58] described a feedback loop in which miR-132 decreases MECP2 levels, thereby decreasing the drive to express the miRNA. MECP2 expression leads to increased transcription of the cortical trophic factor BDNF, which then promotes transcription of miR-132. Thus, miR-132 acts to decrease its own production, and may function to "protect" the cell against Rett-causing swings in MECP2 levels.

1.2.2.3. Autism

The many stochastic features of miRNA biology raise the possibility of miRNA dysregulation in complex genetic disorders such as autism. Using multiplex quantitative polymerase chain reaction (PCR), Abu-Elneel et al compared the expression of 466 human miRNAs from postmortem cerebellar cortex tissue of individuals with Autism Spectrum Disorder and a control set of non-autistic cerebellar samples [59]. Most of the miRNAs levels showed little variation across all samples suggesting that autism does not induce global dysfunction of miRNA expression; however, some miRNAs among the autistic samples were expressed at different levels compared to the mean control value. Due to the small sample size the study will need replication. None of the reported miRNAs were consistently dysregulated across the entire set of autistic samples supporting the increasingly likely idea that autism is a complex genetic to which many rare variants contribute. Interestingly, among the predicted targets of the putatively dysregulated miRNAs are genes with known genetic links to autism such as neurexin (*Nrxn1*) and SH3 and multiple ankyrin repeat domains 3 (*Shank3*). Microdeletions or duplications at 15q13.2q13.3 with breakpoints BP4-BP5 can result in a phenotype with features of autism spectrum disorder, and the implicated regions encodes one miRNA as well as three reference genes [60]. Recently Talebizadeh *et al.,* found dysregulated miRNAs from lymphoblastoid lines of autism patients [61].

1.2.2.4. Fragile X.

Fragile X syndrome is a common cause of mental retardation caused by loss of function of *FMRP1,* which encodes the Fragile X Mental Retardation Protein 1 (reviewed in [62]). Patients and animal models of the disease have normal gross anatomy of the brain, but defects in synapse morphology and function. Changes in neurogenesis have also been noted in a cell culture model [63]. *FMRP1* was first linked to the miRNA pathway by

immunoprecipitation studies which found it complexed with the RISC components ARGONAUTE (AGO) and DICER in *Drosophila* and mammalian cell lines [64]. Furthermore, FMRP1 is located in processing bodies (P-bodies), and cytoplasmic granules thought to be the location of miRNA-mediated transcript repression. FMRP1 repression of mRNA translation was shown to be physiologically relevant in a fly model of learning. Memory defects present in the FMRP1 knockout were rescued by a protein-synthesis blocking drug [65]. These data suggest that aberrant increases in protein synthesis follow loss of FMRP1 in neurons, resulting in cellular dysfunction. The particulars of the relationship between the miRNA pathway and FMRP1 remain unclear. While FMRP1 is associated with the miRNA machinery (RISC), and can directly bind and repress mRNA targets, it is not known whether small RNAs play a role in this process (reviewed in Gao [37] and Li [66]). The mechanism of FMRP1 in miRNA-mediated repression is also unresolved. There is one report describing miRNA mediated cell cycle dependant increase in TNF-alpha levels which implicates the FMRP related protein FXRP1 [67]. Whether or not FMRP1 and miRNAs directly interact, their shared mechanism of action (through RISC) means that investigations of each will inform our understanding of the other. Of note, FMRP1 likely works in multiple subcellular compartments. The protein sequence contains nuclear import and export domains, and FMRP1 can shuttle between the nucleus and cytoplasm [68], suggesting that it may also control mRNA translation by regulating mRNA localization.

1.2.2.5. DiGeorge syndrome

DiGeorge syndrome results from hemizygous deletion of a 1.5-3 Mb deletion on human chromosome 22q11. Patients have disruptions in morphogenesis of a variety of cranial and trunk organs, including bony skeletion, heart, thymus, and the CNS. One of the genes falling within the deleted region is DGCR8, a component of the Microprocessor complex, which cleaves the primary miRNA transcript to its precursor form. Stark *et al.*

generated a mouse model with a genetic microdeletion of the syntenic region [69]. The significant increase in mental retardation and mental illness in DiGeorge patients versus healthy controls (e.g. schizophrenia, which occurs in 30% vs. 1%) led the researchers to assess cognitive performance both in the DiGeorge mice and in another model with a more focused deletion of DGCR8. They found significant increases in anxiety measures and also hyperactivity in the DGCR8 heterozygotes. Another group specifically knocked out the DGCR8 gene in embryonic stem cells, and found defects in the ability of those cells to switch from pluripotent to differentiated program [70]. Particular miRNAs have not been implicated in the disease.

1.2.2.6. Fetal Ethanol Exposure

Fetal exposure to teratogens, including ethanol, decreases neuroblast proliferation and neuron production [71]. Sathyan *et al.* (2007) found that miRNA expression changes in neural progenitor cells after ethanol exposure [72]. In particular, miRNAs are expressed which are predicted to work in cell damage response pathways.

1.2.3. miRNAs regulate known molecular pathways that modulate neural development

The hedgehog signaling pathway is especially well-described with respect to its pro-proliferative role in brain development and cancer. Sonic hedgehog (SHH) binds Patched (PTC), stopping the inhibitory activity of PTC on Smoothened (SMO). Free SMO then agonizes GLI, promoting proliferation. In the developing cerebellum, Purkinje cells produce SHH to promote proliferation of adjacent cerebellar granular cells. Reactivation of SHH signaling by modulation of pathway components promotes the erroneous proliferation that occurs in the cerebellar granular cell tumor medulloblastoma. Several interactions between miRNAs and the hedgehog pathway were shown in fly [73]. Recent work [74] has identified miRs-125b, 324-5p, and 326 as upregulated in cerebellar development and decreased in medulloblastoma. Since these miRNAs target the HH

pathway members SMO and GLI, they are poised to promote cell cycle exit and differentiation.

One important mechanism to safeguard transcription of neuronal identity genes against activation in non-neural cells is activity of the RE1 silencing transcription factor (REST). Several brain-functioning miRNAs have now been identified which appear to regulate and be regulated by REST. In non-neural cells and neural progenitor cells, transcription of both miR-124a and miR-132 is inhibited by REST interaction with miRNA promoter elements [75, 76]. The regulation of miR-132 is critical for normal brain development, as described above [58]. REST also functions in a homeostatic loop with miR-9 [77].

A recently recognized mechanism important for homeostasis in the CNS is alternative splicing. At least two neurodegenerative diseases, the group of Tau-opathies and Myotonic Dystrophy, involve dysregulation of splicing (reviewed in [78]). miR-124 has recently been found to regulate PTBP1, which controls alternative splicing such that PTBP1 is down regulated with neural differentiation (as miR-124 levels rise), allowing a shift toward brain-specific alternative splice forms. Dominant expression of PTBP1 over its homolog PTBP2, is thought to be a major mechanism promoting the production of non-brain transcripts.

1.2.4. miRNA-target profiles shift during development

Pri-miR-376 is edited in various tissues, with extensive editing (98% of transcripts) occurring in the medulla oblongata. This editing event does not occur at the expense of mature miRNA levels [79]. Kawahara *et al.* found that because the editing sites are located within the 5' end of the mature miRNA (the seed), which is essential for pairing with target mRNAs, the profiling of selected targets differs from the unedited miR-376 [79]. This mechanism amplifies the possible protein targets for miRNA-mediated regulation, and may reduce or improve those targets that were marginal in the

unedited state (Figure 2). Editing events outside of the critical seed region might be particularly interesting in developing tissues. This scenario may be ideal to accomplish needed shifts in the proteome to effect developmental transitions, e.g., from neural stem cell to more rapidly cycling but still multipotential progenitor cell.

1.2.5. miRNA function is required during development

Initial studies of miRNAs function in mammalian development largely focused on hematopoiesis (reviewed in [80, 81]) and limb development (reviewed briefly in [82]). A variety of microRNAs have been identified which modulate the developmental transitions that occur during hematopoietic cell maturation. Some of these microRNAs have also been implicated in tumorigenesis. DICER is an RNAse III enzyme that is required for mature miRNA production. Conditional deletion of *Dicer* enzymatic domains by cre-lox technology has proved a powerful tool to study the requirement for microRNAs. The first conditional DICER knockouts in mouse were activated in developing T cells [83, 84], where defects in progenitor cell survival and differentiation were observed, and in developing limb, where the requirement for DICER was immediately evident due to gross pathology [85]. If miRNAs were similarly required for brain development, miRNA depletion would impair differentiation, with stronger phenotypes apparent when depletion was induced at robust differentiation stages. Recent work with conditional deletion of DICER in the nervous system supports this thesis.

Zebrafish which are null for DICER in the embryo (but retain some DICER protein from the maternal cytoplasm) have only mild morphological changes in the brain [86] that can be resolved by miR-430 replacement. Global genetic depletion of DICER or DGCR8 in mammals causes very early embryonic lethality, which precludes analysis of neural development [70, 87]. Furthermore, even conditional deletion of DICER in the developing mammalian nervous system results in gross histological aberrations and

embryonic lethality [69, 88-93], suggesting a more critical role for miRNAs in these organisms (Table 1).

DICER loss in the developing brain in mice seems to be more devastating during progenitor cell differentiation than during self-renewing divisions. For example, Dicer depletion in forebrain [88, 91] or olfactory progenitor cells [89] results in neuron loss that occurs days before progenitors stop dividing or decrease in number. Furthermore, NPCs do not accumulate, so the loss of neurons is likely due to cell death of committed cells rather than failure of NPCs to differentiate. Dicer depletion in early forebrain development does yield increased neuronal apoptosis within three days (by E12.5). Eventually, NPC defects contribute to the phenotype, as proliferation defects are observed by E14.5, followed by apoptosis in the proliferative zones. It is also interesting to consider the neuronal subtypes that are produced in these animals. They generate "early-born" neurons throughout corticogenesis, seemingly failing to switch to the "late-born neuron" program, and so are not able to properly laminate the cerebral cortex. Similarly, ES cells can be differentiated toward a neuronal phenotype by chemical induction in culture, but DICER null ES cells are strongly hampered in their ability to produce neurons [90]. Interestingly, production of dopaminergic neurons was much more profoundly affected than was production of other neuronal subtypes. These findings are consistent with the idea that miRNAs are required to alter a cellular program, that directs a progenitor to make a neuron. To examine these new results in light of this and other hypotheses, it is useful to methodically summarize the work, proceeding from earliest depletion through development into adulthood.

1.2.5.1. DICER ablation in neural progenitors at/before the onset of neurogenesis

To address the differential requirement for DICER in progenitor cells versus mature neurons, Choi *et al.* [89] depleted DICER in first olfactory progenitor cells, then in

mature olfactory neurons. They used the floxed *Dicer* mouse generated by Harfe and McManus [85], in which the second Rnase III domain of *Dicer* is excised upon cre recombination. To ablate miRNA processing in olfactory neural progenitor cells, they used the FoxG1-cre mouse, which expresses cre in the developing olfactory epithelium and throughout the forebrain starting at ~E8. With respect to olfactory neurogenesis, within two days, both neuron-committed progenitor cells and also mature neurons were reduced. By five days after recombination, at E13.5, decreased staining for olfactory progenitor markers and loss of staining for mature olfactory neuron markers were accompanied by decreased neuroepithelial thickness. The neuron loss appears to be due to cell death: apoptotic cells were frequent already at E10.5 and still present at E12.5. However, neither "pile-up" of non-differentiating progenitor cells, nor defect in progenitor cell proliferation was detected. The ablation in this model also affects the cerebral cortex, and the authors report that the embryos had remarkably small heads and died in utero. However, detailed histological analysis of the brain was not reported. The same model was analysed by Makeyev *et al.* [94], including histological studies of tissue sections from E13.5 brain. They observed disorganization throughout the cortical thickness, with ectopic expression of the neural progenitor cell splicing regulator PTBP and loss of the post-mitotic post-migratory marker MAP2. Though the number of mitoses was grossly unchanged (cell counts were not reported), apoptotic cells were greatly increased in the DICER null animals. Analysis of other stages, however, was not included.

De Pietri Tonelli and colleagues sought to define the requirement for DICER specifically in corticogenesis. In order to prolong animal survival and to focus their analysis on one region of interest, they employed the Emx1-cre mouse, which drives CRE expression only in neuroepithelial cells in the developing cerebral cortex, not in midbrain or hindbrain structures. Recombination occurred very early in cortical neurogenesis, with in situ evidence of miRNA loss by E10.5. Like the FoxG1 mice,

these animals were microcephalic, but they did survive beyond birth, only failing to thrive with weaning at postnatal day 21. As in the olfactory epithelium, loss of DICER resulted in defects in maturing and mature cells before problems were observed in progenitor cells. By four days after depletion, at E13.5, the cerebral cortex was thinned. However, markers of NPCs in the VZ and SVZ were intact, as was TIS21, the marker of neuron-committed progenitors. Furthermore, proliferative zone mitoses were unchanged at E12.5 and E13.5, first decreasing at E14.5, with a more profound change in the more committed SVZ cells than in the VZ cells. Later, at E16.5, decreased staining with radial glial cell markers and less BrdU uptake suggested loss of NPCs. However, increased apoptosis compared to controls was observed throughout the cortical thickness by E12.5, and was seen to increase through E14.5. Since neurons are lost early without an apparent decrease in NPCs, the apoptotic cells located in the proliferative zone at E12.5-13.5 are likely to be neuron-committed progenitors, but this was not confirmed by co-labeling. As time goes on, the increase in apoptosis, and continued intensity of signal in the proliferative zone is likely to reflect increased cell death of progenitors. Cells marked by BrdU pulse at E12.5 or E13.5 are much less likely to acquire mature neuronal markers in the DicerKO than the control animals. Since increased cell density in the proliferative zones was not observed, this failure to differentiate may be compensated by cell loss along with the observed decrease in mitoses. Cell differentiation is also compromised in the DicerKO cortex, as the cell differentiation promoting marker FOXP2 is absent by birth, and the switch from production of early born (TBR1+) neurons to late born (BRN1+) neurons is inefficient, resulting in low numbers of BRN1+ cells and disorganized cortical lamina.

Three studies have ablated DICER early enough to observe differentiation defects, and effected the ablation in undifferentiated cell types. The above two studies both recorded decreased ability of progenitor cells to produce neurons. Another study in cell culture had similar results. Using well-established protocols for differentiation of ES

cells to dopaminergic neurons, Kim *et al.* [90] found that DICER null cells cannot produce TH+ neurons (dopaminergic cells), and make roughly half the expected number of other neurons. It is not known whether the undifferentiated progenitors persist or apoptose.

In summary, loss of miRNAs in neural progenitor cells early in corticogenesis profoundly and rapidly impacts on neuron production, and soon afterward, decreases progenitor cell renewal. The mechanism of failed neuron production with DICER withdrawal is not clear, though the evidence points to defects in both differentiation and newborn neuron survival.

1.2.5.2. DICER ablation in post-mitotic neurons during corticogenesis

Moving on to mid-corticogenesis in the mouse embryo, Davis *et al.* have crossed the Harfe-McManus mouse to the R1AG-5 α-CaMKII Cre mouse, resulting in DICER loss at ~E15.5 in post-mitotic excitatory forebrain neurons, including cells in the cortex, striatum, hippocampus, and few cells in the thalamus. Analysis of these results permits further examination of the role of DICER during differentiation (described above) versus maintenance of newborn neurons. The DICER null mice in this study are born, but 50% die by postnatal day 10, and none survive beyond weaning. They are ataxic by 15 days after birth. They are microcephalic with enlarged lateral ventricles. Embryonic analyses were not reported, but apoptosis was present by the time of birth throughout the recombined regions. However, the increased apoptosis did not persist, as levels in postnatal day 15 animals were comparable to controls. The authors also tested the ability of DICER null newborn neurons to produce morphologically appropriate and electrically active neurites. They detected changes in both dendrite shape and axon path finding, but cells were able to give and receive electrical signals normally.

In this model of later miRNA depletion, the authors describe a slower onset of neuron loss, which does, however, strongly impact on brain size and ultimately result in failure to thrive. Taken together, this data and the above progenitor cell DICER knockout phenotypes show that while newborn neuron apoptosis occurs and contributes to the observed dysfunction in the progenitor cell knockouts, it is not sufficient to explain the severe and rapidly developing phenotype (as it is much more severe than with depletion only in newborn neurons).

1.2.5.3. DICER ablation in early retinal progenitor cells

One other recent study does describe the effect of DICER ablation during neural differentiation. Damiani *et al.* reported DICER removal from retinal progenitor cells during mouse eye development. The Chx-10 promoter expresses in retinal progenitor cells as the optic vesicle forms, and then persists only in retinal bipolar cells in the mature eye [95]. Expression is mosaic, with intermingled populations of expressing and non-expressing cells both numerous. The Chx-10-cre mouse was crossed to the Harfe/McManus mouse. Perhaps surprisingly, there was no developmental defect at the histological level. However, miRNA levels were found to persist much longer in the retina after Dicer ablation than has been observed in other Dicer depletion experiments. One month after cre expression, miRNA levels were unchanged. Three months after cre expression, they had fallen to 30% of control levels. This remarkable stability of the mature microRNAs combined with the presence of non-ablated cells may explain the lack of histopathology during development.

1.2.5.4. DICER ablation in mature neurons results in slow-onset, varied neuropathology

Though DICER ablation in the retina did not result in developmental pathology, the researchers did find progressive functional deficits on electroretinogram in both DICER null and DICER haploinsufficient animals when they were tested at 1, 3, and 5 months of

age. Also, disorganization of initially normal histology developed between postnatal days 16 and 45, followed by cell death and structural degeneration of the retina by 3 months of age. In contrast to the other neural systems described above, the requirement for DICER in the retina is more evident in maturity than during development. DICER ablation has been effected in several other mature neuronal subtypes, with the usual result of slow neurodegeneration (in dopaminergic neurons in the substantia nigra, in medium spiny neurons in the striatum, and in cerebellar purkinje cells). However, in contrast to the retinal story, although lack of DICER in olfactory progenitor cells had profound consequences (described above), removal in mature olfactory neurons [89] did not result in histopathological or functional phenotype.

Cuellar *et al.* [92] removed DICER from cells expressing the dopamine receptor: mostly post-mitotic neurons in the striatum, also deep cortical neurons. They crossed the DR1-cre mouse onto the Harfe-McManus mouse. The DICER null mice exhibit progressive motor phenotypes beginning at 4 weeks of age, and begin to waste at 6 weeks of age. The mice die at 10-12 weeks of age. Microcephaly, apparent by 5 weeks of age, is apparently due to cell shrinkage without concomitant neuronal apoptosis or loss. However, astrocyte activation, a marker of toxicity in the brain, was widespread within the DICER-ablated region.

In addition to testing the requirement for DICER in dopaminergic neuron differentiation, Kim *et al.* also tested the effect of DICER ablation in post-mitotic dopaminergic neurons *in vivo* [90]. They crossed the DAT1-cre mouse to the Murchison floxed *DICER* mouse [96], which was made in DICER heterozygous cells by inserting loxP sites to flank *DICER* exons 22 and 23 such that cre-mediated recombination excises portions of both Rnase III domains. The resulting DICER null mice lack DICER in the midbrain dopaminergic neurons that project into the striatum and are dysfunctional in Parkinson's disease. Loss of TYROSINE HYDROXYLASE stained cells (a marker for

dopaminergic neurons) occurred by 3 weeks of age, and apoptosis was present by 6 weeks of age.

DICER removal has also been effected in newborn post mitotic cerebellar purkinje cells (PCs) [97] by crossing the Pcp2-cre mouse [98] to the Yi floxed *DICER* mouse [99], which targets most of the first Rnase III domain of *DICER* and part of the second. In the cerebellum, the pcp2 promoter expresses specifically in PCs starting at ~2 weeks after birth in mouse. Cerebellar development is largely postnatal, with mouse PCs all in place by three weeks after birth. There is also expression from the pcp2-cre transgene in retinal bipolar cells, though those cells were not studied in this work. Recombination and miRNA depletion were both detected in PCs at 4 weeks of age. However, in situ hybridization revealed some PC miRNA signals which did not fall even months after the others were undetectable. The reason for this ongoing expression is not clear. There was no difference in PC number, morphology, or electrical activity at either 8 or 10 weeks of age. Mild morphological changes began in the dendritic arbors at 13 weeks, and progressed from anterior to posterior by 17 weeks of age. By 17 weeks, apoptosis were evident in both the purkinje cell and granule cell layers (likely due to lack of support from PCs). Motor phenotype developed in the animals at time points coincident with onset of histopathology: mild tremor and ataxia were detected at 13 weeks, and were grossly apparent at 17 weeks.

1.2.6. Individual miRNAs modulate decision points in neural development.

1.2.6.1. Cell differentiation *in vitro*.

Several investigations of neural differentiation in cell culture point to miRNAs regulators. There is a direct relationship between the levels of miRNAs 9, 124, 125, and 22 and the ratio of neurons to glia after neural progenitor cell differentiation in culture [36]. Another group found that miR-23 is required for retinoic-acid induced

differentiation of NT2 cells [100]. Also, miR-9 falls with maturation of oligodendrocytes, and represses the myelin component PMP22, suggesting a role in the differentiation of oligodendroctye progenitor cells [101].

miRNAs also regulate the shape of neurons. Vo *et al.* [102] found that loss of miR-132 decreases neurite outgrowth in a cell culture model of neuronal differentiation. Schratt *et al.* [103] have shown that miR-134 represses lim kinase, which promotes dendritic spine formation, thereby decreasing spine volume. They further found that the interaction of miR-134 and lim kinase is disrupted in the presence of BDNF. miR-124 is of particular interest because it is stronger and widely expressed in the CNS. Expression increases with days of development in mouse brain [94], and seems to be specific to post-mitotic neurons [35]. In fact, a 2005 report showed that over expression in the non-neural cell line HeLa shifted the contents of the transcriptome toward a "neural" complement of mRNAs [104], and a more recent publication found that neuroblastoma cells develop differentiated morphology after miR-124a over expression [94]. This correlation of miR-124a with "neuron-ness" holds up in functional studies. The length of cellular processes extended during differentiation of P19 cells in culture varied directly with miR-124a levels [105]. This effect was likely mediated through control of cytoskeletal regulators, including CDC42 and RAC1.

1.2.6.2. Cell differentiation *in vivo*.

One of the first studies to demonstrate a role for miRNAs in cell fate decisions *in vivo* was Oliver Hobert's elegant description of left-right asymmetry decisions in worm sensory neurons [106-108]. Several interesting studies have followed, as reviewed by Gao et al [37]. One important caveat to all of this work is that many studies are effected by gross gain and loss of function, whereas the biological role of miRNAs may well be to tip the balance to enforce one biological state over another [109]. Several recent reports highlight the role of individual miRNAs in cell differentiation in the nervous system.

Leucht *et al.* [110] found that miR-9 expression avoids the midbrain-hindbrain boundary organizing center in zebrafish, a site of progenitor cells in the developing CNS. Gain of miR-9 in that region drives premature/inappropriate commitment, and thus, loss of the progenitor pool. This is consistent with miR-9 function in the Notch/Hes pathway [111] in flies (Figure 3). In this system, miR-9 probably acts by repression of the NOTCH/HES pathway gene senseless.

While miR-9 sequence and CNS expression is conserved (as reviewed in Gao [37]) conserved genes can have opposing roles during neural commitment in varied models. One example of this phenomenon is numb, which in fly facilitates asymmetric divisions, but in mouse maintains progenitor cells (reviewed in Johnson *et al.* [27]). In fact, miR-9 does appear to function differently in mammals than fly and fish (Figure 3). In the mouse cortex, miR-9 works to maintain progenitor cells in the cortical hem, a narrow strip of tissue in the developing forebrain that lies between the emerging choroid plexus and the more rostral neural tissue [112]. Over expression of miR-9 at e11.5 but not at e14.5 caused ectopic production and location of Cajal-Retzius (CR) neurons. The implication is that not only do progenitors prematurely differentiate, but they also specify an inappropriate fate (CR neurons not cortical progenitor or cortical projection neurons). Application of anti-miR9 oligonucleotides caused loss of cortical hem and neuronal markers with regression of the cortical hem cells. Shibata and coworkers showed that this effect is mediated through repression of the progenitor marker FoxG1 in the cortical hem [112].

Two conflicting papers speak to the requirement for miR-124a in vertebrate neural tube development. Cao *et al.* found that loss of miR-124a expression did not change the number or morphology of neurons in the chick ventricular zone. However, Visvanathan *et al.* found that miR-124 over expression in the chick neural tube drove neural progenitor cells to differentiate [113]. As detailed above, Makayev *et al.* found that miR-

124a represses the splice regulator PTBP1 in nervous tissue, allowing neuron-specific alternate splicing to occur, and so promotes changes in cell phenotypes [94].

1.2.7.miRNAs are implicated in disorders of cell cycle regulation (e.g. cancer), and regulate cell cycle regulatory genes.

Loss of miRNAs early in development causes rapidly developing pathology, defects in cell differentiation and declines in progenitor proliferation and survival (Table 1) [88]. Interestingly, in the embryo, the effect of synchronous loss of all miRNAs tends toward cell death and decreased proliferation rather than overgrowth. By contrast, Dicer loss in mature neurons results in an exquisitely slow onset of dysfunction and degeneration. In fact, in medium spiny neurons in the striatum, there is cell shrinkage at 5 weeks of age, but animals die several weeks later without cell dropout [92]. Thus, loss of miRNAs early in development has much more rapidly-developing and profound consequences on tissue architecture and animal survival than do later loss.

Early studies of miRNAs function *in vivo* in fly found that DICER loss slows cell cycling in Drosophila germ cells but not in other tissues (tested in imaginal discs) [114].

miRNA profiling has been conducted in pathological samples from two of the more common brain tumors: glioblastoma multiforme (GBM) and anaplastic astrocytoma. Dysregulation of miRNAs 7, 124, 129, 137, 139, and 218 was demonstrated [115]. Several of these miRNAs have been implicated in differentiation events, for example miR-7 in photoreceptor differentiation, miR-124 in red blood cells and brain differentiation, miR-218 in neuronal differentiation of embryonic carcinoma cells. Furthermore, miRNAs 137 and 124 increase during *in vitro* differentiation of adult neural stem cells (aNSCs). However, miR-218, miR-7 did not change, and miRs-129 and -139 were reduced. aNSCs are thought to be the source of GBM tumors: re-expression of growth factors may promote de-differentiation (which would then repress miRNAs 124

and 137). Consistent with this model, chemotherapeutics which decrease epigenetic silencing rescue the lost miRNAs expression. Over-expression of miR-124 or miR-137 promoted neuronal differentiation and cell cycle exit, and for miR124, also decreased production of astrocytes after differentiation of aNSCs, oligodendroglioma cells, or human GBM stem cells. The miR-124/137 mediated shift to quiescence may be due to repression of cyclin dependent kinase 6 (CDK6), a checkpoint gene that promotes advancement through the cell cycle.

miR9/9* expression is sufficient to distinguish tumors of brain origin from brain-located metastases from non-brain tumors. This suggests that miR9/9* are markers of un/de-differentiated cells in the brain [116]. However, in cerebellar granule progenitor cells, increased expression of the pro-proliferation signal GLI is associated with loss of miR-9 [74].

Another brain-enriched miRNA implicated in cell cycle regulation is miR-34a. Levels are inversely correlated with cell proliferation levels in cancer cell lines and worsening prognosis in patient tumors [117, 118]. Transcription is promoted by the tumor suppressor p53, which, if constitutively active in neural stem cells, reduces their regenerative capacity and reduces numbers of mature neurons [119, 120]. Also, loss of p53 promotes expansion of neural progenitor cells [121]. These data suggest that miR-34a may also play an anti-proliferative role in the CNS.

1.2.8. Conclusion

Until recently, the hypotheses we formed about the role of miRNAs in neural development were based on very focused, difficult to generalize, models, and analogies to other organ systems. However, the rapid development of the miRNA field, in particular the recent spate of publications describing conditional DICER depletion in the developing nervous tissues, taken together with profiling studies and functional analyses of individual miRNA function, greatly informs

our thinking. It is now clear that miRNAs are most important in early development, likely facilitating coordinated transitions in the proteome that accompany phenotypic change. Further studies will place particular miRNAs in regulatory pathways, and will improve our understanding of control of and by miRNAs in the developing brain.

Table 1. Consequences of Dicer depletion in the developing mouse nervous system.

	FoxG1-cre X dicer$^{flox/flox}$	Emx-1 cre X dicer$^{flox/flox}$	22q11.2 microdeletion
location/time of enzyme loss	**BRAIN:** At E8.0 telen-cephalon and sensory placodes. By E12, restricted to wnt3a+ forebrain regions	From E9.5 in the telencephalon.	**1.** Genetic deletion of DGCR8-containing region, also deletes a variety of other genes in the region: tested hemizygous mice
	NOSE: "as early as E9.5" in presumptive OE		**2.** Bgal knock-in to DGCR8
confirmed time of miR loss	e13.5 (4 days post-cre) miR200 is gone from OE	E10.5 by ISH	pri-miRs rise, but most mature miRs are not reduced (19% of miRs expressed in prefrontal cortex and 10% of miRs expressed in hippocampus).
survival	death in utero	To weaning	normal in hemizygous deletion or heterozygous knock-in/truncation. homozygous knock-in/truncation is embryonic lethal
patterning	patterning: defined regions of olfactory structure are all present	Normal	
brain size	small forebrain	Small forebrain	normal with DGCR8 haploinsufficiency.
cell loss	present by E10.5, profound by E16.5, appears to be cell autonomous	Yes, in emerging lamina, early (by e12.5), later in proliferative regions	
apoptosis	present by E10.5, persistent at E12.5. Without any change in proliferation in OE.	Present by e12.5, widespread by e14.5.	
histopath	AT E10.5 no gross change in OE; 18% neuron loss; AT E13.5 marked thinning with loss of OE progenitor markers and abnormal LACK of olf. neuron markers.	Decreased proliferation affects SVZ > VZ, present by e14.5.	in HC, decrease in dendrite complexity and spine number and size.
cortical layers	not assessed	Distinct cortical layers fail to form.	
behaviour	NA	NA	Hyperactive, but more fearful of novelty (travel in center/edges was less). poorer performance on fear-context task, also on spatial memory task.

Table 1 continued

Rag1AG-cre X dicer$^{flox:flox}$:	Chx10cre X dicer$^{flox:flox}$
From E15.5 in forebrain projection neurons and hippocampal pyramidal layer. No recombination in midbrain, hindbrain, or thalamus	Mosaic expression in developing retina: normally dicer ish signal is in inner segments (inner nuclear layer and ganglion cell layer)
looked at P15: 15-20% loss of miR132, 60% by P21 (stNB)	no change in miR96 etc. at ~P30, but strong decreases at 3 months and 7 months (this is when cell loss became prominent!).
homozygotes die early postnatally (40% by P2, 100% by P20)	normal
	normal
50% reduction in brain mass at P21	NA
enlarged lateral ventrices (4th v. normal), small ant. commissure (with defasiculation).	
P0: apoptotic cells near VZ. P15: little apoptotic signal.	
P20, HC small, esp. DG: decrease in dendritic branching and arbor complexity	rosettes: could represent inappropriate increase in proliferation, but none was detected. could also represent loss of neuroepithelial polarity, but this is not likely as lamination, location of cells within lamina, and cell-cell connections were all normal during retinal development. rosette architecture became more complex between P16 and P45.
normal	
at P14, ataxia, unison hindlimb movement, clasping	ERG amplitudes decreased in homozygous and **heterozygous** animals

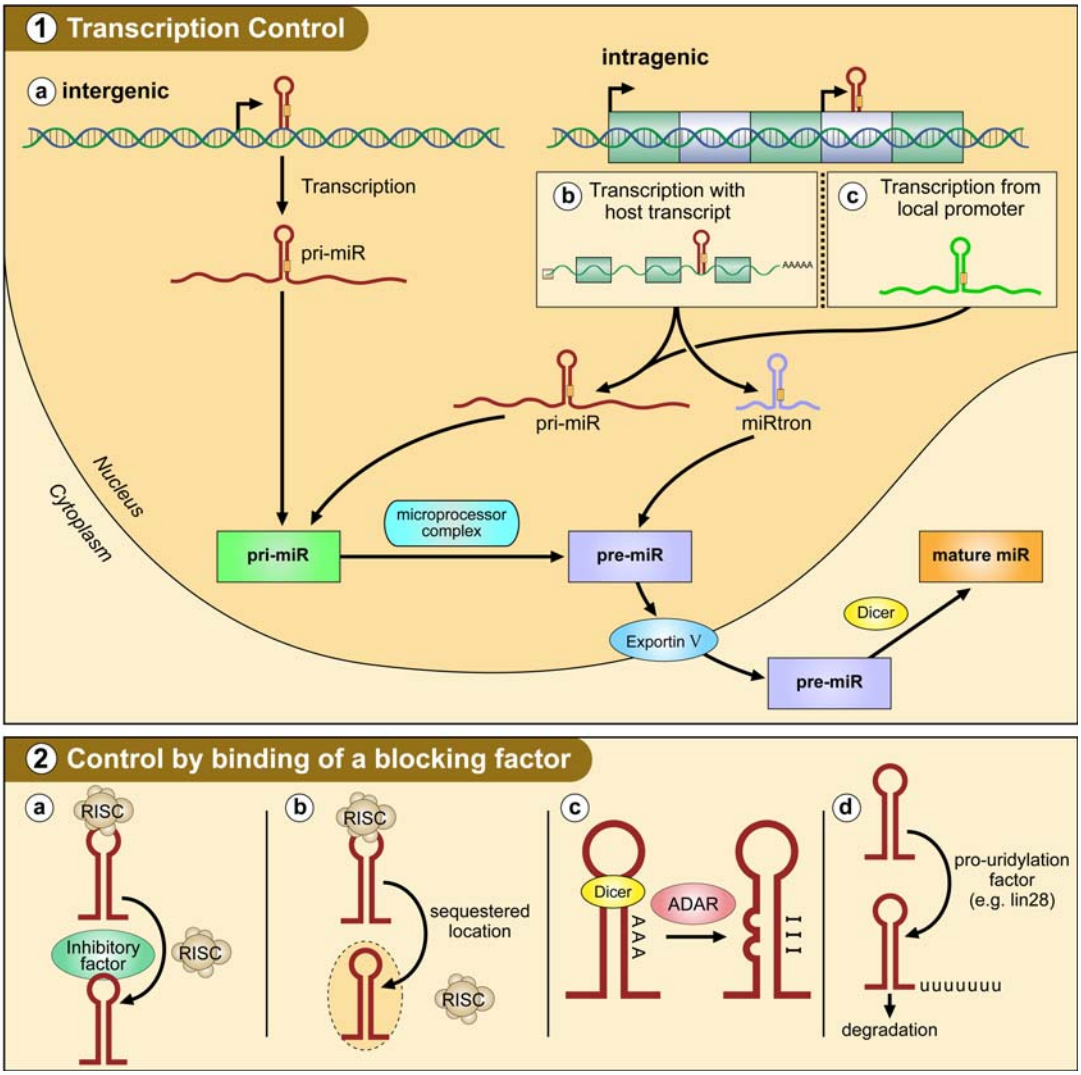

Figure 1. Control of miRNA processing 1. miRNA levels are controlled at the level of transcription. 1a) Some miRNA hairpins are expressed from genomic loci outside of known transcripts. These intergenic miRNAs can be expressed from RNA polymerase II promoters quite distant from the hairpin locus and also from RNA polymerase III promoters [43]. 1b) For miRNA hairpins that are located within the introns of host genes, regulation of host gene transcription directly modulates miRNA levels. The miRNA is released from the host transcript during mRNA processing. There are two possible forms of miRNA produced. The first, better studied form is the "pri-miRNA", a longer RNA molecule with significant flanking sequence beyond the hairpin structure. Pri-miRs enter the canonical miRNA processing pathway at the top, undergoing Drosha cleavage in a set of molecular events that, for intronic miRNAs, can be coincident with splicing [42].

Figure 1 continued

The second form, the mirtron, is a short RNA molecule with little sequence flanking the hairpin [122, 123]. Mirtrons are released by splicing of the host mRNA and enter the miRNA processing pathway after the canonical first step, and thus, are directly exported from the nucleus without DROSHA processing. 1c) There is also evidence for expression of intronic miRNAs from promoters located proximal to the hairpin sequence within the intron. Among these local promoters, there are examples of RNA polymerase II and RNA polymerase III driven loci. Production of miRNA from a local promoter introduces a level of regulation independent from control of host gene levels. Data suggests that expression by both mechanisms can occur concurrently [44]. 2. miRNA levels are also controlled at the level of processing. The canonical miRNA pathway involves processing of the pri-miRNA in the nucleus by an enzyme complex called the Microprocessor (including the RNase DROSHA). This cleavage, which occurs at the base of the hairpin, yields an ~70nt stem-loop structure referred to as a pre-miRNA. The pre-miRNA is transferred to the cytoplasm by the enzyme EXPORTIN V. Once in the cytoplasm, the loop is removed from the pre-miRNA by the enzyme DICER, a component of the RNA induced silencing complex (RISC). Regulation of both DROSHA and DICER cleavage has been demonstrated.. These mechanisms are drawn separately for clarity, but are likely interacting and possibly interdependent. We have depicted control of processing for an individual miRNA species, but changes in levels of processing enzymes are known to occur and to regulate global rates of miRNA processing [46]. 2a) Binding of some factor to a miRNA hairpin could block interaction with processing enzymes [45]. 2b) Sequestration of a miRNA hairpin to an inaccessible subcellular location could prevent processing. 2c) Deamination of pri-miRNA sequences changes adenosine residues in the double-stranded "stem" region of the hairpin structure to inosine residues, which function similarly to guanisine. These A to I edits can therefore alter hairpin structure, and so change interactions with processing enzymes. Due to higher expression levels of the ADAR deaminase enzymes, the prevalence of edited transcripts is higher in the brain than in other tissues [124]. 2d) Uridylation of some miRNA transcripts has been demonstrated, and it has been suggested that this alteration may impact on stability. An interesting recent report links the regulation mechanisms, denoted "2a" and "2d" [52]. Binding of Lin28 to the pre-miR-let7 hairpin leads to uridylation, and so blocks DICER processing of the pre-miRNA.

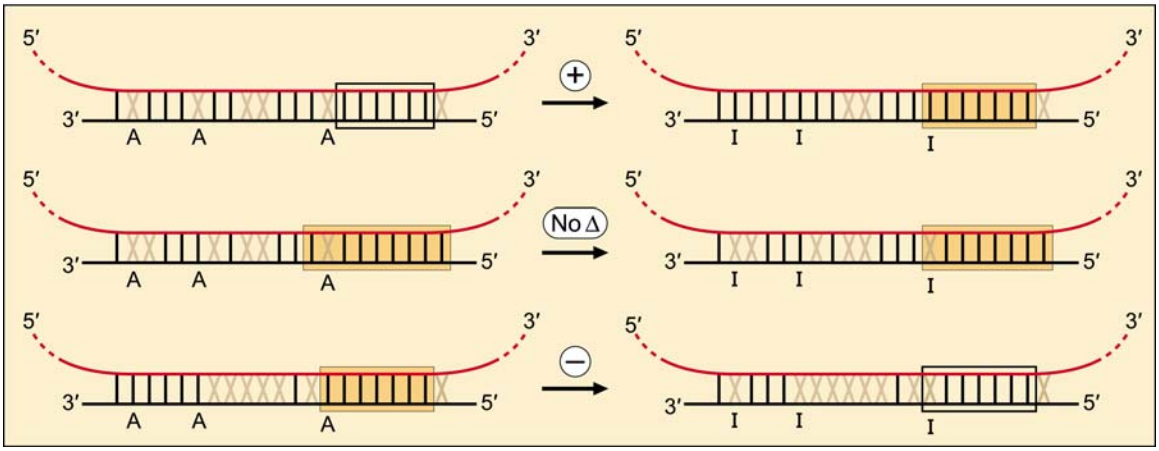

Figure 2. Deamination of mature miRNA sequence can shift the set of target transcripts. A) Weak or moderate binding partners could be strengthened, especially if the sequence changes extended base pairing in the critical "seed" region of the miRNA (nucleotides 2-8 are minimal, additional binding at positions 1 or 9 increases the likelihood of miRNA-target interaction). B) After the same deamination events, many miRNA-target pairs will still be associated, and the target repressed. C) Some weak miRNA-target pairs will lose binding after deamination, as the remaining base pairs will be insufficient for translational repression.

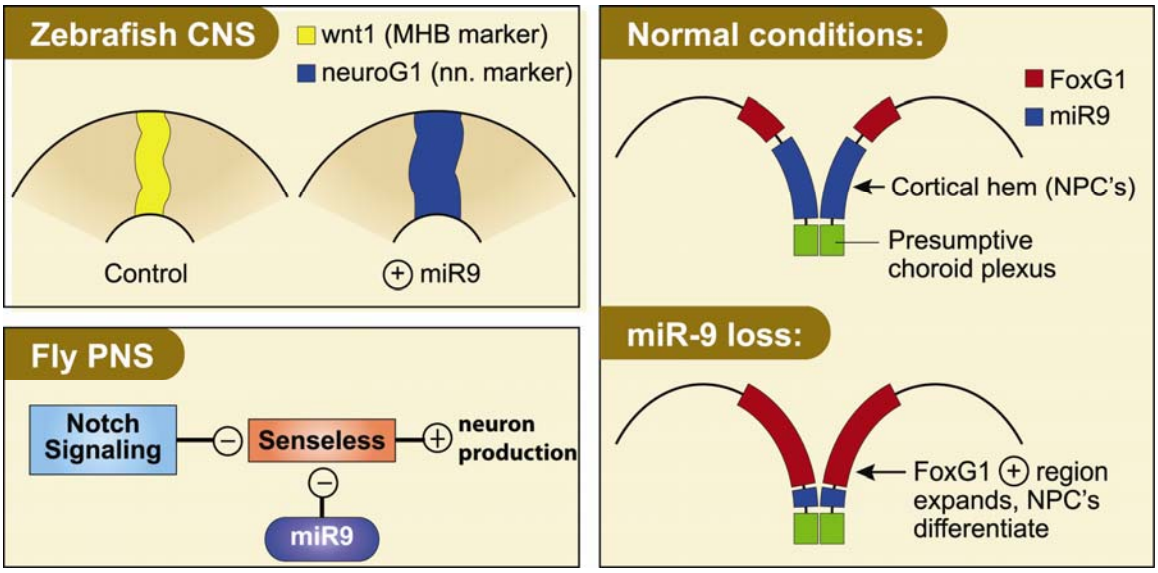

Figure 3. miR-9 activity differs in fly and fish versus mouse brain. A) In the developing nervous system in fly, miR9 inhibits the Notch effector Senseless, permitting neural differentiation to occur. B) In zebrafish, miR-9 is normally excluded from the midbrain-hindbrain boundary where neural progenitor cells reside. Ectopic expression of miR-9 in that region results in inappropriate commitment of progenitors to neurons. C) During mouse corticogenesis, miR-9 is expressed in the progenitor-containing cortical hem. In this context, miR-9 expression is adjacent to, but non-overlapping with, its pro-differentiation target, FOXG1. miR-9 loss of function allows ectopic expression of FOXG1 in the cortical hem, which results in premature neural differentiation of progenitor cells.

CHAPTER TWO: CENTRAL NERVOUS SYSTEM DICER DEPLETION IN VIVO

miRNA function is known to be required in mature neurons, with loss leading to slowly developing neurodegeneration ([89, 91-93, 97]). Until recently, only a small body of functional data supported the hypothesis that miRNAs are also important in the developing vertebrate nervous system ([89, 103]. For this reason, we sought to deplete mature miRNAs in the developing nervous system to determine if miRNAs are implicated in developmental processes and to test which miRNA players are relevant.

During the final stages of this study, others reported that miRNAs are required for nervous system development. These studies were described in Chapter 1. Three recent reports are most relevant to my work, and describe miRNA loss in early corticogenesis. These studies, and my experiments, employ a mouse model in which loxP sites flank a critical exon of *Dicer,* an essential enzyme in the miRNA biosynthetic pathway. Choi *et al.* disabled *Dicer* in mouse olfactory epithelium and CNS tissue starting around embryonic day 8 (E8). They effected recombination of the floxed *Dicer* by breeding to the FoxG1-Cre mouse. Recombination occurs throughout the telencephalon coincident with the onset of cortical neurogenesis [89]. They observed lethality *in utero* and microcephaly, but did not describe the CNS phenotype in detail. Makayev *et al.* performed the same cross, and in addition to microcephaly, characterized some aspects of histology in the embryonic day 13 brain [94]. They noted disorganization of cortical layers with a specific decrease in newborn neurons. De Pietri Tonelli and colleagues bred the floxed *Dicer* mouse to Emx1-Cre, removing *Dicer* specifically in the developing forebrain [88]. They carefully described the histological phenotype of dicer dysfunction in the developing brain, clarifying the cellular mechanism of the observed microcephaly.

My experiments characterized a similarly timed and located *Dicer* depletion. I crossed the floxed *Dicer* mouse (fd) to a mouse in which the Cre recombinase is driven

by the neural progenitor cell specific *NESTIN* promoter (ncre), which drives recombination in neural progenitor cells and their progeny. Our model recapitulates several key aspects of the Emx1-Cre *Dicer* knockout, allowing us to further examine the cellular and molecular phenotype. I extend the published findings in several ways. I tested the hypothesis that disruption of migration contributes to the observed lamination defects. I found that Cajal-Retzius neurons, which emit critical guidance signals to migrating neurons, are present in the expected location and density in the Dicer null cortex. I also inspected the radial glial cell processes that serve as a scaffold for newborn neuron migration. I found cortex-spanning radial glial processes at decreased density in null versus control animals. Lastly, to implicate particular miRNA players in neurogenesis, I profiled miRNAs in NPCs isolated from depleted and control littermate forebrains. From these results, I suggest several candidate miRNAs for the observed phenotype.

2.1. Results of *Dicer* depletion in the developing CNS

We bred mice with loxP sites flanking the essential Rnase III domain of *DICER* (fd mice) to mice expressing Cre recombinase from the NPC-specific nestin promoter/enhancer (ncre mice) [85]. Resultant embryos were haplo-insufficient (fd/-;ncre) or null (fd/fd;ncre) for DICER in NPCs (Figure 4). Mendelian ratios predict that one-fourth of the animals from this cross would be null. However, based on the reports of developmental lethality following DICER ablation in the forebrain [88, 89, 94], we anticipated loss of animals, perhaps even at prenatal timepoints. Indeed, only 14% of embryos were null at either e16.5 or e18.5 (7 litters counted at each timepoint, n=50 embryos at E16.5, n=34 embryos at E18.5), and even fewer, 7% (5/72 animals) survived to birth (Figure 5). Since these “survivors” appeared grossly normal (data not shown), we checked if recombination had occurred at the DICER locus. Recombined and un-recombined RNA products of the floxed *DICER* allele were quantified after RT-PCR was

performed using samples from survivor tissues (Figure 6). We found that tissue from the five surviving DICER null animals had lower ratios of recombined/normal *DICER* in several different brain regions than did heterozygous (fd/+; ncre) littermates. Therefore, we did not conduct further analysis of the survivors.

To evaluate the brains, we prepared paraffin sections of whole embryos in the sagittal plane. Nissl staining revealed decreased brain size with enlarged lateral ventricles and marked cortical thinning in the null embryos compared both fd/+;ncre and fd/fd;+ embryos (Figure 7). For the rest of the studies described here, we used fd/fd;+ littermate embryos as controls. Developmental malformations of the cortex are often categorized into defects in NPC proliferation *vs.* defects in migration or differentiation [25]. Since microcephaly is commonly caused by decreased proliferation of NPCs, I began by assessing the proliferative regions of the developing cerebral cortex.

I inspected NPCs in e16.5 embryos by immunostaining for the NPC marker NESTIN. I observed a layer of NESTIN+ cells bounding the lateral ventricle in both null and control brains at both ages (Figure 8). To learn if these cells were dividing normally, I stained dividing cells with the M-phase marker PHOSPHOHISTONE H3 (Figure 9). I found that both the number and the distribution of stained cells was different. In wildtype animals, stained cells were notable in the VZ and SVZ. Null animals had fewer cells in the VZ, and a near absence of PHOSPHOHISTONE H3 positive cells in the SVZ.

To test if this late defect in cell division was accompanied by earlier failure of cells to divide and commit (which could be responsible for thinned cortex), I inspected NPC cells two days earlier in development. At this stage, a difference in cortical thickness was not apparent in brain sections (data not shown). Next, I examined NESTIN+ cells, and found a reduction in staining intensity in the proliferative regions of e14.5 null vs. control brains (Figure 10). To test NPC function, I pulsed animals once at e13.5 with bromodeoxyuridine (BrdU), then harvested embryos one day later at e14.5. In sections from these brains, I detected robust numbers of newborn cells in the cerebral

cortex by immunodetection of BrdU (Figure 11). Though not quantitative, this qualitative assessment suggests that there is already a defect in NPC number at e14.5, but the cells are still able to divide and move out of the VZ/SVZ.

However, my data also suggest defects during the later developmental stage when committing neurons undergo migration and differentiation. In e16.5 null embryo brains, NESTIN expressing cells were present in the upper layers of cortex, which normally house only committed cells (Figure 12**)**. Also, immunostaining for the mature neuronal marker NEUN revealed that neurons were so disorganized by e16.5 that cortical lamina were not recognizable (Figure 13). In control animals at e16.5, neurons had inserted into the cortical plate, dividing the subplate (arrows) from the uppermost cortical layer where Cajal-Retzius neurons reside. However, in the null embryos, we observed poorly organized NEUN positive cells throughout the non-proliferative region of developing cortex, suggesting retardation in preplate splitting. These results are consistent with the cortical layer phenotype reported for the Emx1-Cre Dicer knockout mice [88].

One explanation for the observed disorganization is a problem with migration. Newborn neurons normally sense extracellular REELIN near the pial surface of the developing cortex, and as a result, cease surface-directed migration at a precise cortical level. The source of REELIN protein is a superficially-located layer of Cajal Retzius neurons. The Cajal Retzius neuron marker CALRETININ revealed these cells at the pial surface at e16.5 without gross differences between genotypes (Figure 14). Stereological counts would be needed to eliminate the possibility of subtle differences in cell number. However, staining for REELIN revealed a broadened swath of expression in null versus control cortex at e14.5 (Figure 15) and e16.5 (data not shown).

Migration of newborn neurons occurs in close association with the processes of radial glial cells, which form a scaffold for newborn cell movement [3]. To test the integrity of the radial glial scaffold, I examined the NESTIN+ processes at e14.5 and e16.5 (Figure 16). These processes were marked less dense in null versus control

animals. Thus, both REELIN distribution and radial glial morphology likely contribute to the observed lamination defect.

Based on the observation that some cells in the nonproliferative zone are NESTIN-expressing in null but not in control brains, I tested if acquisition of mature fate was impaired. I tested this using the newborn neuron marker DOUBLECORTIN, and found reduced staining intensity in the null animals at e16.5 (Figure 17). These newborn neurons were fewer in number at the correct location at the superior aspect of the developing cortex. Also, in contrast to controls, DOUBLECORTIN-expressing cells were also found in the SVZ in null embryos.

2.2. Expected and novel miRNAs are regulated during cortical neurogenesis

To pinpoint individual miRNAs working in the developing cortex, we quantified expression of 384 miRNAs and endogenous small RNAs from null and control NPCs using a q-RTPCR based platform (Tiling Low Density Array (TLDA), Applied Biosystems). We collected NPCs from null and control embryos at e15.5, cultured them for two passages *in vitro*, and measured miRNAs in three samples of each genotype.

As an initial evaluation of of the effectiveness of the depletion we evaluated two miRNAs that are highly expressed in brain [88]. miR-9 has been found specifically in NPCs and expression is low to undectable in post-mitotic neurons in the embryo. miR-124a has the opposite expression pattern, with specific localization to post-mitotic neurons. Indeed, we found that in the control samples, miR-9 was among the most strongly expressed miRNAs, and miR-124 was not detected. We also looked at the heart specific miRNA, miR-1, and found that it was also not detected in the control NPCs. We next tested for changes observed in miR expression from control to null cells. We found that of the miRNAs that were detected, 65/247 showed a significant change in expression level ($p<0.05$, Student's t-test) (Table 2). Of these, 70/73 had decreased levels, and

interestingly, 3/65 were increased. This is consistent with the expectation that mature miRNAs will be lost after DICER depletion. One intriguing finding from this work was that the levels of 182/247 miRNAs were not significantly different after DICER depletion, and the levels of others, though significantly decreased, were not reduced to undetectable levels. Several new candidate actors in neurogenesis are identified by these results.

2.3. Discussion

2.3.1. Efficiency of miRNA depletion by this method

We have depleted DICER in the developing nervous system by irreversibly disabling the genomic locus in neural progenitor cells. In this way, the progenitors and all of their daughters will fail to produce DICER protein. With rare exceptions, removal of DICER in other systems has resulted in miRNA depletion. However, some miRNAs are quite stable, persisting for months in slowly dividing and quiescent cell types, for example, in developing retina and purkinje cells [93, 97]). In the Emx1-Cre model, loss of DICER did result in rapid loss of the several highly expressed miRNAs tested after recombination in neuroepithelial cells at E8-9. Neither miR-9 nor miR-124a was detected by *in situ* hybridization at E10.5. We found a modest reduction in miRNAs in our system. In neural progenitor cells collected at e15.5 (~ six days after recombination) and cultured for two passages (~12 divisions, assuming 20h cycle time ([125, 126]) and passage every 5 days), most miRNAs that were expressed in wild-type cells were reduced by ~50% in knock-out cells. There is no data in the literature to suggest an alternative to DICER for processing of precursor to mature form of miRNA. However, the persistence of some miRNAs after DICER loss invites speculation. Are there alternate enzymes capable of executing miRNA biosynthesis in particular tissues, such that miRNA levels fall less precipitously after DICER loss in those settings? Are there particular miRNAs that can be processed by an alternate pathway in the absence of DICER function (or

maybe even as a regular mechanism)? The sets of miRNAs that are less efficiently depleted after DICER loss merit close consideration.

2.3.2. Selection of DICER ablation as a technique to investigate miRNAs' role in CNS development

Clearly, the DICER depletion has broad impact on neurogenesis. There are may be nearly one thousand miRNA individuals in human, and nearly as many in mouse. While only a fraction of these are present in any given tissue, that fraction is likely hundreds of mature miRNA sequences. In this study, I found that 255/384 miRNAs represented on the TLDA were expressed in pimary NPCs in culture. One very powerful aspect of the DICER loss model is the ability to perform subtractive profiling. We analyzed the miRNAs present in wild-type vs. depleted cells and also wild-type vs. depleted developing brain. This unbiased approach to candidate selection has uncovered a set of miRNAs which are present in NPCs with information about their changing levels during corticogenesis *in vivo.* Combined with other profiling studies, for example, at timepoints during neural differentiation, this information will facilitate development of more specific hypotheses about miRNA function in neural development.

Of note, the histological devastation accompanying miRNA loss is anti-correlated with animal age at the time of deletion. Surprisingly, it is not progenitor cell populations that confer sensitivity, as progenitors are apparently normal for days to weeks after DICER loss. Instead, it is the cells in the process of differentiation and migration. Without DICER, cells fail at differentiation and are subsequently lost.

Based on my results, it is difficult to even speculate whether the depletion of these regulators as a group is <u>more</u> disruptive (many regulators missing) or <u>less</u> disruptive (coordinate removal of balanced positive and negative regulators) than would be the loss of individual miRNAs. Future studies in our lab and by other groups will address this question. Several reports of miRNA function in the nervous system implicate single, and

sometimes multiple, miRNAs in feedback loops [77, 86, 107, 108]. This study, together with the similar published reports, points to the initiation and completion of cell differentiation as a rich model to study the impact of miRNAs in brain development.

2.3.3 Extending the published histological analysis

Other groups have found that the neuron loss after DICER depletion occurs before NPCs drop out or stop dividing. De Pietri Tonelli *et al.* describe increasing apoptosis in the cortical lamina from e12.5 to e14.5, with a strong increase in TUNEL signal in the proliferative layers (VZ and SVZ) at e14.5. They suggest that because there is no decrease in layer thickness or cell density, it is newborn neurons that are dying. I would like to verify that prediction by co-staining e14.5 sections to detect the apoptotic marker activated caspase 3 together with markers of cellular identity.

Another approach to this question would be to observe the kinetics of apoptosis onset in cultured cells by qPCR or flow cytometry in NE experimental or control animals.

2.3.4. Further miRNA profiling

We have also collected forebrain samples at timepoints early and mid-way through cortical neurogenesis. The analysis of these samples is underway, and may point to important miRNA players in cortical development that are located <u>outside</u> NPCs/newborn neurons. For example, the role of glia in brain development is clearly important, the glial biologist Ben Barres calls it “magical” [127]. To investigate these miRNAs, we could focus on some of the miRNAs found in both sets (control and null), but not in the control cultured NPCs (a purer population). We could easily confirm location outside the neuronal lineage by *in situ* hybridization.

2.4. Methods

2.4.1. Animal Care and Use

Floxed *dicer* (fd) mice were transferred from Michael McManus at UCSF and rederived at the University of Iowa Animal Care Facility. Animals were bred to homozygosity, and genotyped using published protocols [85]. Nestin-Cre (ncre) mice were purchased from Jackson Labs (Strain name B6.Cg-Tg(Nes-Cre)1Kln/J; Stock number 003771) and genotyped as recommended. Animals were housed and handled according to protocols approved by the University of Iowa Institutional Animal Use and Care Committee.

For harvest of adult mouse tissues, animals were anaesthetized with 0.01ml/g ketamine/xylazine (1%/10%) solution, then transcardially perfused with 25ml normal saline. Brains were removed and sub-structures dissected. Hearts were also collected as a negative control.

2.4.2. Embryo collection

For timed matings, male and female mice were co-housed overnight. We defined noon the following day as E 0.5. On the day of harvest, the pregnant dam was over-anaesthetized with 0.015 cc/g intraperitoneal ketamine/xylazine (10%/1% solution in normal saline) or inhaled isoflurane, then euthanasia was confirmed by cervical dislocation. For paraffin immunohistochemistry, embryos were harvested and anaesthetized for 5 minutes in weigh boats on wet ice. After weighing, tails were removed for genotyping. Whole embryos were stored for 8-12 hours at 4 °C in zinc-formalin fixative, then hemissected in the sagittal plane, wrapped in permanent paper (Sally Beauty Supply), and stored in embedding cassettes at 4 °C overnight in zinc-formalin fixative. Cassettes were paraffin embedded according to standard protocols and blocks were sectioned at 6 uM thickness. Sections were transferred to Superfrost plus (Sigma) slides and stored at room temperature until use.

2.4.3. Primary cell culture

For preparation of primary embryonic neural progenitor cells, timed matings and anaesthesia were performed as described above. Embryos were collected into ice-cold PBS/2% glucose. Each embryo was decapitated, and the forebrain was removed and diced. The remaining head tissue was used for DNA isolation and genotyping. Diced forebrain was subjected to trituration with a glass Pasteur pipette to dissociate cells. Repeat supernatant collections and triturations were performed 4-5 times. Cells were pelletted at 800 rpm for 5 minutes at 4 °C, then resuspended in Mouse Neural Stem Cell proliferation media (Stem Cell Technologies) containing human recombinant epidermal growth factor (hrEGF) with added penicillin/streptomycin (1%).

Cells were cultured for two passages to enrich cultures for dividing stem/progenitor cells. These cells were subjected to flow cytometric analysis of cell cycle distribution. Nuclei were stained by propidium iodide in hypotonic solution as described [128] and analysed by flow cytometry (Becton Dickinson Facscan) followed by curve fitting in Modfit (Verity Software).

2.4.4. RT-PCR

RNA was isolated from tissue using Trizol (Invitrogen), and reverse transcribed using Superscript III reagents (Invitrogen). cDNA was amplified using primers as described [85], and products visualized on 1% agarose gel with 0.5 ug/ml ethidium bromide. Relative quantification of bands was performed using image analysis software (Labworks).

2.4.5. Histology

Sections were prepared as described above. Before staining, they were deparaffinized by warming, washing in xylenes, then dehydration through an ethanol series followed by incubation at 95 °C for 5 minutes in the microwave in Citrate buffer. Nissl stains were performed according to standard protocols. For immunostaining, block

was for one hour in 5% goat serum in PBS at room temperature, and primary antibody incubation was overnight at 4 °C. Antibodies used were Nestin (mouse anti-Rat401, Developmental Studies Hybridoma Bank, 1:5), NeuN (mouse anti-NeuN, (Chemicon, 1:200), PH3 (rabbit anti-phosphohistone H3 (ser10), Upstate division of Millipore, 1:6000), Doublecortin (goat anti-Doublecortin (N-19), Santa Cruz, 1:200), Calretinin (mouse anti-Calretinin, Chemicon, 1:200) and BrdU (mouse anti-BrdU, Becton Dickinson, 1:200). Biotin-labelled secondary antibodies (Jackson Immunoresearch) were used at 1:500 in PBS for one hour at room temperature. Immunohistochemistry was developing using the Vectastain ABC Elite Kit (Vector Labs) according to the manufacturer's instructions. These slides were mounted using S-100 permanent mounting media. For BrdU fluorescent stain, goat anti-mouse Cy3 (Jackson Immunoresearch) was used at 1:500 in TBS for one hour at room temperature. These slides were mounted using Vectashield (Vector Labs).

2.4.6. Analysis of TLDA data

Raw data files were processed using RQ Manager Software, which calculates the Cycle Threshold (Ct). Ct is the PCR cycle number at which the fluorescence from any well hits a common pre-selected threshold level that falls within the range of linear amplification for most samples. I used the default value of 0.2. I normalized the Ct values in each sample to the mouse U6 small RNA control: deltaCt = Ct(miR) – Ct (mU6). For samples that were not detected, I assigned the Ct to the maximum (40). I then compared the three control deltaCt values to the three null ones by Student's t-test using Excel (Microsoft). For the samples with $p < 0.05$, I then calculated fold-change for each miRNA probe: Fold change = 2 ^ -((meanDeltaCt(experimental) – meanDeltaCt(control)). I then ranked the samples by fold change, and displayed probe name, fold change, and p value in tabular format.

Table 2. miRNAs which were significantly changed after Dicer depletion in NPCs

Detector	Fold change	TTEST
mmu-miR-127	0.0163	0.0000
mmu-miR-153	0.0280	0.0001
rno-miR-346	0.0317	0.0001
mmu-miR-187	0.1011	0.0096
rno-miR-219-2-3p	0.1077	0.0100
mmu-miR-687	0.1986	0.0440
mmu-miR-491	0.2454	0.0265
mmu-miR-138	0.2572	0.0305
mmu-miR-210	0.4275	0.0309
mmu-miR-195	0.4522	0.0198
mmu-miR-125a-5p	0.4527	0.0451
mmu-miR-488	0.4628	0.0158
mmu-miR-204	0.4629	0.0064
mmu-miR-450a-5p	0.4711	0.0068
mmu-miR-135b	0.4729	0.0092
mmu-miR-126-3p	0.5052	0.0212
mmu-miR-16	0.5250	0.0335
mmu-miR-685	0.5358	0.0043
mmu-miR-126-5p	0.5359	0.0026
mmu-miR-30e	0.5461	0.0062
mmu-miR-30c	0.5495	0.0315
mmu-miR-24	0.5531	0.0367
mmu-miR-322	0.5538	0.0103
mmu-miR-101a	0.5556	0.0060
mmu-miR-350	0.5675	0.0002
mmu-miR-340-5p	0.5790	0.0016
mmu-miR-30d	0.6028	0.0119
mmu-miR-146a	0.6092	0.0211
mmu-miR-351	0.6095	0.0096
mmu-miR-140	0.6106	0.0125
mmu-miR-186	0.6180	0.0450
mmu-miR-484	0.6184	0.0177
mmu-miR-9	0.6214	0.0035
mmu-miR-19a	0.6324	0.0237

Table 2 continued

mmu-miR-324-5p	0.6342	0.0430
mmu-miR-872	0.6424	0.0321
mmu-miR-27a	0.6502	0.0589
mmu-miR-106b	0.6555	0.0087
mmu-miR-26a	0.6573	0.0012
mmu-miR-26b	0.6583	0.0071
mmu-miR-106a	0.6592	0.0002
mmu-miR-344	0.6597	0.0272
mmu-miR-301a	0.6637	0.0028
mmu-miR-155	0.6672	0.0032
mmu-miR-19b	0.6674	0.0008
mmu-miR-384-5p	0.6697	0.0381
mmu-miR-30b	0.6709	0.0169
mmu-miR-132	0.6873	0.0528
mmu-miR-181a	0.6876	0.0195
mmu-miR-222	0.6905	0.0344
mmu-miR-99a	0.6911	0.0369
mmu-miR-17	0.6946	0.0009
mmu-miR-130a	0.6993	0.0066
rno-miR-351	0.7046	0.0114
mmu-miR-21	0.7165	0.0211
mmu-miR-30a	0.7257	0.0213
mmu-let-7g	0.7295	0.0573
mmu-miR-93	0.7414	0.0070
mmu-let-7i	0.7571	0.0175
mmu-miR-29c	0.7960	0.0394
mmu-miR-672	0.8317	0.0163
mmu-miR-190	1.8642	0.0338
rno-miR-598-5p	7.4666	0.0498
mmu-miR-150	19.2196	0.0213

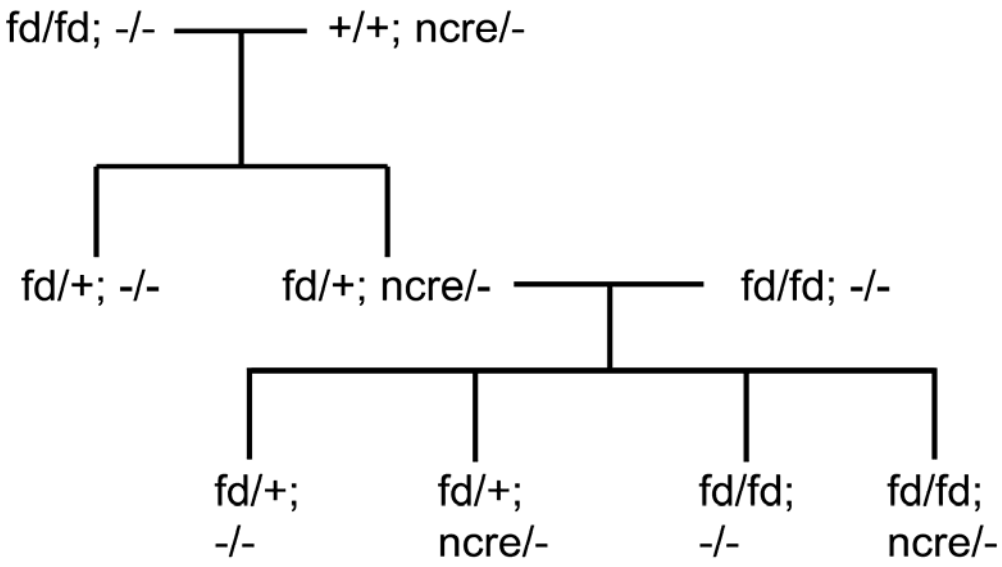

Figure 4. Breeding scheme to yield mice with dicer-depleted NPCs.

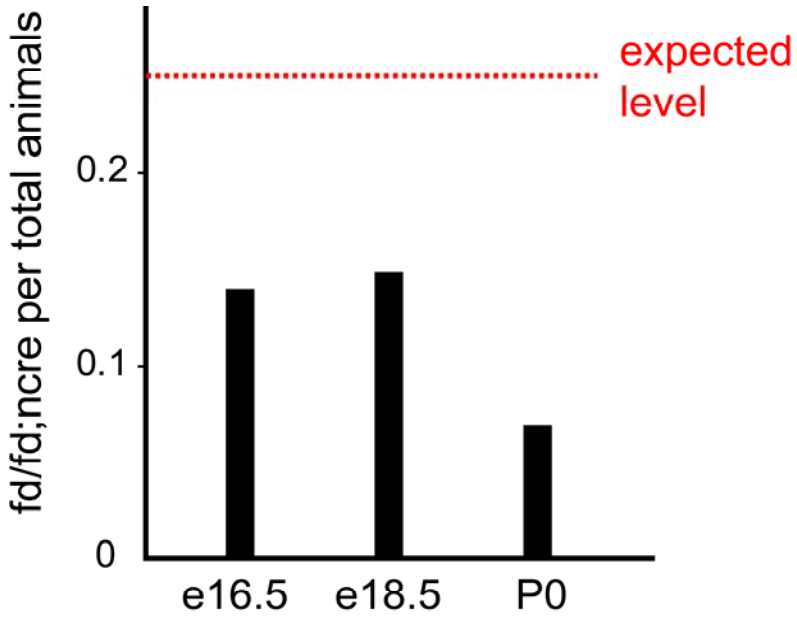

Figure 5. Fewer than the expected number of null animals were present at the three measured timepoints.

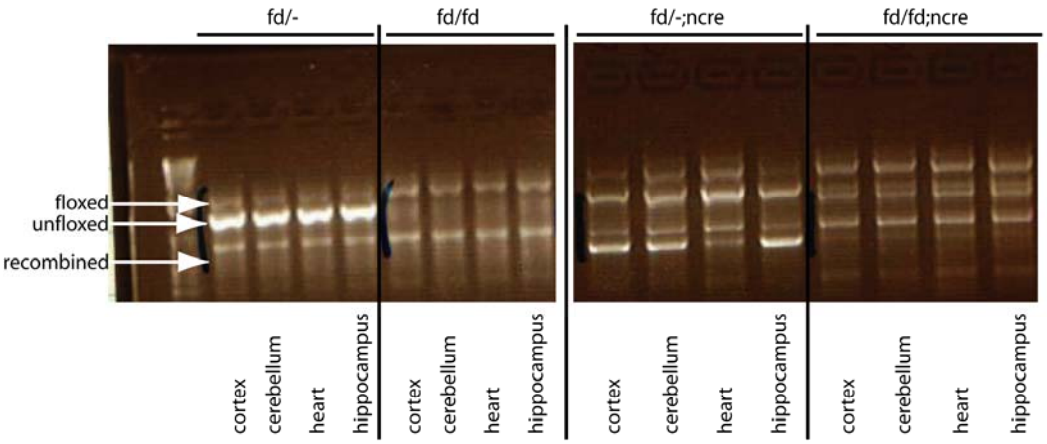

Figure 6. RT-PCR was used to verify recombination at the *Dicer* locus in young postnatal animals. Heterozygous animals have two upper bands (floxed and unfloxed). Homozygous animals only have the upper floxed band. Heterozygotes have a distinct additional band in the presence of Cre. Homozygous animals that survive beyond birth show only minimal recombination.

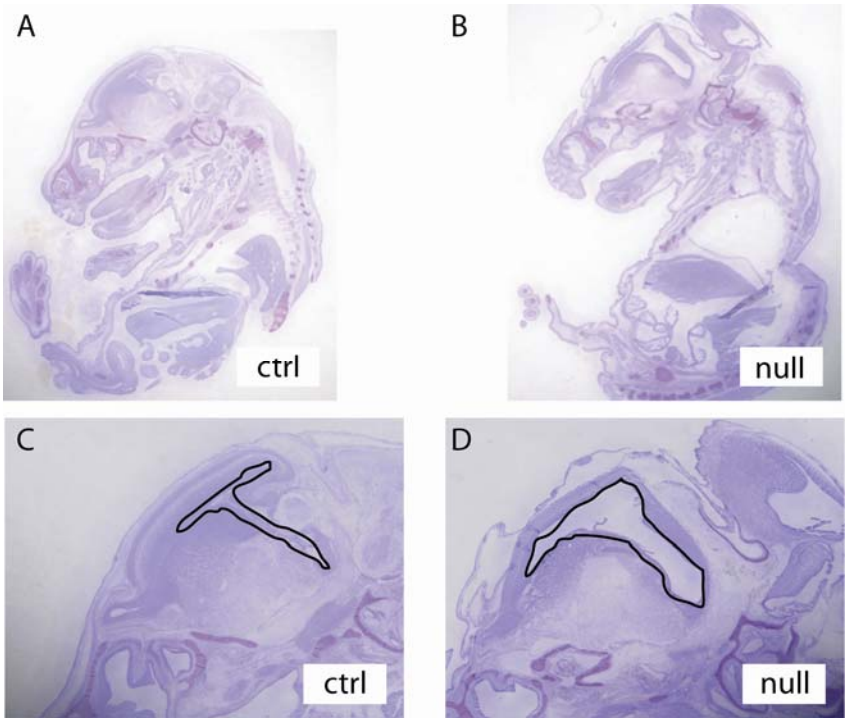

Figure 7. Nissl staining in DICER null animals at e16.5 shows gross dilation of the lateral ventricle. A,B low-power sagittal sections. C,D high-power view of same sections, lateral ventricles outlined in black.

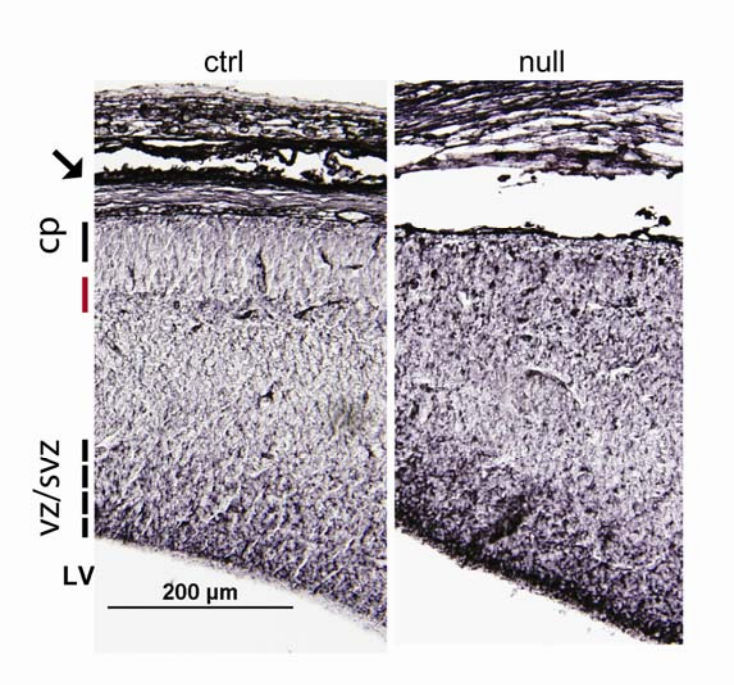

Figure 8. NPCs are detected in control and Dicer null animals in the VZ and SVZ. Lateral ventricle (LV) at inferior aspect of micrograph, pial surface at superior aspect.

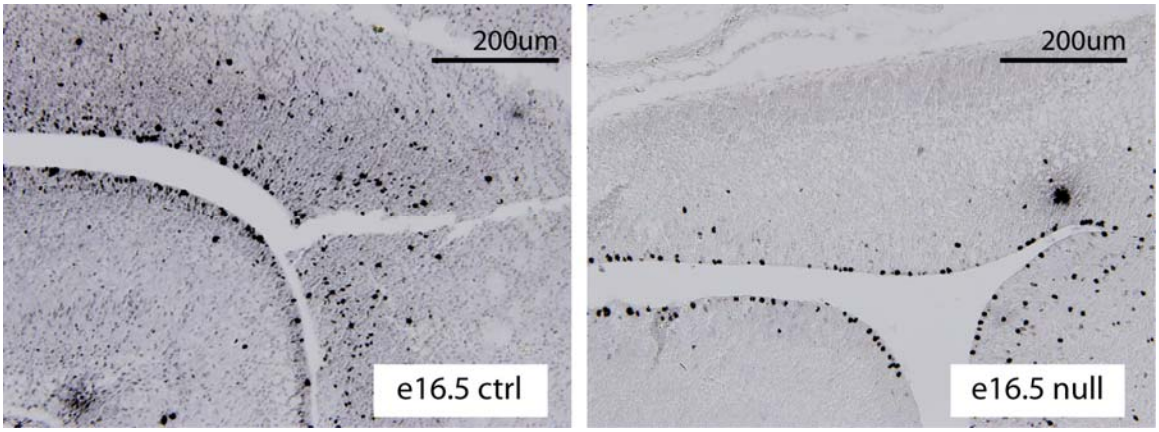

Figure 9. Staining with the mitotic cell marker PHOSPHOHISTONE H3 at e16.5 reveals loss of dividing cells in the proliferative zones, with profound loss in the SVZ.

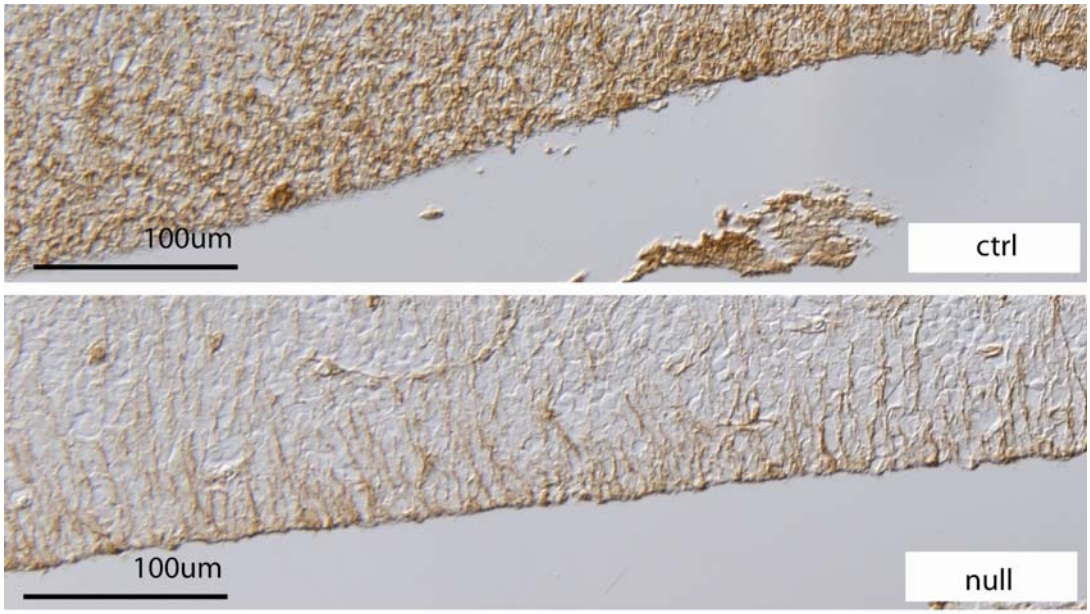

Figure 10. At e14.5, the NPC marker NESTIN reveals a lower density of progenitor cells near the ventricular surface (located at the bottom of this image).

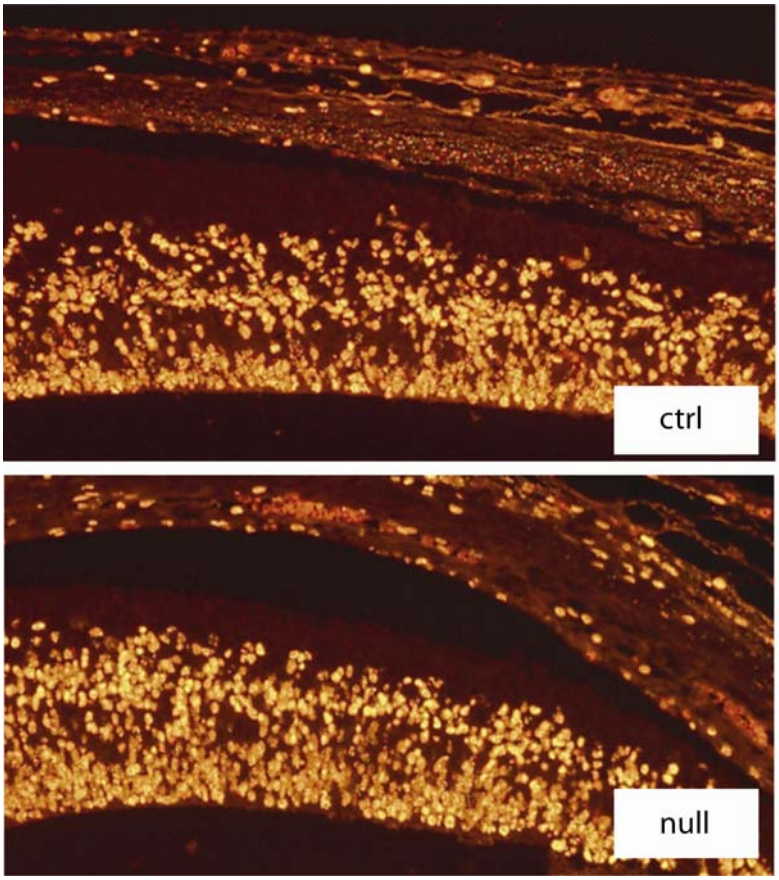

Figure 11. Cell division and migration did not differ from e13.5 to e14.5. Number and distribution of marked cells is indistinguishable one day after a single BrdU pulse. Micrograph shows sagittal section of cerebral cortex with lateral ventricle at the inferior aspect of the tissue.

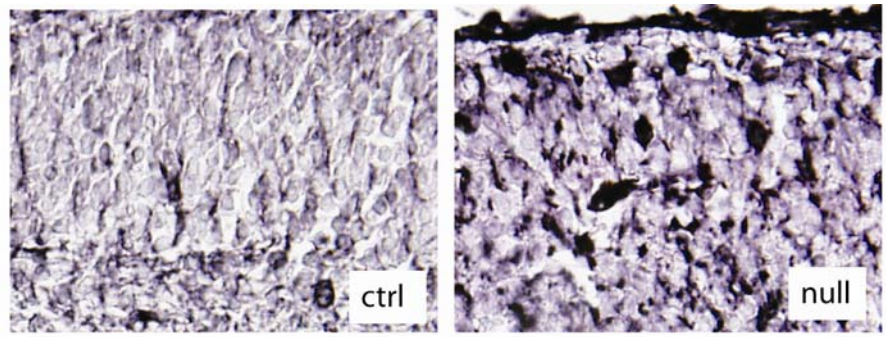

Figure 12. High powered image of the superior aspect of cerebral cortex shows the numerous ectopic cells in the DICER null, but not the control, cortex at e16.5.

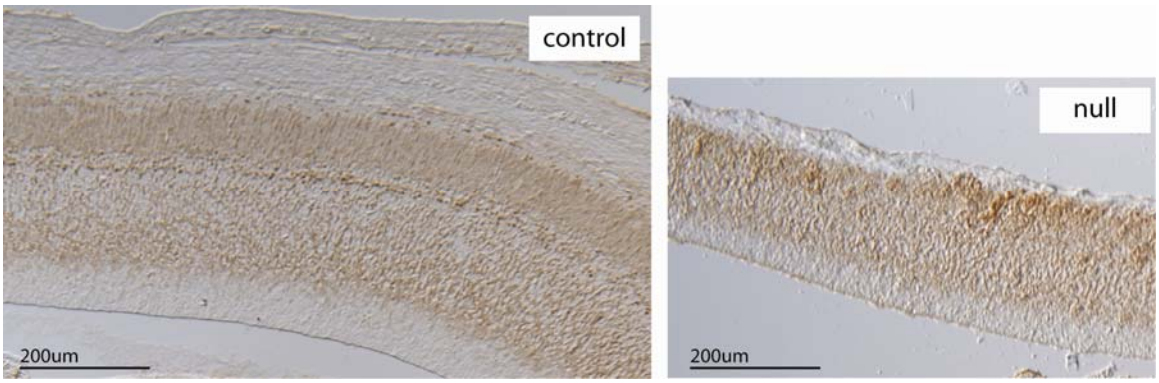

Figure 13. Neurons are few and disorganized in null brain at e16.5 compared to control. NEUN staining marks post mitotic neurons, and shows distinct layers in the control, but not null, brain.

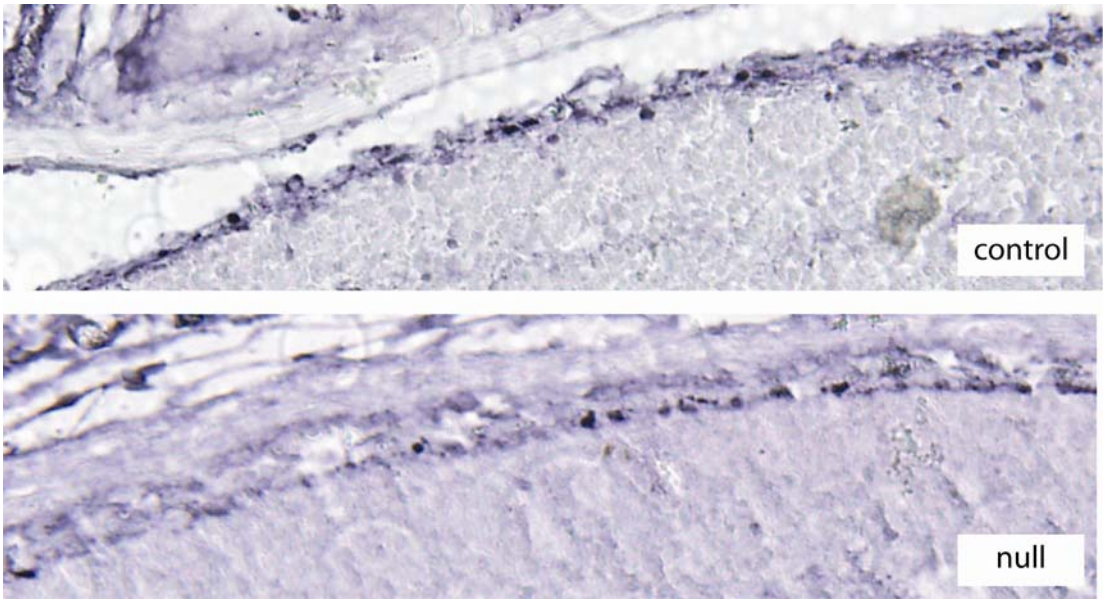

Figure 14. Cajal Retzius neurons do not differ in number or location between null and control mice. Staining with CALRETININ antibody revealed cells in a single layer at the pial surface.

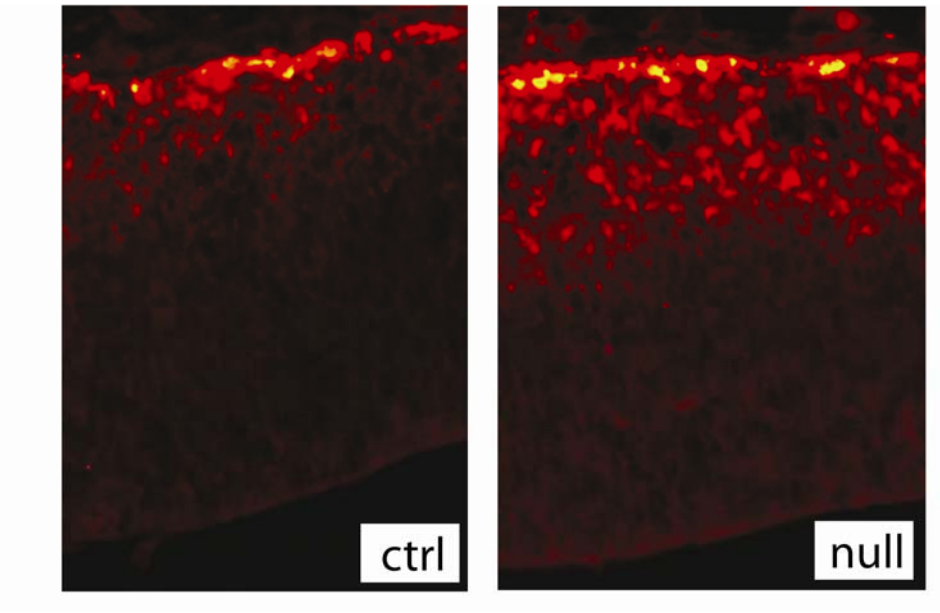

Figure 15. Immunostaining for REELIN in e14.5 cerebral cortex reveals increased area in which REELIN is distributed. Micrograph shows coronal sections in which the superior/pial surface is aligned with the top of the image.

Figure 16. At e14.5, NESTIN-positive radial glial cell processes are cortex-spanning in both null and control brains. Micrograph shows full thickness of cerebral cortex with lateral ventricle at the bottom.

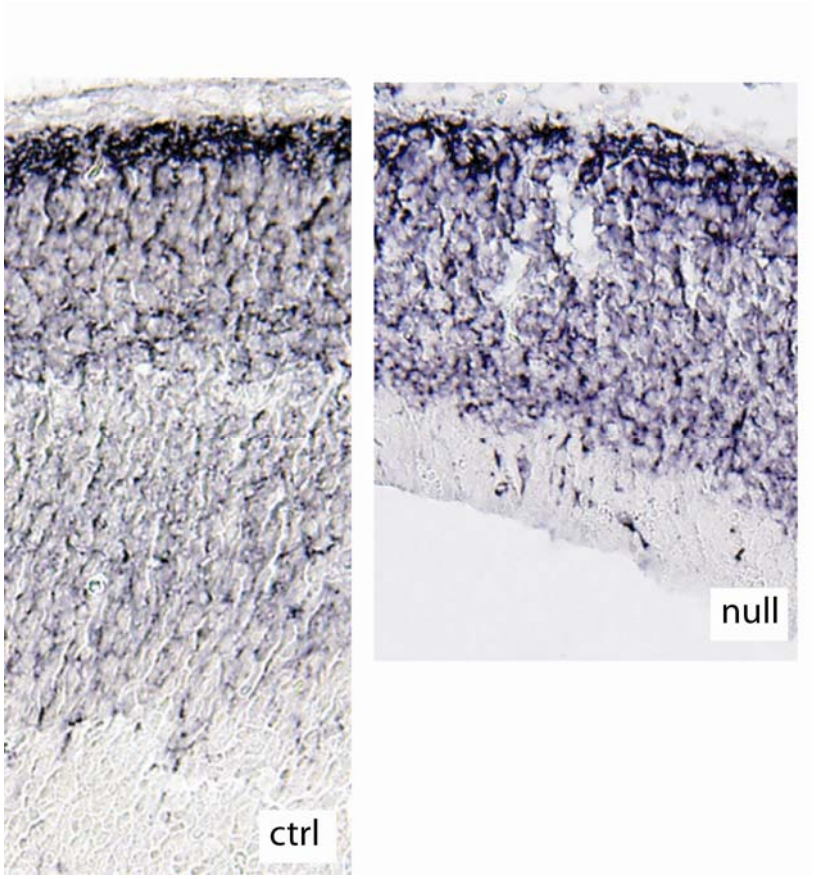

Figure 17. In null brain, newborn neurons are left behind in the proliferative zones and fail to populate the upper cortical layers as densely as they do in the control brain. DOUBLECORTIN staining was used to mark newborn neurons.

CHAPTER THREE: MICRORNA CANDIDATES TO MODULATE NEURAL DEVELOPMENT

At the outset of my project, miRNAs had only very recently been described, and the first profiling studies were being published [28, 35, 86]. For the reasons set out in Chapter 1, in particular the specific and dynamic expression patterns of miRNAs coupled with their ability to coordinately downregulate sets of proteins, we hypothesized that brain-expressed miRNAs modulate neurogenesis. During the course of this work, a great deal of supporting data has been published. This chapter details the process I took for early candidate selection, development of tools to manipulate miRNA levels in NPCs, functional analyses of a few miRNA candidates in NPCs, and the results of some recent unbiased profiling studies I have undertaken.

3.1. Selection of miRNA candidates

To begin, I conducted a review of the literature, including articles that described miRNA profiling or detection and included samples of neural tissue. I compared the results of these studies to a 2005 publication which described *in situ* hybridization results after testing the then-complete panel of miRNA probes on developing zebrafish. These results are summarized in Table 3**.** For each of these miRNAs, I examined the genomic locus from which is it expressed. Several of these miRNAs were encoded by multiple genomic loci which generate the same miRNA precursor. These are designed as mmu-miR-#-1, mmu-miR-#-2, etc. . . To simplify future analyses, I elected to begin with the miRNA candidates thought to be expressed from a single locus. Some miRNAs share such significant homology in the mature miRNA sequence that functional overlap is likely. These nearly-identical mature miRNA "family members" are named as mmu-miR-#-a, mmu-miR-#-b, etc. . . Data regarding the presence of multiple loci and nearly-identical family members is included in Table 3 parenthetically under the miRNA name.

3.2. Strategies to experimentally alter miRNA levels in NPCS

To test the function of the selected miRNA candidates in the developing nervous system, I planned to effect gain and loss of function *in vitro* in primary embryonic mouse neural progenitor cells (NPCs). These cells were collected from embryonic day 15.5 mouse forebrain and cultured as neurospheres for fewer than eight passages, as described by Reynolds *et al.* [129]. By changing growth factors and adding serum to the culture, the NPCs are induced to differentiate into neurons, glia, and oligodendrocytes.

3.2.1. Gain of function in NPCs

3.2.1.1 Vector Selection

Work from the Davidson Lab had shown that feline immunodeficiency virus (FIV) vectors pseudotyped with the lymphochoriomeningitis (LCMV) envelope glycoprotein can transduce NPCs, and the cells can subsequently continue to grow in culture as progenitors [130]. The other viruses tested in that study were not effective: adeno-associated virus subtypes did not transduce NPCs, and adenoviral infection resulted in NPC differentiation to astrocytes, precluding further analysis of progenitor cells. Therefore, I opted to express the candidate miRNA hairpins from FIV, following a strategy conceived by Scott Harper in the lab based on a report by Cai et al. [131] (Figure 18). He inserted miRNA hairpins into an EcoRI site in the 3' untranslated region of a protein reporter gene in FIV. We used two reporter genes in these studies: green fluorescent protein (GFP), with emits green light under epifluorescence, and neomycin phosphotransferase II (NPTII, here called neoR), which confers resistance to neomycin and neomycin-analogs (we used geneticin (Gibco)) . The miRNAs were transcribed along with the reporter gene. We expected the excision of miRNA from some transcripts to result in reduced reporter protein, but found adequate levels of both reporter and miRNA (data detailed below). We selected this strategy over one in which two vectors

would be delivered, each bringing one sequence (reporter or miRNA), for two main reasons. First, although there were already plentiful reports in the literature of functional short hairpin RNA (shRNA) vectors (designed to deliver RNAi) expressed from independent transcription units, we did not have much information about the transcriptional and processing requirements of endogenous mammalian miRNAs. We did know that some of these sequences were produced from 3'UTRs *in vivo*, so we hoped to mimic a successful *in vivo* strategy. Second, the use of a single vector eliminates questions about efficacy of co-delivery, ensuring that reporter-expressing cells also contain the miRNA expressing sequences.

We also tested the ability of FIV vectors enveloped with the vesicular stomatitis virus glycoprotein (VSVG) to transduce NPCs. In the University of Iowa Gene Transfer Vector Core (GTVC), VSVG enveloped vectors can be produced at ~100fold higher titers than can L-CMV enveloped vectors.

3.2.1.2. Vector cloning

I constructed these expression vectors as follows. For the selected miRNA candidates, I designed DNA primers to amplify 200-500 nucleotides of genomic sequence surrounding the miRNA hairpin by polymerase chain reaction (PCR). For convenience in subcloning strategies, I cloned the PCR products into the TOPO2.1 vector using the TOPO TA cloning kit (Invitrogen), which contains a rich multiple cloning site. I subcloned the miR-containing sequences, each separately, into the FIV vectors, and verified the clones by restriction digests and DNA sequencing across the clone/vector junctions (data not shown). We named these vectors as FIV-(reporter)-miR-(#) (Figure 19). The first several clones I generated expressed miR-21, miR-34a, miR-23b, and miR-182. I then used these vectors for functional studies.

3.2.1.3. Tests of vector functionality

Before employing the miRNA expression vectors in functional studies, I confirmed that they were functional. I tested for detectable levels of reporter protein and miRNA hairpin, and miRNA activity. Much of this data is published in Harper *et al.* [132].

To assess reporter gene levels, we infected HT1080 cells with 100-fold diluted FIV-GFP-miR21 viral supernatant or FIV-GFP as a control. In protein lysates from these samples, western blotting revealed GFP protein, and, as expected, a weaker band in the FIV-GFP-miR21 infected samples than control (Figure 20). I confirmed this result by flow cytometry (Figure 21). I detected GFP+ cells in both samples, however the number of GFP+ cells and the mean fluorescence of each cell were reduced in the FIV-GFP-miR21 cells compared to control. To test if this finding extends to NPCs, I repeated the infections and flow cytometry in NPC culture. Indeed, flow cytometry results were similar (Figure 22). I also tested reporter expression from the neoR vectors. I infected NPCs with FIV-neo or no virus, and found that 0.5 μg/mL geneticin was sufficient to kill uninfected cells without impacting infected cell numbers (Figure 23). I then applied this dose of geneticin to FIV-neo and FIV-neo-miR34a infected cells and found that neurospheres grew in both cultures within one week (data not shown).

We next tested expression of the miRNA hairpins and mature forms from the vectors. Scott Harper infected HT1080 cells with FIV-neo-miR21 and FIV-neo-miR34a, selected infected cells, and collected RNA. He observed both precursor and mature forms of each miRNA on Northern blotting (Figure 24).

I also tested miRNA expression from these vectors in NPCs. For *in vivo* overexpression studies, I wanted to confirm that the miRNAs were produced in NPCs after infection, and that the increase in miRNA levels was a small increase, likely to fall within reasonable expectations of biological changes. I infected NPCs with the vectors and used miRNA assays (Applied Biosystems) to quantify relative amounts of each

miRNA by qRTPCR (Figure 25). I found that infection with these vectors resulted in a 2-5 fold increase of mature miRNA compared to control.

As a tool for verifiying miRNA activity, I cloned two "perfect targets" (sequence exactly antisense to the mature miRNA) into the 3'UTR of the firefly luciferase gene in a dual reporter plasmid (psi-check2, Promega) that contains a second, undisturbed, luciferase gene from the marine organism, *Renilla*. In this way, I can detect changes in miRNA activity by measuring the ratio of firefly to *Renilla* luciferase in co-transfected cultures. Indeed, upon co-transfection, I observed that the luciferase reporters were repressed by the matched FIV-GFP-miR (for example, the luciferase-miR182target was repressed by FIV-GFP-miR-182) but not by the control plasmid or the mismatched FIV-GFP-miRs (FIV-GFP or FIV-GFP-miR-34a) (Figure 26).

3.2.2. miRNA loss of function

To effect loss of function of mature miRNAs in NPCs, we tested two approaches: antisense oligonucleotide transfection and expression of shRNAs directed against the pre-miRNA loop.

3.2.2.1 Antisense oligonucleotides

A variety of approaches to miRNA knockdown via antisense oligonucleotides, generally called "anti-miRs" have been reported (reviewed in [133]). In particular, naked DNA oligonucleotides have been modified to increase stability, uptake, and binding to target sequences. By phosphothioate modification of the sugar backbone, the anti-miRs are considered degradation-resistant. In contexts in which complexing with transfection reagents is not practical (intravenous delivery), lipid moieties have been conjugated to the anti-miRs to improve cellular uptake. Lastly, binding to target sequences can be improved by nucleic acid composition. It has long been known that ribonucleic acid (RNA) binding to RNA exhibits a stronger strength of hybridization than does deoxynucleic acid (DNA) binding to DNA, with hybrid pairs showing intermediate

melting temperatures (Tms). In collaboration with Integrate DNA Technologies, we designed and tested locked-nucleic acid modified oligonucleotides. Locked nucleic acids (LNA) are a chemically synthesized nucleic acid structure that does not occur in nature. The 2'C is linked to the 5'C via an O-methyl bridge, which stabilizes the sugar ring, hence the term "locked". Importantly for biologists interested in hybridization applications, the strength of binding between LNAs and other nucleic acids is greater than RNA:RNA binding, allowing more stable interactions at lower temperatures. For example, for the sequence antisense to mature miR-34a 5'acaaccagctaagacactgcca 3', at 115 mM salt, Exiqon, the company holding copyright on LNA production, predicts the following melting temperatures. For 22 DNA nucleotides the Tm is 66 °C; if every third nucleotide is an LNA in a background of DNA nts (7LNA+15DNA), the Tm is 80 °C (http://lna-tm.com/). The IDT-designed anti-miRs we used were both one-third LNA, two-thirds DNA, and also phosphothioate modified. We transfected them into HEK-293 cells, and found we could rescue FIV-GFP-miR mediated repression of the luciferase-target reporter constructs (Figure 27). However, transfection into NPCs is known to be difficult, and in fact, we did not observe any decrease in miR levels after transfection of a wide dose range of anti-miR into NPCs with either of two transfection reagents tested (data not shown).

3.2.2.2. Si-miRNA constructs

Since knockdown of miRNAs in NPCs by the most commonly used reagent, anti-miRs, was not effective, I planned a knockdown strategy that would depend instead on a viral vector delivered reagent. In their paper describing miRNA target profiling by identification of polyribosome-associated transcripts, Nakamoto *et al.* [134] required stable knockdown of the miRNAs of interest. They developed an shRNA which produces a mature sequence antisense to the loop region of the target pre-miRNA. In this way, they decreased expression of the target mature miRNA. I used a vector in which the

U6 promoter drives the “miR-30 shuttle”, a commonly used and well-described shRNA vector system, to express a 94 nucleotide long sequence directed against the miR-182 loop (Figure 28**)**. The cleavage sites in the miR-30 hairpin have been very well characterized [135], allowing replacement of the mature sequences with other sequences of interest, and increasing the likelihood of Dicer cleavage releasing the intended mature siRNA. I called this new vector U6-simi182. I then subcloned U6-simi182 into FIV-GFP at an MfeI site that occurs upstream of the GFP reporter expression cassette. At the time that this vector was cloned, it had been demonstrated that high-level miRNA expression and processing could be achieved by coupling the miR-30 shuttle to the RNA polymerase III driven U6 promoter [135]. I tested the U6-simi182 plasmid against the luciferase-182T reporter by co-transfection into HEK-293 cells. At the dose range tested (5ng to 100ng plasmid vector), simi182 did not rescue luciferase activity (Figure 29). It was not tested further.

3.3. Analysis of miRNA function in NPCs

Having developed reagents to modulate miRNA levels in NPCs, I proceeded to tests of the effects of those reagents on key miRNA functions. To further implicate miRNAs in differentiation, I first assessed expression pattern: both cell types expressing the miRNAs in mouse brain *in vivo* and miRNA levels during NPC differentiation in culture. To extend understanding of the specific expression patterns of miR-34a and miR-182, I also investigated the transcription factors that may regulate their expression. I have also tested the effect of miRNA overexpression on NPC proliferation and differentiation in culture. Finally, to relate the neuromodulatory effects of miR-34a to known pathways functioning in neural differentiation, I tested the ability of miR-34a to repress some of the most relevant targets predicted by bio-informatic databases.

3.3.1. Mouse miR-182

As described above, and in Table 1, miR-182 is a brain-expressed miRNA with strong enrichment in the zebrafish eye. *In situ* hybridization in both embryonic zebrafish [28] and mouse eye [136] reveals an identical expression pattern for miR-182 and its genomic neighbors miR-183 and miR-96 with enrichment in the retina. We tested the hypothesis that these miRNA hairpins are co-expressed by using RT-PCR to amplify the region as one fragment. We were unable to amplify across the three hairpin locus in cDNA from mouse cerebellum, but we did confirm expression of miR-182, and confirm the co-linear expression of miRs 96 and 183 (Figure 30). The miR-182-96-183 cluster has recently raised interest in medicine because it is expressed in cochlear hair cells in the inner ear ([137]). Furthermore, a single nucleotide polymorphism in *Serotonin receptor IB* ablates a miR-96 binding site and is correlated with increased aggressive behavior [138]. I first tested the levels of miR-182 in NPCs during early differentiation time points in culture. I found that miR-182 levels rise, peaking at thirty minutes, and return to baseline within an hour (Figure 31).

In order to predict which transcription factors might regulate expression of miR-182, I presented a 7kb segment of genomic sequence in the putative regulatory region (5kb upstream and 2 kb downstream of the hairpin) to the rVISTA search engine [139]. This web-based utility searches for highly conserved sequence based on regions of homology between species (here, mouse and human), then looks for known transcription factor binding motifs within these regions. The logic goes that conserved regions are likely to be functional, so we can turn first to those sequences in a search for regulatory elements. The database of transcription factor binding motifs is based on a position-weight matrix assembled in the TRANSFAC database [140]. In this way, I identified Pax6 and BACH2 as candidate transcription factors that may regulate miR-182 levels (Figure 32)**.**

Next, I wanted to learn how miR-182 impacts cellular phenotypes relevant to neural differentiation. First, I tested the effects of miR-182 overexpression on NPC proliferation. I found that FIV-neoR-miR182 cultures did not grow well enough to permit further analyses. Five days after infection of 1 million cells, there were too few cells to count (<10,000) remaining in the culture. Control cultures had become thick with cells, numbering in the millions, by this timepoint.

Since they are co-expressed, I wondered whether these miRNAs might reinforce each others' activity. I compared the mature sequences, and noticed significant sequence homology (Figure 33).

3.3.2. Mouse miR-23b

miR-23b came to our attention initially in reports from Kawasaki and Taira [100], in which they describe the repression of the pro-neural gene hairy enhancer of split 1 (Hes1) by miR-23b, and also the glial localization of the miRNA after neural differentiation in culture. This work was later retracted due to data inconsistencies not related to this finding [141]. I assessed the location of miR-23b in adult mouse brain, revealing expression throughout the brain, especially in olfactory bulb, rostral migratory stream, deep cerebellar nuclei, and cerebellar folia (Figure 34). After miR-23b overexpression in NPCs, I differentiated cells and used immunostaining combined with morphological characteristics to identify neurons and glia. I found that neuron production was decreased in miR-23b overexpressing cultures compared to control (Figure 35 n=10 fields counted for control, 5 fields counted for miR-23b, $p=0.008$, Student's t-test).

3.3.3. Mouse miR-34a

3.3.3.1. Review of recent data and profiling work provides additional evidence for miR-34a as a candidate regulator of differentiation

miRNA (miRNA) profiling studies have defined strongly expressed brain-enriched miRNAs and their regional localizations. For example, miR-124a is robustly expressed throughout the brain, while the miRNA cluster 183-96-182 is remarkable for its specific localization to neurosensory tissue [136]. Functional studies have defined the roles of some highly expressed miRNAs in neurons and neural tissue [86, 89, 103, 113, 142]. However, *in situ* hybridization in developing zebrafish suggests that other miRNAs are expressed in intriguingly specific patterns in the brain [28]. Recent deep sequencing and more exhaustive cloning studies [38, 143, 144] may suggest why these other miRNAs have not been further investigated: several of them are expressed at such low levels that they passed under the radar of many earlier profiling analyses [36, 145-152]. For example, in one study, miR-34 was cloned three times when miR-124a was cloned 59 times [146]. However, it seems likely that low-level expression and small changes in miRNA levels may have significant functional consequences.

miR-34a is a case in point: its expression is low throughout the body in profiling studies. In fact, it was expressed weakly enough to escape notice in many studies to date, but the difference between weak expression and none at all is critical: loss of miR-34a in non-small cell lung cancer is associated with worse pathologic grade and worse prognosis [153]. Furthermore, re-expression in mouse tumor models was sufficient to significantly decrease aberrant cell proliferation and decrease tumor size [154-157]. Interestingly, expression profiling in developing zebrafish suggests that the strongest expression of miR-34a is not in lung or gallbladder, where it is now known to play an anti-tumorigenic role, but in the central nervous system (CNS) [28, 158]. Furthermore, miR-34a

expression is regulated by both the Notch and Hedgehog signaling pathways in zebrafish [159]. The enrichment of miR-34a expression in the developing brain together with its well-demonstrated role in cell cycle control led us to investigate its role in neural commitment. We reasoned that miR-34a might function similarly in brain and promote cell cycle exit. In this manner, miR-34a could facilitate acquisition and/or maintenance of mature cellular fates.

3.3.3.2. Results of miR-34a functional analysis

miR-34a shows conservation of the mature miRNA sequence in human, mouse, fish, and fly. There is only one nucleotide variation between vertebrates and *Drosophila melanogaster*. Based on the strong enrichment of miR-34a expression in the zebrafish CNS with respect to non-nervous tissue, we predicted expression in the developing mouse brain. To test this, we performed *in situ* hybridization on brain tissue at e16.5, a timepoint during cortical neurogenesis (Table 4). We observed miR-34a signal in the NPC niche surrounding the lateral ventricle with less expression in the cortical lamina**.** We also found miR-34a signal in the hindbrain in the external granular layer of the developing cerebellum (data not shown)**.**

To test whether miR-34a expression is maintained in the cells that arise from these embryonic neural progenitors during animal aging, we performed *in situ* hybridization on adult mouse brain sections. miR-34a is expressed in cortical neurons (Figure 36 A,B) and cerebellar Purkinje cells (Figure 36 C,D) in the mature brain. However, we did not observe expression in the subventricular zone (Figure 36 E), where adult neural progenitor cells reside before migrating to commit to the interneuron fate. To confirm that miR-34a expressing cells in the cerebral cortex were neurons, we co-labeled cells by *in situ* hybridization (to detect miR-34a) and immunostaining (to detect the mature neuronal marker NEUN) (Figure 37). We observed significant co-localization

in the middle cortical layers, with few cells singly labelled by each marker. Few cells were labeled by miR-34a in the upper layers.

I also assessed miR-34a levels by qRT-PCR during the onset of differentiation in culture. I found a rapid decrease in miR-34a levels, with a significant decrease after 5 minutes (Figure 38).

Based on our observation that miR-34a is expressed in the differentiating neuronal lineage, we tested if miR-34a can impact differentiation. We infected cultured NPCs to overexpress either miR-34a or a control hairpin. We then plated the cells in differentiation-promoting conditions. Five days later, immunocytochemistry and cell morphology were used to identify neurons and glial cells (Figure 39). Cell counts revealed a decrease in the neuron/glia ratio ($p<0.01$, Student's t-test).

To investigate the mechanism of the observed neuron loss, we first looked at cell cycle regulation. Dysregulation of cell cycle has been observed in a variety of cell types following changes in miR-34a levels (reviewed in He *et al.* [160]). First, we assessed the distribution of unsynchronized cells through the cell cycle during differentiation *in vitro*. After chemical dissociation, cells were re-plated in proliferation or differentiation conditions. Under proliferation conditions, miR-34a overexpression did not change secondary neurosphere number (Figure 40, $p=.25$ Student's t-test), or distribution of cells through the cell cycle (Figure 41, $p>0.05$, Student's t-test). However, secondary neurosphere size was slightly reduced (Figure 40, Median size was 136 vs. 160 pixels, $p<0.001$, Mann-Whitney rank sum test), suggesting a defect in either cell proliferation or survival.

To test the ability of miR-34a to effect changes in cell cycling during differentiation, we sought a mechanism to effect slightly higher levels of miRNA overexpression. For this reason, we tested another expression vector in which the miRNA hairpin is expressed from an independent U6-promoter driven expression cassette located upstream of the reporter gene (FGUM, shown in Figure 19). This vector

expresses reporter, as measured by green fluorescence in infected NPCs (data not shown), and slightly higher levels of miRNA, as measured by qRTPCR on infected NPC RNA (Figure 25).

Also, during differentiation, there was a subtle but significant decrease in the percent S phase nuclei at five hours (Figure 41, $p<0.01$, Student's t-test).

To assess the molecular mechanism(s) of miR-34a action, we tested if miR-34a reduces expression of a target cell cycle controller in NPCs, similar to what was found in cancer cells [160]. By RT-PCR, we confirmed expression of many putative miR-34a targets in this system (Figure 42). Western blot revealed that miR-34a over-expression impacts CDC25A levels (Figure 44). Interestingly, although RRAS, CDK2, CDK4 and E2F5 are expressed in NPCs, and are predicted targets, we did not find changes in their levels of protein expression upon low-level miR-34a over-expression (Figure 44 B).

We also tested a set of brain-specific targets predicted by Targetscan.org [161]. Several genes in the Notch pathway are predicted targets of miR-34a, including the pro-differentiation factors *Delta*, *Numbl*, *NeuroD1*, and *Mash1*, and the anti-differentiation factors *Notch* and *Cbf1* (Figure 43). We found that NUMBL and NEUROD1 are indeed decreased with overexpression of miR-34a in cultured NPCs (Figure 44). We confirmed the direct repression of *Numbl* by miR-34a using a luciferase reporter assay (Figure 45, $p<0.001$, One-way ANOVA, Holm-Sidhak pairwise comparison). The *Numbl* 3' untranslated region (UTR) contains two predicted binding sites for miR-34a. We used site-directed mutagenesis to ablate either the first or the second binding site in the luciferase reporter plasmid, and subsequently challenged these reporters with miR-34a over-expression. We found that ablation of the either binding site abrogated repression by miR-34a (Figure 45, no significant difference, One-way ANOVA, Holm-Sidhak pairwise comparison). The data suggest that the two target sites likely cooperate to effect miR-34a-mediated repression of *Numbl*.

Using the prediction method described above for miR-182/96/183, I developed a list of transcription factors that might regulate transcription of miR-34a (Figure 46**)**. At the time that I began these studies, no information was available about transcription of this intergenic miRNA. So, as described above, I first considered transcription factor binding sites 5kb upstream and 2kb downstream of the miR-34a hairpin using the rVISTA database. Based on this search strategy, I predicted that *Pax6*, a critical transcription factor during neural development, might regulate miR-34a levels. *Pax6* is a reasonable candidate because it is expressed in neural progenitor cells (in fact, it has been used as an NPC marker), and its loss in mouse (small eyes; *Sey*) leads to neurodevelopmental defects (reviewed in [162]). Particularly well-described aspects of the *Sey* mouse phenotype are disruptions in the eye (micropthalmia with aniridia) and cerebellum (leading to ataxia). Human mutations have been identified in the *Pax6* gene leading to anterior segment malformations in the eye as well as loss of anterior commissure and changes in auditory cortex function. I used RT-PCR to amplify the two prevalent isoforms of *Pax6* from perinatal mouse brian RNA, and I cloned them into the pcDNA3.1 (Invitrogen) expression vector (Figure 47A). I verified expression of *Pax6* transcript from the vector by transfection into HEK-293 cells followed by RNA isolation and RT-PCR. Transfected but not untransfected cells expressed mouse *Pax6* mRNA (Figure 47B). Neither PAX6(5A) overexpression (data not shown) nor low dose PAX6 overexpression changed activity of luciferase-34T, but high dose PAX6 overexpression weakly increased luciferase activity, suggesting that PAX6 may repress miR-34a production (Figure 47C).

While this work was underway, several different groups identified miR-34a as the miRNA most responsive to levels of the tumor suppressor gene p53 [154-157]. As part of those studies, p53 binding sites that control miR-34a expression levels were identified more than 20kb upstream of the miR-34a hairpin in mouse and human. A short first exon near that binding site is followed by a very long exon and a short, miR-34a containing,

second exon. Though the cDNA is less than 2kb, the primary transcript is more than 20kb in both species. Based on this new data, I collected mouse genomic sequence surrounding the reported transcription start site, and subjected it to transcription factor binding site prediction (Figure 46**)**. I identified a putative binding site for PITX2, a homeodomain protein working in head and neck development [163]. Dysregulation of PITX2 levels leads to Reiger syndrome, a cause of developmental anomalies, the best characterized of which is dysgenesis of the anterior segment of the eye (reviewed in [164]). As described for *Pax6*, I cloned and overexpressed *PitX2* together with the luciferase-34T reporter. I did not observe any significant differences in luciferase activity (data not shown).

3.4. Discussion

The work described in this chapter began with selection of miRNA candidate modulators of neural development. I selected candidates based on the available data, and have characterized aspects of expression and function for three of those. In particular, miR-34a has been shown to work through multiple mechanisms to modulate neuron production in a cell culture model of neural differentiation.

3.4.1 Gain and loss of function approaches

Modulation of miR levels in NPCs was complicated by poor transfection efficiency in these cells. However, using viral vectors, I was able to deliver constructs that overexpress miRNAs of interest and report infection by GFP or neoR expression. Unfortunately, efforts to effect loss of miRNA function in NPCs were not successful. I first tried the most common approach in the field: anti-miR oligonucleotides. I tested transfection of this reagent at a large dose range (from the lowest doses shown effective in previous studies in the Davidson Lab (data not shown) to the highest doses shown to tolerated in cell culture). However, despite efficacy in transformed cell lines, I saw no difference in miRNA levels by qRTPCR. This result could be simply transfection failure,

which I think is most likely. However, it could also reflect a failure of anti-miR function in NPCs due to differential miRNA stability. It has been shown that miRNA levels can be quite stable in neural tissue [93, 97]. I also attempted shRNA vectors targetting precursor miRNAs. However, testing of the simi182 construct in HEK-293 cells did not rescue repression of the luciferase reporter. This result could be due to inadequate simi182 levels. Future studies could try increasing the plasmid amount (the maximum dose I tested was the moderate 100 ng/well). Also, production of the mature siRNA could be measured by small transcript Northern blotting. A third approach which should be tested in NPCs to reduce miRNA levels is the "miRNA sponge" in which a chain of target sites for a miRNA are expressed, in this case, from a viral vector [165]. Usually, the target sites are embedded in the 3'UTR of a reporter gene to allow both localization of vector delivery and also to see loss of the reporter upon miRNA binding. Expression of enough reporter/target-site fusion transcript will sequester mature miRNA, so acting as a "sponge", sopping up matched miRNA. However, since transfection in NPCs is difficult, vectors which infect at multiple copies per cell would be required.

3.4.2 miR-182

miR-182 expression increased transiently after the onset of differentiation in culture. It will be interesting in the future to consider levels of the co-expressed members of this transcript to learn whether or not processing is differentially regulated. The mature sequences of these miRNAs show intriguing similarity, suggesting possibly overlapping function.

3.4.3 miR-23b

Consistent with published data from cell culture studies, miR-23b was found to be expressed in astrocytes in mouse brain. Preliminary data suggests that miR-23b may increase proliferation of cultured NPCs. One recent study showed an opposite effect in a non-neural context, finding that the oncogenic factor C-MYC represses miR-23a/b in

order to increase cell proliferation. It will be interesting to see how further work relates the role of miR-23b in cancer to its expression in nervous tissue.

3.4.4. miR-34a

In the mouse embryo, miR-34a expression is enriched in both cortical and cerebellar NPCs and found at lower levels in neurons in the emerging cortical layers. Accordingly, in cultured NPCs, miR-34a levels fall rapidly with the onset of differentiation. However, expression persists in the cells derived from embryonic NPCs; most NeuN+ cells in the adult mouse cortex express miR-34a, and cerebellar Purkinje cells (products of the expressing cells in the embryonic hindbrain) represent the strongest expressing cells in the adult mouse brain. The strong expression in NPCs, and to a lesser extent, in the neurons they produce, led us to examine the role of miR-34a by miRNA overexpression. We found that miR-34a overexpression disrupts neuron production.

We reasoned that loss of neurons could reflect changes in the progenitor cell cycle, consistent with prior reports of miR-34a function in tumor cells. In transformed cell lines and mouse cancer models miR-34a functions as a p53 effector gene. miR-34a expression level correlates with tumor severity, and re-expression in inappropriately proliferating cells restores quiescence. Cell cycle progression in NPCs is intimately involved with the state of differentiation. The proliferative regions of the embryonic cortex, the ventricular zone (VZ) and the subventricular zone (SVZ), house multipotential neural stem and progenitor cells. Slow dividing stem cells give rise to progenitors and ultimately neuroblasts, which are committed to differentiation. Studies *in vitro* suggest that cultured NPCs recapitulate the *in vivo* progression [125]. Analysis of the *Tis21*-GFP mouse has helped to clarify the relationship between cell cycling and neural differentiation [126]. TIS21 is an immediate early gene expressed in cells that are still dividing, but are committed to the neuron fate. Transcription increases during the G1 phase of the cell cycle as NPC nuclei migrate away from the ventricular surface.

Examination of BrdU uptake in *Tis21*-GFP animals revealed a 20% increase in cell cycle length in differentiating (GFP+) vs. proliferating (GFP-) cells (19.1 vs. 14.8 hours). Importantly, the longer cycle was due to increased G1 transit time, and was not accompanied by a decrease in growth fraction (percent cells that are cycling). Also, G1 transit time was two hours longer in the more committed SVZ NPCs than in VZ NPCs.

In undifferentiated NPCs, over-expression of miR-34a (at levels 2-5 fold higher than endogenous expression levels) did not change self-renewal capacity or percent cells in S phase. And although CDC25A was reduced, other predicted targets of miR-34a, including RRAS, CDK2, CDK4, and E2F5, were unaffected. However, in differentiating cells, miR-34a over-expression had a subtle but significant effect on the rate of decline of cycling cells. While miR-34a did not potently inhibit proliferation as noted in rapidly dividing cancer cells, this small difference in slowly dividing, differentiating NPCs could contribute to the noted decrease in neuron production. Mathematical models of NPC proliferation and differentiation have been generated and tested *in vivo.* Caviness *et al.*[8] measured the effects of the 5% shift of cells out of G0/G1 in the p27KO mouse, which has a disabled G1 checkpoint. They found an 8% increase in cortical thickness and a 23% increase in the late formed layers at postnatal day 21. Therefore, the observed 2.5% change noted in our system may be sufficient to alter cell fate.

In addition to the effect on percent cells in S-phase, we found that miR-34a represses at least two targets in the Notch pathway. The small increase we effected in miR-34a levels was sufficient to decrease levels of Numbl and NeuroD1. These regulators of the Notch pathway are important for execution of asymmetric divisions, and so maintaining a balance between neuron production and progenitor cell maintenance. It is therefore not surprising that repression of these pro-neural genes would be associated with ultimate neuron loss, perhaps by premature depletion of the progenitor population.

In summary, we tested miR-34a as a candidate modulator of differentiation in mouse cortical neural progenitor cells. We found that small increases in miR-34a levels

in cortical neural progenitor cells resulted in decreased neuron production after *in vitro* differentiation. The anti-proliferative role of miR-34a may allow moderate but not excessive proliferation, but the subtlety of the changes in cell cycle we observed suggests that the mechanism of miR-34a action in the developing nervous system is likely multifactorial. Our findings fit with a model in which tight regulation of miR-34a levels (perhaps by p53, as in other tissues, or by NOTCH and HEDGEHOG pathways, as demonstrated in developing fish) allows appropriate cell division, and a ratio of symmetric and asymmetric divisions by committing neuroblasts.

3.5. Methods

3.5.1. Animal Husbandry

C57BL/6J mice were purchased from The Jackson Labs or bred in house. Animals were housed in the University of Iowa Animal Care facilities, and maintained on a 12h:12h light:dark cycle. For timed matings, one male and one to three females were co-housed in the male's home cage from one afternoon until the next morning. We defined noon on the day the animals were separated as embryonic day 0.5.

3.5.2. Euthanasia

For *in situ* hybridization studies and NPC preps, pregnant dams were over-anaesthetized with 0.2ml/g of a 1% ketamine/10% xylazine mixture, then cervical dislocation was performed. Embryos were rapidly removed and decapitated.

3.5.3 Animal Care

All experiments were approved by the University of Iowa Animal Care and Use Committee, and procedures were performed in accordance with those guidelines.

3.5.4. In situ hybridization

Heads were fixed for four hours at 4 °C in 4% paraformaldehyde, then frozen in OCT on a dry-ice ethanol slurry. Twelve micron sections were cut on a cryostat microtome (Microm, Walldorf, Germany) and transferred to SuperFrost Plus slides (Sigma, Saint Louis, MO) using the CryoJane adhesive system (Instrumedics, Saint Louis, MO). Slides were stored at -80 °C for up to three months. Slides were allowed to warm to room temperature and dry for 10 minutes, then fixed in 4% paraformaldehyde for 20 minutes at 25 °C. Slides were washed 3 times for 5 minutes each in PBS with shaking, dried on a slide warmer for 10min, and washed again 3 times for 5 minutes each in PBS. Sections were dehydrated through an ethanol series (70%, 90%, 100%), then air dried for 15 minutes. Sections were acetylated by a 3 min wash in triethanolamine solution (1.32% triethanolamine, 0.5% HCl in water) and 10 minutes in acetic anhydride solution (0.22% acetic anhydride in triethanolamine solution). After one rinse in PBS, sections were prehybridized at 55 °C for 30 minutes - 2 hours in a humid chamber with pre-hybridization buffer from the mRNA locator kit (Ambion, Austin, TX). LNA-modified DNA oligonucleotide probes antisense to the mature miRNA sequence were purchased (Exiqon, Denmark) and tailed with digoxigenin-UTP/UTP mixture using the Digoxigenin 3' tailing kit (Roche, Indianapolis, IN) according to the manufacturer's protocol. We diluted the probe 1:100 in pre-warmed hybridization buffer (mRNA locator kit), incubated 5 minutes at 65 °C to decrease viscosity and improve mixing, then vortexed and centrifuged briefly to collect. We added the hybridization buffer/probe mixture to the sections and incubated at 55 °C overnight. We washed off the hybridization buffer in 2X SSC with four 30 minute washes at 55 °C, then five washes for five minutes each in PBS/0.05% tween-20 (PBST) at 25 °C. Slides were blocked in 2% sheep serum, 2 mg/ml BSA in PBST for 1 hour at 25 °C, then sheep anti-DIG AP Fab fragment (Roche, 1:500) was used in blocking buffer at 4 °C overnight in a humid chamber. Slides were washed five times five minutes in PBST, then 3 times 5minutes in

AP buffer pH 9.6 (100mM Tris-HCl, 50mM MgCl2, 100mM NaCl, 0.1% Tween-20). Color was developed with NBT/BCIP One-touch Solution (Pierce #34042, Rockford, IL). Slides were incubated in a humid chamber at 25 °C in the dark**,** with monitoring every 10 minutes until background signal was barely visible. The slides in each experiment were developed to a single stopping time, then washed briefly in PBS and mounted.

3.5.5. Microscopy

Images were captured by using an Olympus BX60 light microscope (Olympus, Center Valley, PA) and DP70 digital camera, along with an Olympus DP Controller software. Overlays were performed using Photoshop CS3 (Adobe, San Jose, CA) "screen" function.

3.5.6. Neural progenitor cells

Embryonic mice were collected at E15.5-16.5 as described above. Embryos were rinsed in PBS with 2% glucose (PBSG), then decapitated. Brains were removed, whole cortex isolated and diced, then triturated in PBSG using cotton-stuffed sterile glass Pasteur pipettes. The solution was transferred to 15mL falcon tubes and diced tissue was allowed to settle. The supernatant was transferred to a fresh tube. NPC maintenance media (Stem Cell Technologies, Vancouver, Canada) was added to the remaining tissue pieces, which were again triturated to dissociate more cells. This procedure was repeated five times, then the remaining tissue pieces were discarded, and the supernatant was centrifuged at 800 rpm at 4 °C for five minutes. A cell pellet was easily discerned, and the clear supernatant was discarded and replaced with ~30 ml fresh maintenance media. Cells were plated into T- 150 filter flasks at a density of 2 X 10^6 cells / 100 ml. Cells were allowed to grow for approximately five days into medium-sized neurospheres in tissue culture incubators at 37 °C and 5% CO_2. They were then used for experiments or passaged. All cells used for experiments had been passaged six or fewer times.

For differentiation experiments, neurospheres were dissociated using HyQtase (HyClone, Logan, UT) for fifteen minutes at 37 °C followed by gentle mechanical trituration. They were then centrifuged at 800 rpm at 4 °C for five minutes, then resuspended in NPC differentiation media (Stem Cell Technologies) or IGF media (DMEM/F12 (Hyclone); 1% penicillin/streptomycin; 1% l-glutamine; 1% FBS; .03% dextrose; 20 ng/mL insulin-like growth factor-1 (Sigma)). For timed differentiation experiments, "zero" minutes is defined as the time at addition of the differentiation or IGF media. Cells were then plated on poly-L-ornithine coated tissue culture plates or glass chamber slides. For NPC infections, 1 X 10^6 cells/well were plated in 12 well tissue culture plates (Costar) and virus was added at a multiplicity of infection (MOI) of three. Cells were transferred to a T-25 flasks with 8 mL of NPC maintenance media 18-24 hours later and cultured for 3 days to medium-sized neurospheres.

For transfection, cells were plated at 1 million cells / mL in optimem reduced serum media (Gibco) in 12 well tissue culture plates (Costar), and exposed to transfection complexes (mixed according to Manufacturer's instructions) for two hours. Cells were then diluted to 10 mL maintenance media, and cultured for two days before RNA collection.

3.5.7. qRTPCR:

Total RNA was collected from cells using Trizol (Invitrogen, Carlsbad, CA) according to the manufacturer's instructions. RNA quantity and quality was measured using a ND-1000 (Nanodrop, Wilmington, DE). For miRNANA qRT-PCR, 140 ng/sample was reverse transcribed using reagents from the High Capacity cDNA Archive kit (Applied Biosystems, Foster City, CA) and miR-34a microRNA assay (Applied Biosystems part number 4395168) according to the Applied Biosystems protocol except that RT primer was used at half the recommended concentration. Samples were diluted 1:3 with water, and one sample was used to make a standard curve, then 1.33 ul/sample

was used in a 20 ul qPCR reaction in triplicate according to the manufacturer's instructions except that the qPCR primer was used at half the recommended concentration. The results reported are the mean of three biological replicates for each point.

3.5.8. Vectors/Plasmids:

Lentiviral vectors with the miRNA expressed from the 3'UTR of the reporter have been previously described (Harper 2006). We also used a lentiviral vector with a mouseU6-miRNA34a-polyT cassette cloned into the MfeI site upstream of the CMV promoter in those vectors as an alternative to expression from the 3'UTR. Viral vector production was done by triple transfection according to standard protocols in the University of Iowa Gene Transfer Vector Core. Vectors were pseudotyped with the VSVG envelope protein and titered at 1-6 X 10^8 transducing units/mL. The luciferase reporter constructs are based on psi-check2 (Promega, Madison, WI) and cloned as described previously (Harper 2006).

3.5.9. RT-PCR

Total RNA was collected from NPCs using Trizol extraction (Ambion), and reverse transcribed using Superscript III according to the manufacturer's instructions for oligo-dT extension (Invitrogen). PCR was done according to standard protocols at 30 cycles with Taq polymerase (Bioline).

3.5.10. Small transcript Northern blotting

Small RNA was extracted using a mirVana miRNA isolation kit (Ambion), and 900 ng was loaded on a 15% acrylamide-bisacrylamide (19:1) gel containing 8 M urea (48%, wt/vol) and 1x Tris-borate-EDTA. The decade marker (Ambion) was radiolabeled using the manufacturer's protocols and diluted 1:50, and 2.5 µl was loaded on the gel as a size reference. DNA oligonucleotides (1 and 0.1 pmol) containing shLacZ guide strand

sequences were loaded as positive controls. Following a 30-min pre-run, electrophoresis proceeded at 20 mA until the bromophenol blue loading dye reached the gel halfway point. RNA was then electrotransferred (Bio-Rad Transblot SD) to Hybond N^+ nylon membranes for 45 minutes at 200 mA in 0.5x Tris-borate-EDTA, and then membranes were UV cross-linked (Stratalinker; Stratagene). Following overnight prehybridization, the blot was hybridized overnight in ULTRAhyb-Oligo hybridization buffer (Ambion) at 36 °C with a ^{32}P-end-labeled (Ready-To-Go T4 polynucleotide kinase; Amersham) oligonucleotide probe that detects the active guide strand of miR34a RNA. The blot was then washed in 2x SSC (1x SSC is 0.15 M NaCl plus 0.015 M sodium citrate) and exposed to film (Kodak BioMax MS).

3.5.11. Immunoblotting

Protein was collected in RIPA buffer with freshly diluted protease inhibitor (Complete Protease Inhibitor, Roche). Samples were quantified using a colorimetric assay vs. a BSA standard curve (DC Protein Assay, Bio-rad). SDS-PAGE was executed using 4-20% gradient gels (Biorad), and samples were transferred to PVDF at 100V for 75min at 4 °C. Block was for 1 hour in PBS, 0.05% Tween-20, and 2% milk. Antibody incubation was in blocking solution at 4 °C overnight. Antibodies were GFP (rabbit anti-GFP, Molecular Probes), CDC25A (rabbit anti-CDC25A, Abcam, 1:500), NUMBL (rabbit anti-NUMBL, Abcam, 1:1000), NEUROD1 (rabbit anti-NEUROD1, Chemicon, 0.5ug/mL), BETA-ACTIN (mouse anti-BACTIN, Sigma, 1:5000).

3.5.12. Luciferase Assays

For luciferase assays, lentiviral vector shuttle plasmids and luciferase reporter constructs at a ratio of 8ng:1ng were transfected into HEK-293 cells using lipofectamine 2000 accordingly to the manufacturer's instructions. Lysates were collected 18-24 hours after transfections and luciferase activity was measured using the dual-luciferase kit (Promega) according to manufacturer's instructions and the Monolight 3010C

Luminometer (Becton Dickinson, Franklin Lakes, NJ). For NPC infections, 1 X 10^6 cells/well were plated in 12 well tissue culture plates (Costar, Lowell, MA) and virus was added at a multiplicity of infection (MOI) of 3. Cells were transferred to a T-25 flasks with 8mL of NPC maintenance media 18-24 hours later and cultured for 3 days to medium-sized neurospheres.

3.5.13. Flow cytometry:

For GFP measurement, cells were trypsinized, pelleted by centrifugation at 1,000 rpm for 5 min, and resuspended in phosphate-buffered saline at a concentration of 10^6 cells/ml. Cells were then filtered (Falcon 2350 mesh filters), stained with propidium iodide (1 µg/ml final concentration), and run on a Becton Dickinson FACScan instrument in the University of Iowa Flow Cytometry Facility. Gating and compensation were set using GFP-positive and GFP-negative cells with and without propidium iodide. The percentage of live GFP-positive cells and mean fluorescence intensity were determined by comparing infected cells to uninfected, GFP-negative samples. FIV.GFPmir21 data are reported as means from two separate FIV infections.

For DNA content analysis, cells were collected by centrifugation and nuclear DNA stained by resuspension in hypotonic solution containing propidium iodide (Krishan, 1990). DNA content analysis with doublet discrimination was performed on a Becton Dickinson FACScan in the U of I Flow Cytometry Facility (http://www.healthcare.uiowa.edu/corefacilities/flowcytometry/). Cells in G1/G0, S, and G2/M phases were quantified from this data by curve fitting using Modfit software (Verity Software House, Topsham, ME).

3.5.14. Immunocytochemistry:

NPCs were differentiated according to standard protocols (Reynolds and Weiss, 1992). After five days, cells were fixed in 4% paraformaldehyde for 20 minutes at 25 °C, then blocked for 30 minutes in 0.05% Triton-X-100, 5% goat serum, PBS. Primary

antibody incubation proceeded at 4 °C overnight to detect neurons (anti-MAP2 antibody, 1:200, Sigma), glia (anti-GFAP-Cy3 antibody, 1:5000, Sigma). Secondary antibody incubation was at 25 °C for 1 hour.

3.5.15. Neurosphere formation assay

After neurosphere formation, infected cells were selected for expression of the neoR gene using 500 ug/ml G418 (Gibco/Invitrogen; Carlsbad, CA) for three days. Surviving NPCs were mechanically dissociated and plated at equal density in 96-well plates. After seven days, number of neurosphere per plate and average neurosphere size were measured in the FIV-CMV-neoR and FIV-CMV-neoR-miRNA34a infected cells using Image J software (Rasband, 1997-2008).

3.5.16 Statistics

Statistical analyses was done using Sigmastat software (Systat, San Jose CA). For comparisons among multiple groups, one-way ANOVA was performed followed by planned pairwise comparisons between relevant groups using Holm-Sidak. Unpaired Student's *t* tests were used for comparisons between two groups.

Table 3 miR candidates selected in 2004 based on available data.

miRNA	Location (fish)	Other expression data	Predicted targets of note
miR-9 (3)		Brain-enriched in human [35]; peaks late in mouse embryo [147, 166]; less in presenilin null brain (has less notch, overgrows, then underdevelops) [166]; in rat neurons [167]; up with neuronal diff. in culture [168].	Id2, cadherin, Kchannel, fmr1, nmdaR, 5htR
miR-17 (1)		Highly expressed in rat embryogenesis, drops in adult [147]	APP, Ataxin1, slitRK3, mnyc, ngn2
miR-21 (1)		Not in neural tissue in adult mouse [169]; found in 2 mouse cell lines [170] up with mouse ES cell diff. [171]	Hox genes, Map2, synaptotagmin, ataxin2 bp, sema4b, protocadherin
miR-22 (1)		In several organs [145]; in mouse neuronal cell line [170]; gets A to I edited [172]	14-3-3, schwannomin, cadherin20
miR-23b (a,b; 1)			**May repress Hes1 [100, 141]**
miR-30 (a-e)		High, brain-enriched [145]; cloned from rat neurons [167]. Another study: not brain-enriched but increases with neural diff. in culture [168].	Homer, K channels, sema7a
miR-34a (a-c; 1)	**Hindbrain**	**Increases in worms [173] and flies [174] during development.**	**Notch and delta targets are shown by luciferase assay. [175] Several other Notch pathway members predicted**
miR-103 (2)		Enriched in cortex and cerebellum, very high in all tissues, not in HeLa cells. Gradual increase during development [35]; high in neurons [170]; found at sites of translation in neurons [146]; increases with neural diff. in culture [168]	Activity dependant neuroprotector, myelin proteolipid, ephrin, bdnf, neuroD

Table 3 continued

miR-124a (3)	Brain, spinal cord	Increases prenatally, stable postnatally [146], enriched in cortex and cerebellum [35, 147, 166]. 10X more in brain than elsewhere. Brain restricted [145, 176]. Up 13X from early to late corticogenesis [35]	Kchannel10, dcx, dystrophin releated protein, ryanodineR
miR-125b (a,b; 2)		Peaks in mouse at e21, brain enriched [177]	Myelin TF1, GABA-R theta subunit, plexinC1
miR128a,b (a,b)		Postnatal expression. Enriched in cortex, cerebellum [145, 166, 168, 177], more with diff. [35] enriched at site of neuronal translation [146]	Sema6d, neuron navigator, Dll1, ngn
miR149		Cloned from mouse heart [145] and rodent neurons [146]. Up in adult vs embryo [147]	Dullard, numbR, protocadherin
miR182	**Eye, identical pattern to miRs 96, 183.**	**Eye specific [176]**	**Bdnf, protocadherin8 sema3f, ngn**
Let-7			Dcx, neuroD1, hox genes, protocadherins,

Table 4. miR-34a enriched brain regions in e16.5 mouse

REGION	LEVELS
Ventricular zone	**+++**
Cerebral cortex	**++**
Ganglionic eminence	**+**
External granular layer (hindbrain)	**+++**

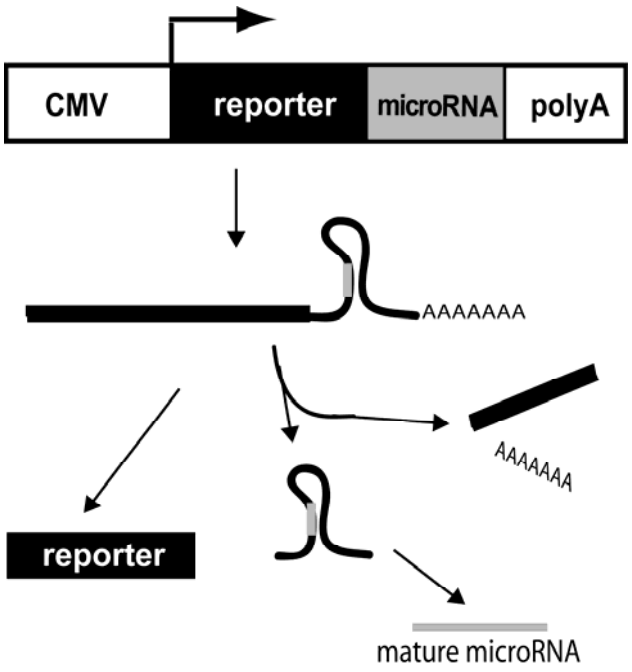

Figure 18. Design of viral vectors for microRNA overexpression in NPCs. A single transcript is expressed in which the miRNA hairpin is embedded in the 3'UTR of the reporter gene (GFP or neoR). Intact copies of the transcript serve as template for translation of reporter protein. Some copies are cleaved by the miRNA processing machinery, yielding mature miRNA.

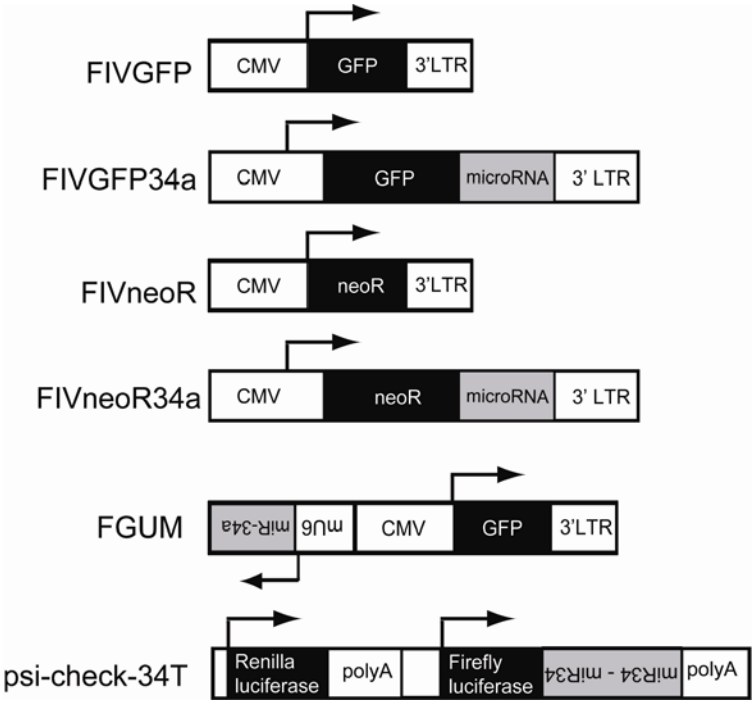

Figure 19 Cartoon showing construction of vectors used in this work.

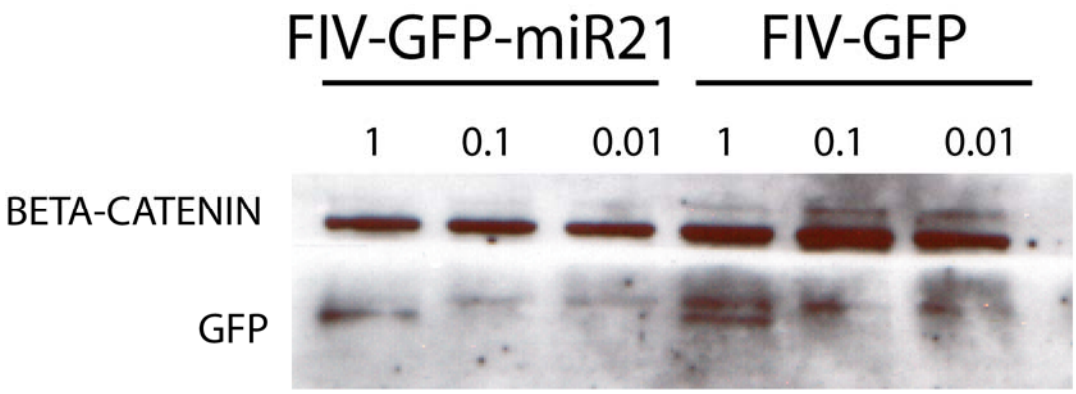

Figure 20. HT1080 cell lysates contain GFP after both reporter and reporter-miR infection. Viral supernatant was applied to HT1080 cells at doses shown (X10^-2). Two days later, cellular, protein was isolated, and GFP and the normalizer gene beta-catenin were visualized by western blotting. GFP is present is all the samples, with decreased levels in the FIVGFPmiR21 infected samples compared to the control FIVGFP infected samples.

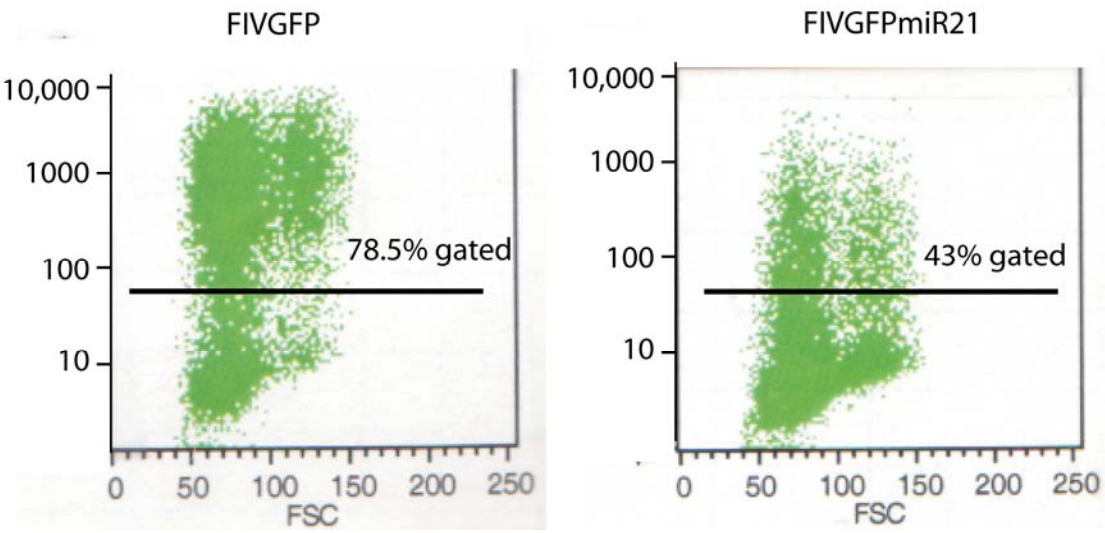

Figure 21. GFP positive cells were detected by flow cytometry in both FIVGFP and FIVGFPmiR21 infected HT1080 cells. However, fewer cells expressed detectable levels of GFP after FIVGFPmiR21 than FIVGFP delivery.

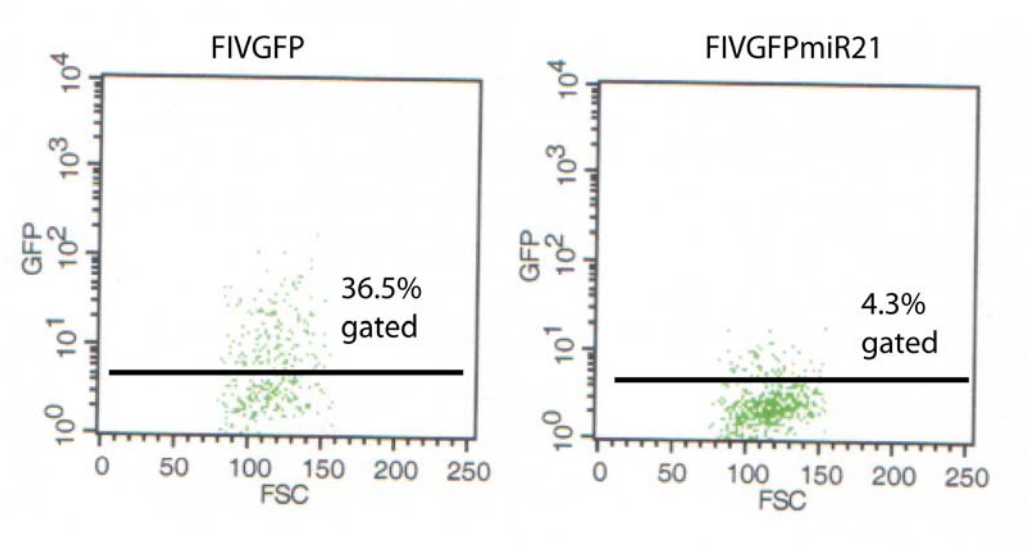

Figure 22. GFP positive cells were detected by flow cytometry in both FIVGFPmiR21 and control infected NPCs. However, fewer FIVGFPmiR21 infected cells than control expressed detectable levels of GFP.

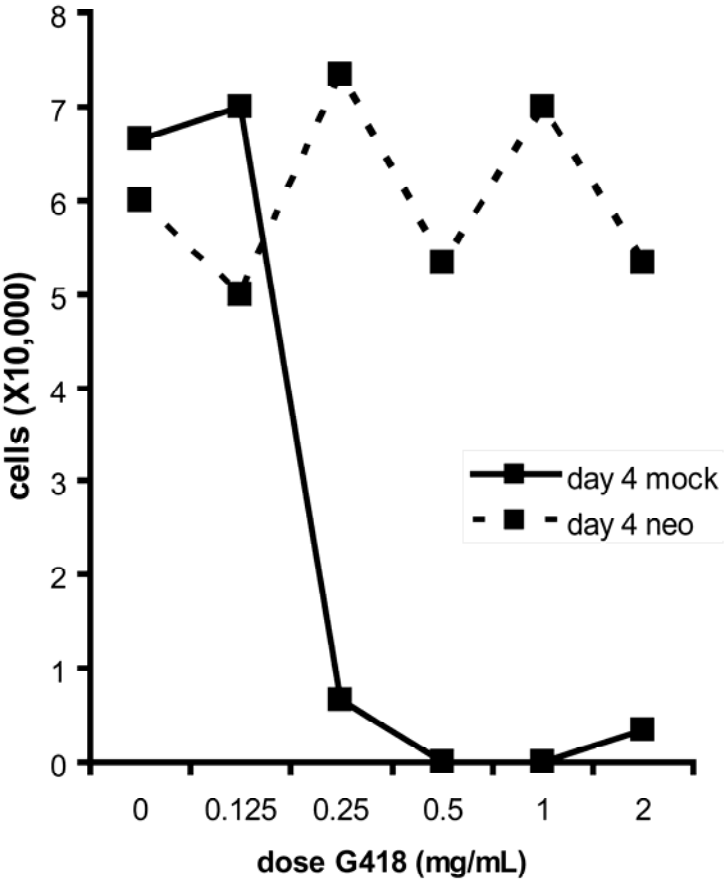

Figure 23.FIV neo and FIV-neo-miR vectors confer neomycin resistance in NPCs.

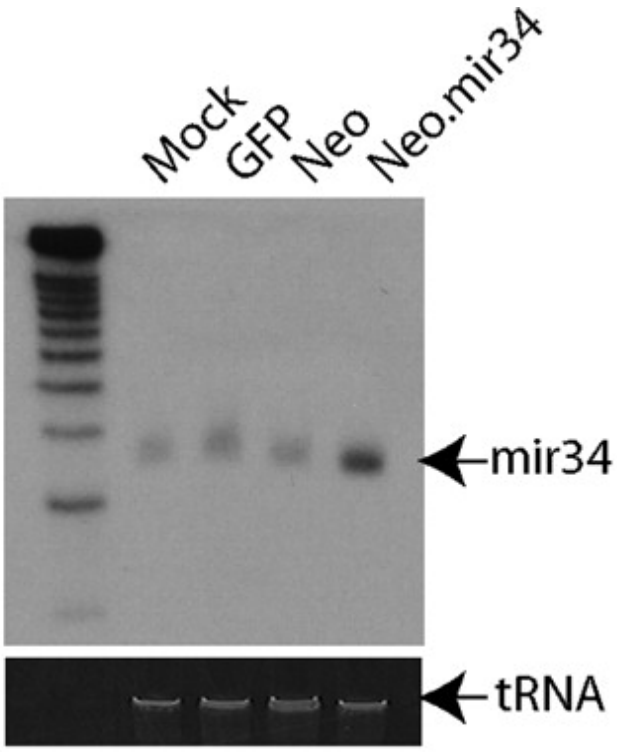

Figure 24. A representative small transcript Northern blot demonstrates production of miR-34a from the FIVneomir34a vector. The mature product is same size as the endogenous product seen in the first three (control) lanes. (This blot was performed, and figure designed, by Scott Harper.)

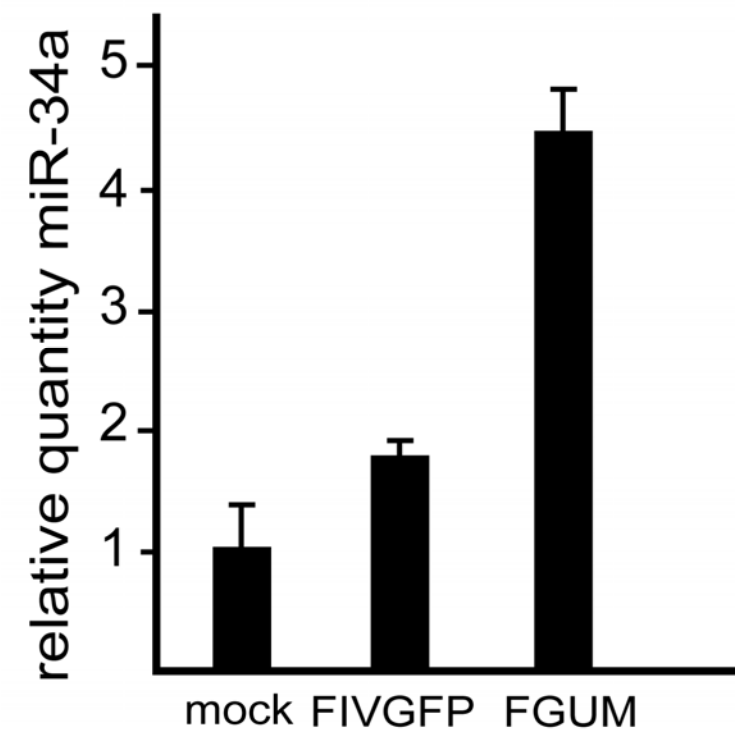

Figure 25 miR-34a is over-expressed at moderate levels 2-5 fold higher than mock in NPCs infected with lentiviruses as labeled.

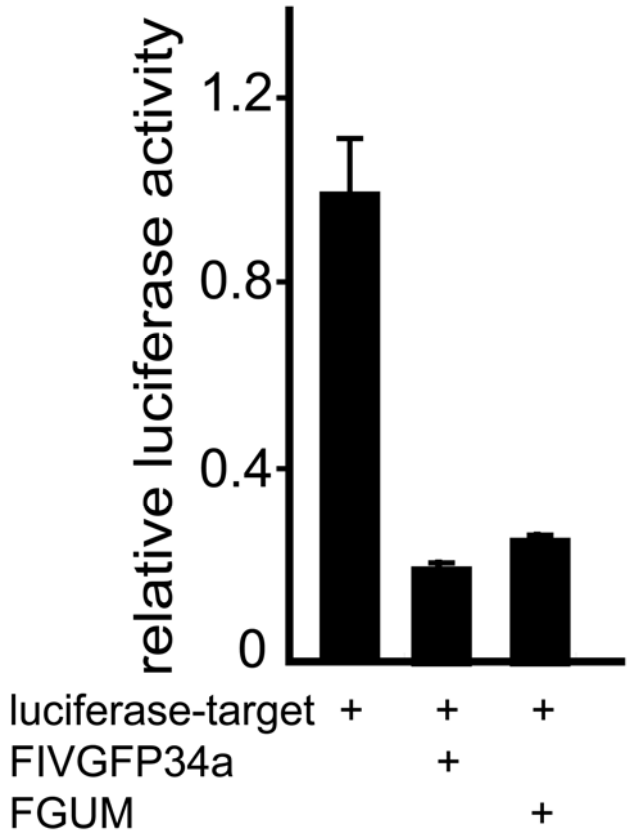

Figure 26. miRNAs produced by the FIV-reporter-miR vectors are active in a luciferase reporter system.

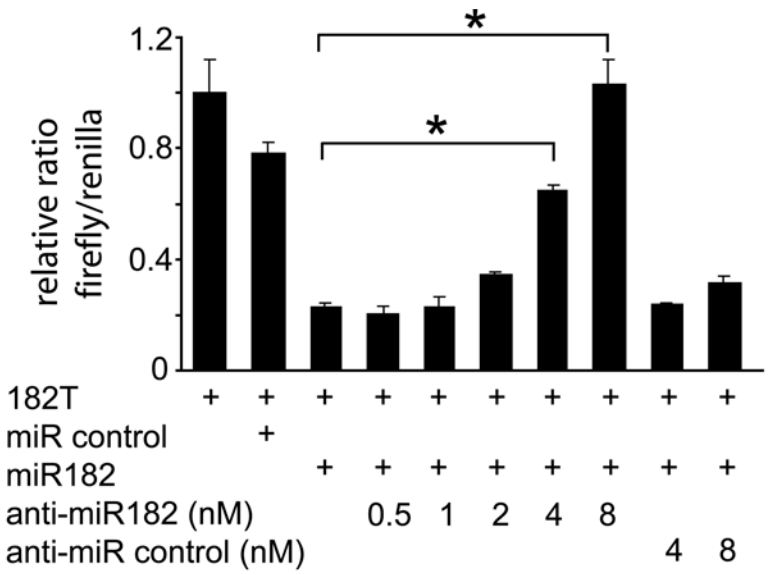

Figure 27. Anti-miR transfection into HEK-293 cells relieves miR-mediated repression of a luciferase reporter. ($p<0.05$, Student's t-test).

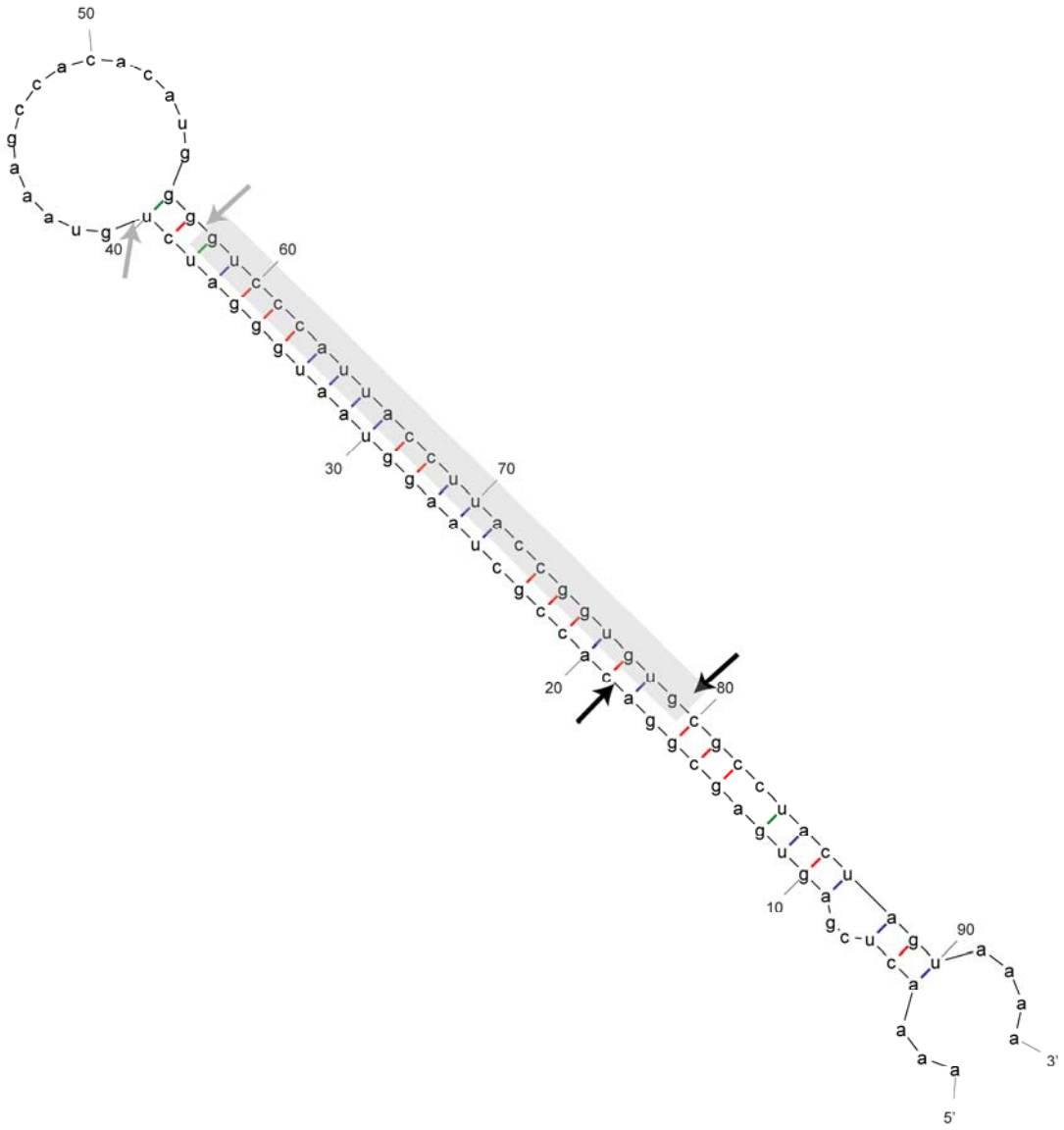

Figure 28. This cartoon of the shRNA designed to target the precursor miR-182 shows several key aspects of the miR-30 shuttle. It was adapted from a predicted structure of our designed seququence from the mFOLD software maintained by Mark Zucker (http://mfold.bioinfo.rpi.edu/). Black arrows mark the expected Drosha cleavage sites. Gray arrows mark the expected Dicer cleavage sites. Based on these predicted cleavage sites, the gray shaded region is region and strand expected to be loaded into the RNA-induced silencing complex (RISC). This sequence is perfectly antisense to pre-miR182 sequence spanning and extending beyond the loop.

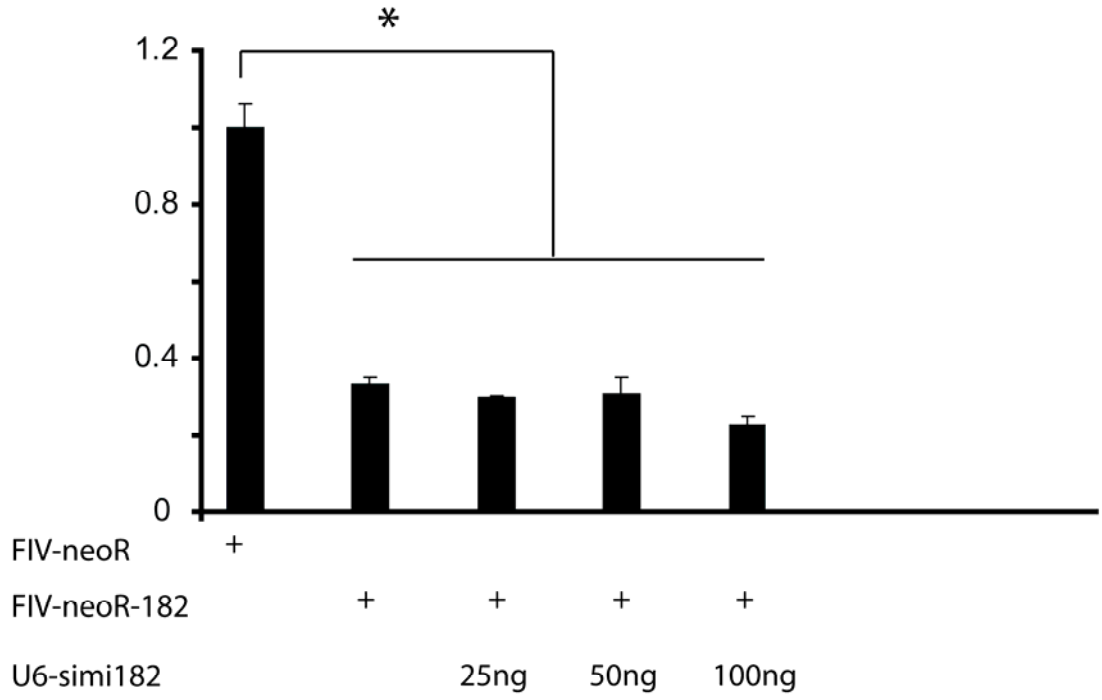

Figure 29. Transfection of U6-simi182 into HEK-293 cells did not rescue miR-182 mediated repression of the luciferase reporter. One way ANOVA with Bonferroni post-hoc noted that all of the FIV-neoR-182 transfected wells repress the luciferase reporter compared to the FIV-neoR samples, $p<0.05$. However, there were no significant differences between the transfection of FIV-neoR-182 alone or with any of the U6-simi182 doses tested.

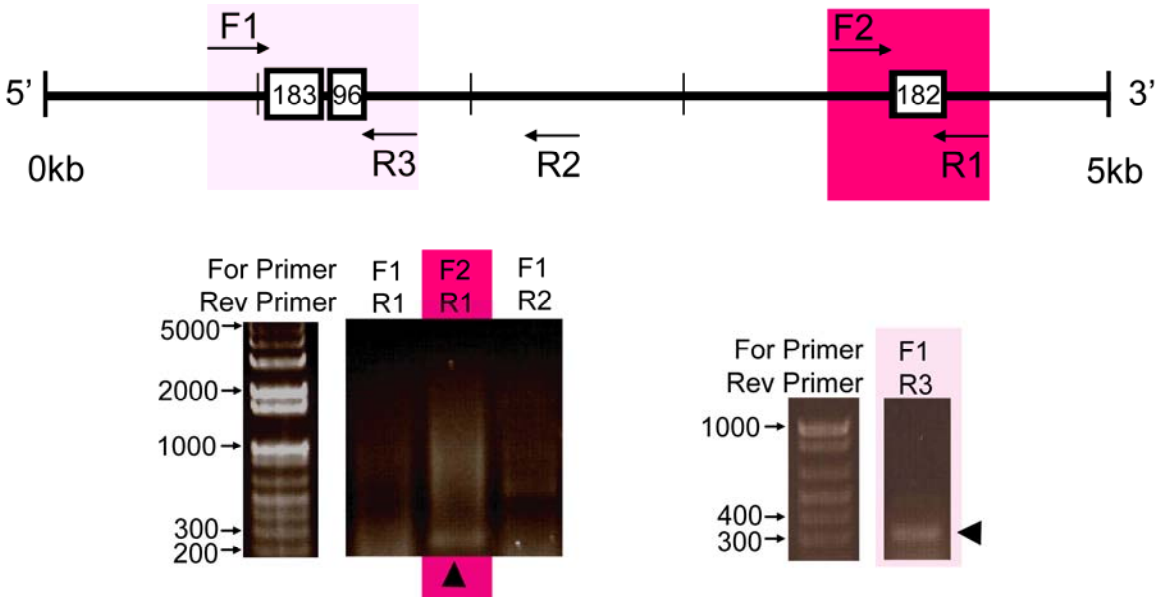

Figure 30. Cartoon showing genomic locus encoding the miRNAs -182, -96, and -183. We used RT-PCR to confirm expression and to test for collinear expression in mouse cerebellar cDNA. All three miRs were detected, the colinear expression of miRs -96 and -183 was demonstrated.

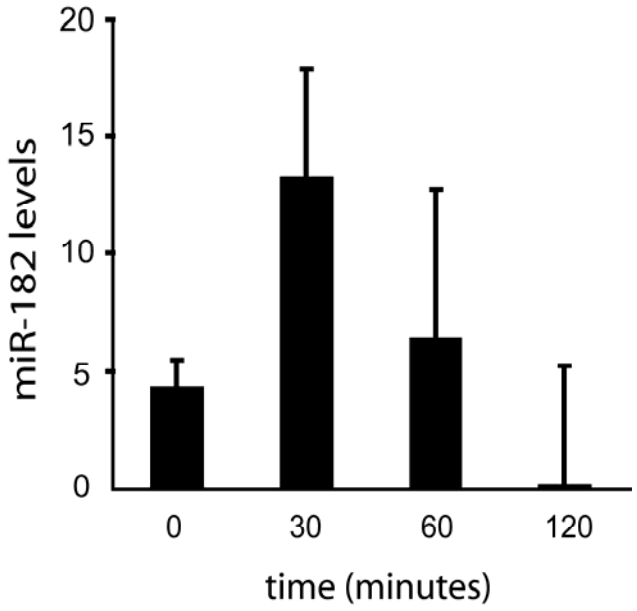

Figure 31. miR-182 levels were measured by q-RTPCR at early timepoints during differentiation of embryonic neural progenitor cells in culture.

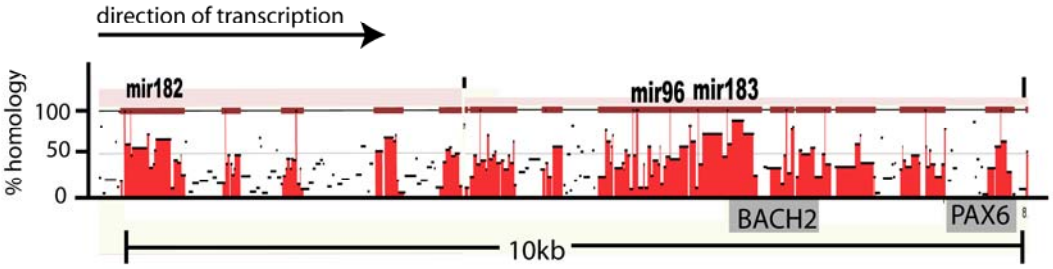

Figure 32. rVISTA results suggest Pax6 and BACH2 as candidate regulators of miR-182/183/96 transcription.

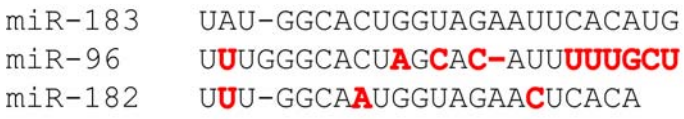

Figure 33. Sequence comparison reveals significant sequence homology amoung miRs 183-96-182 in the mature sequence.

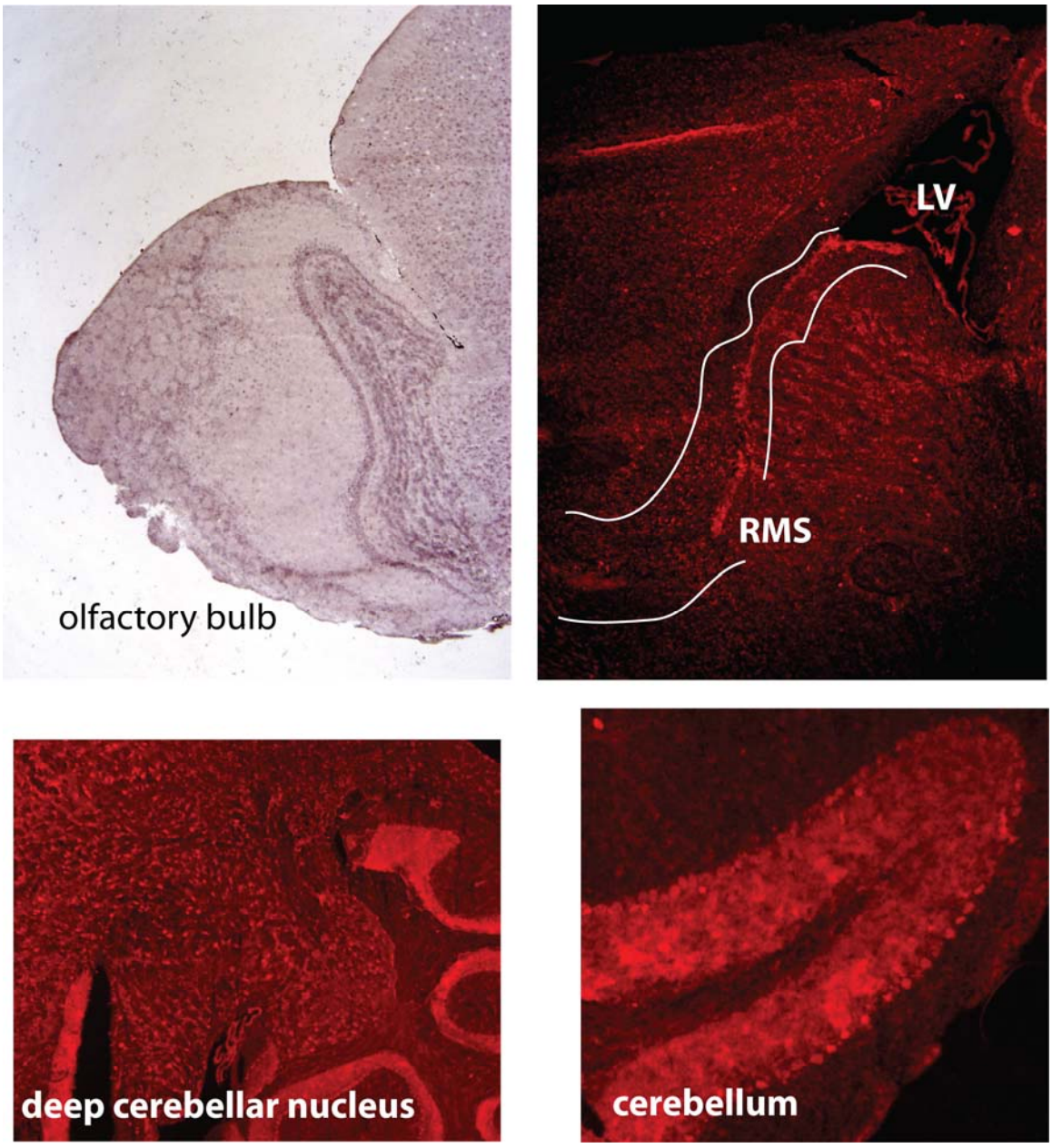

Figure 34. miR-23b expression in the adult mouse brain was visualized using *in situ* hybridization. Signal is developed either with NBT/BCIP (appears purple) or FastRed (appear red), and was enriched in olfactory bulb, rostral migratory stream, deep cerebellar nuclei, and cerebellar folia.

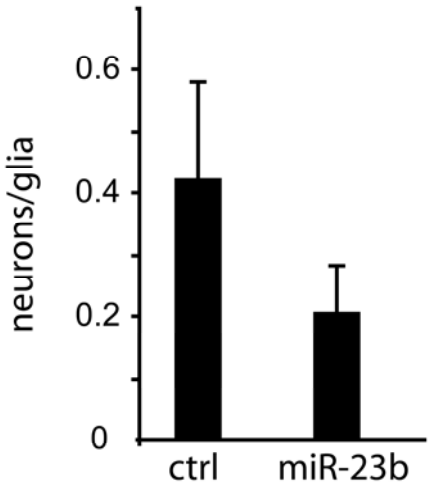

Figure 35. Neuron production is diminished in miR-23b overexpressing cells compared to control.

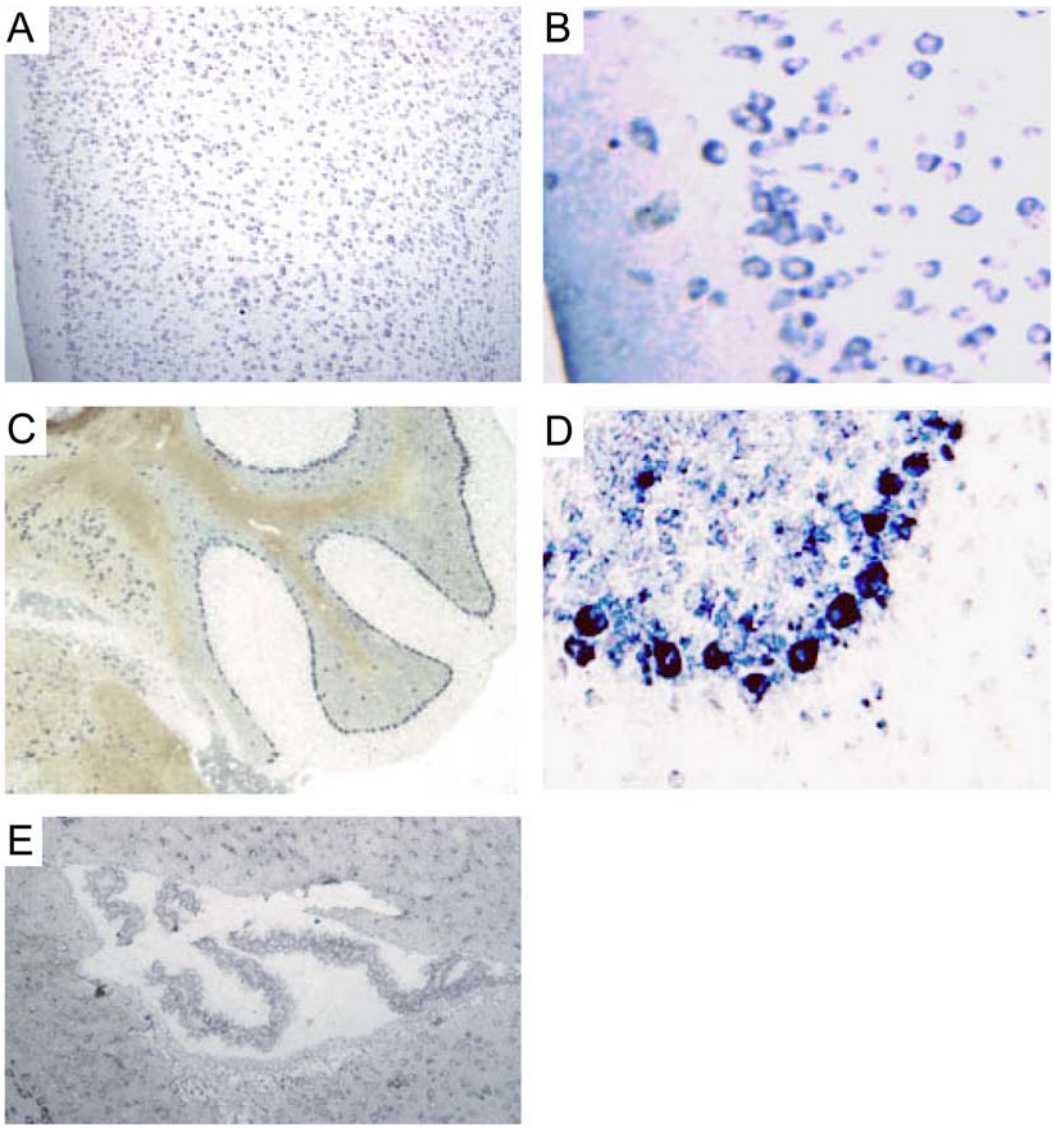

Figure 36. In situ hybridization on sections of adult mouse brain using a probe to detect mature miR-34a. A,B) Cerebral cortex. C,D) Cerebellum. E) Lateral ventricle.

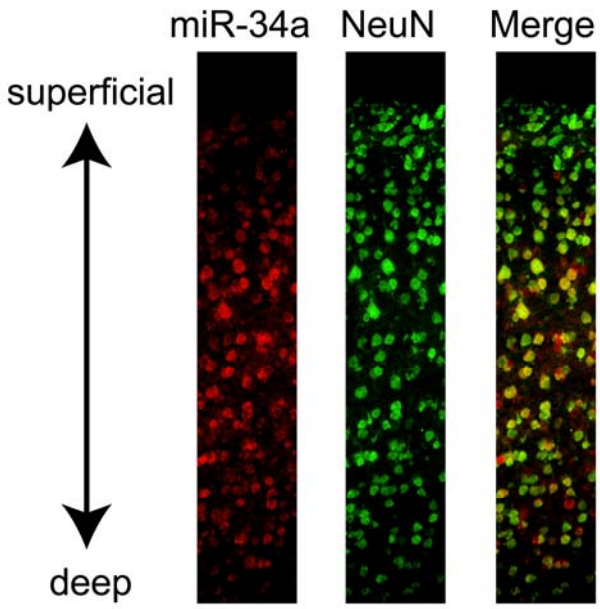

Figure 37. *In situ* hybridization to detect miR-34a (red) was combined with immunofluorescent stain to detect NEUN (green). Merged image shows colocalization (yellow).

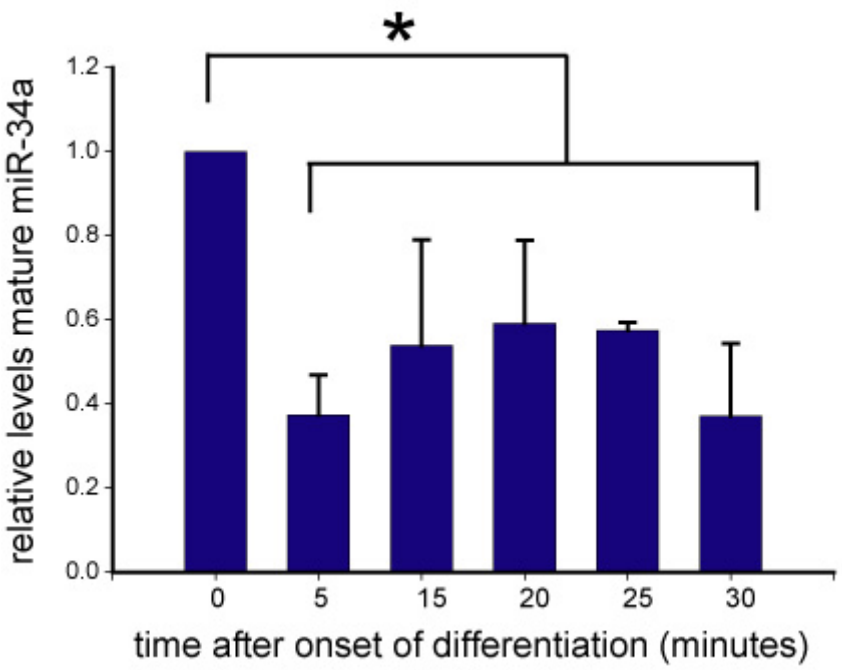

Figure 38. miR-34a levels were measured during the onset of neural differentiation in culture. Levels fell significantly within five minutes ($p<0.001$, One-way ANOVA with Holm-Sidak pairwise comparison).

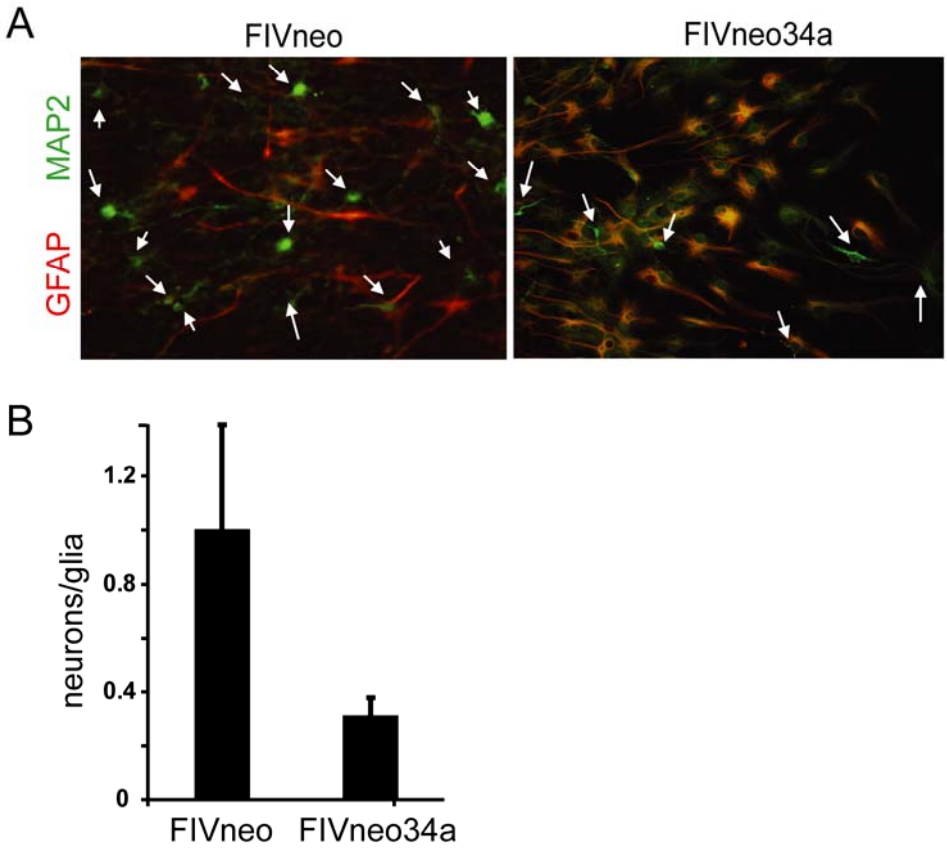

Figure 39. Effects of miR-34a overexpression in differentiating NPCs. *A)* Neurons and glia were identified by MAP2 and GFAP immunofluorescence labeling and morphology. White arrows indicate neurons. *B)* Cell counts in immunostained fields. $p<0.01$ Student's t-test.

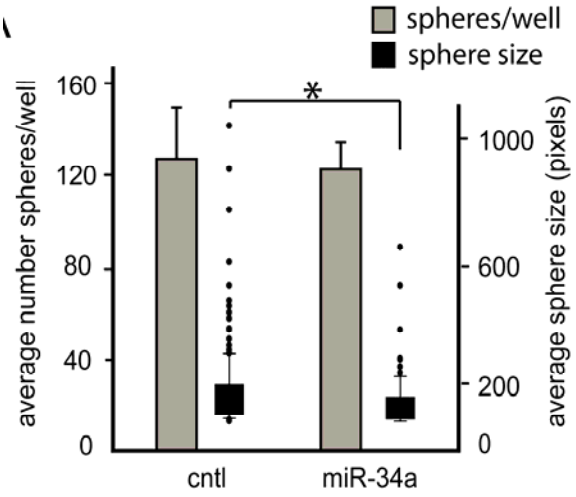

Figure 40. miR-34a effects small changes in cell cycling. NPCs were dissociated and plated at low density. One week later, neurospheres were counted (grey bars) and sphere size measured (black box plots). There was no significant difference in the number of spheres formed by miR-34a overexpressing cells ($p=0.25$, Student's t-test), but a small decrease in sphere size was noted ($p<0.001$, Mann-Whitney rank sum test).

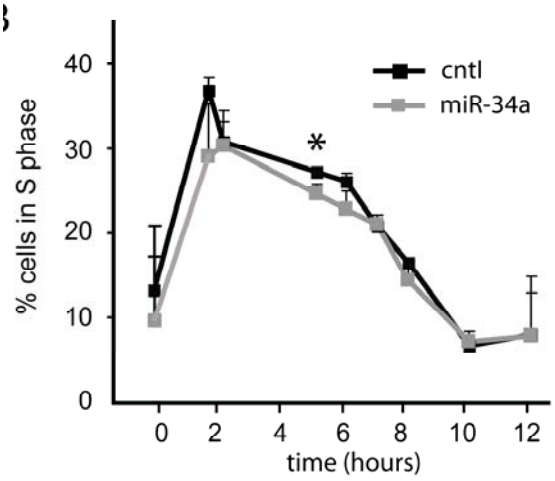

Figure 41. DNA content was measured in dissociated NPCs by flow cytometric detection of propidium iodide stained nuclei. At 5 hours after the onset of differentiation, miR-34a overexpressing cells (grey line) are slightly less likely to be in S-phase ($p=0.02$, Student's t-test) than control cells (black line). There was no significant difference at the other time points tested.

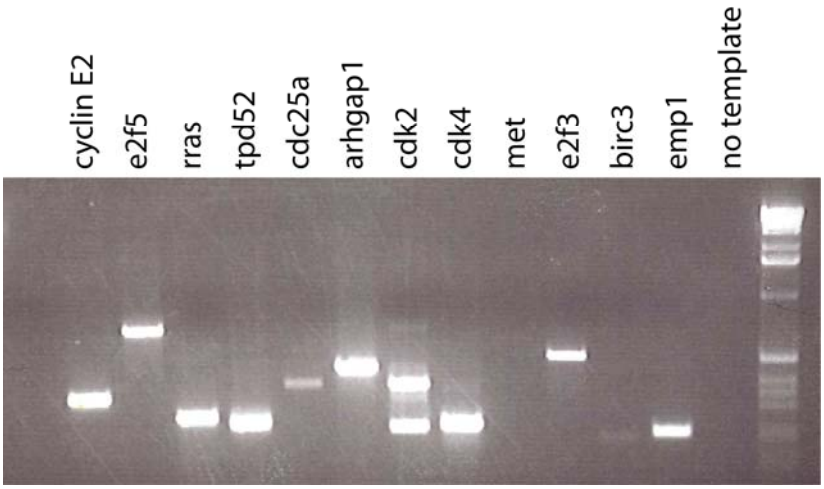

Figure 42. miR-34a targets demonstrated in cancer cell lines were detected by RT-PCR in NPC cDNA.

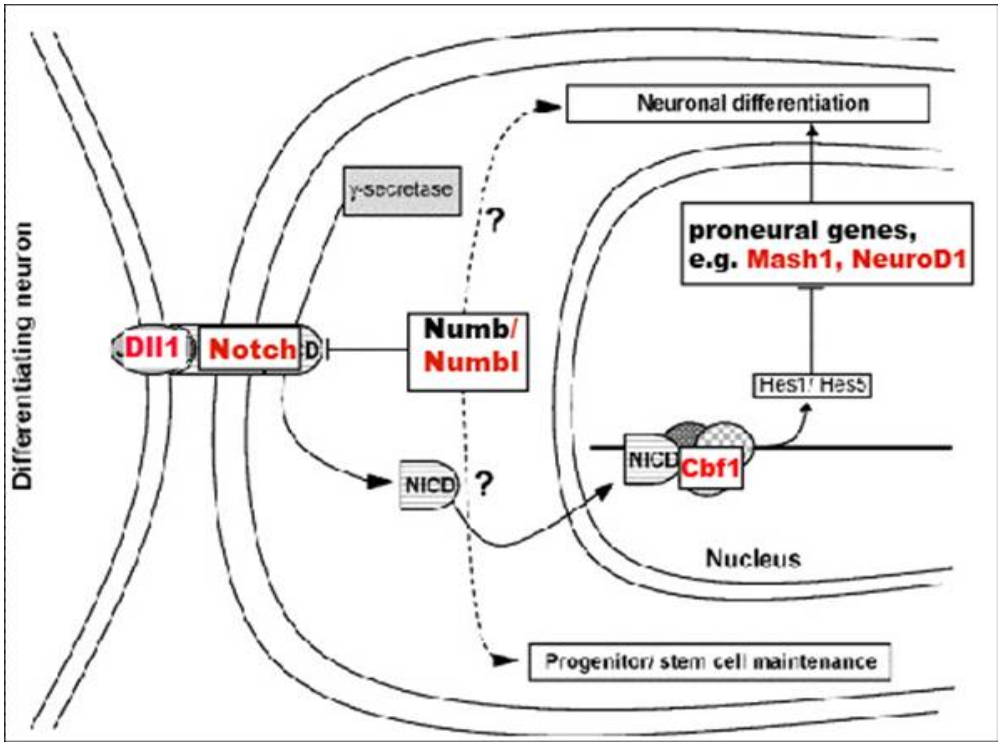

Figure 43. Members of the Notch pathway predicted to be miR-34a targets are marked with red font. Figure adapted from Gregorio *et al.* Schizophrenia research 88 (2006) 275.

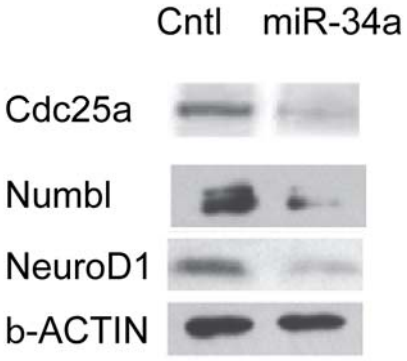

Figure 44. Validation of predicted miR-34a targets in NPCs. Protein levels of the cell cycle regulator CDC25A and the proneural genes NEUROD1 AND NUMBL are decreased in miR-34a overexpressing NPCs. Beta-actin was used as a normalizer (representative blot shown).

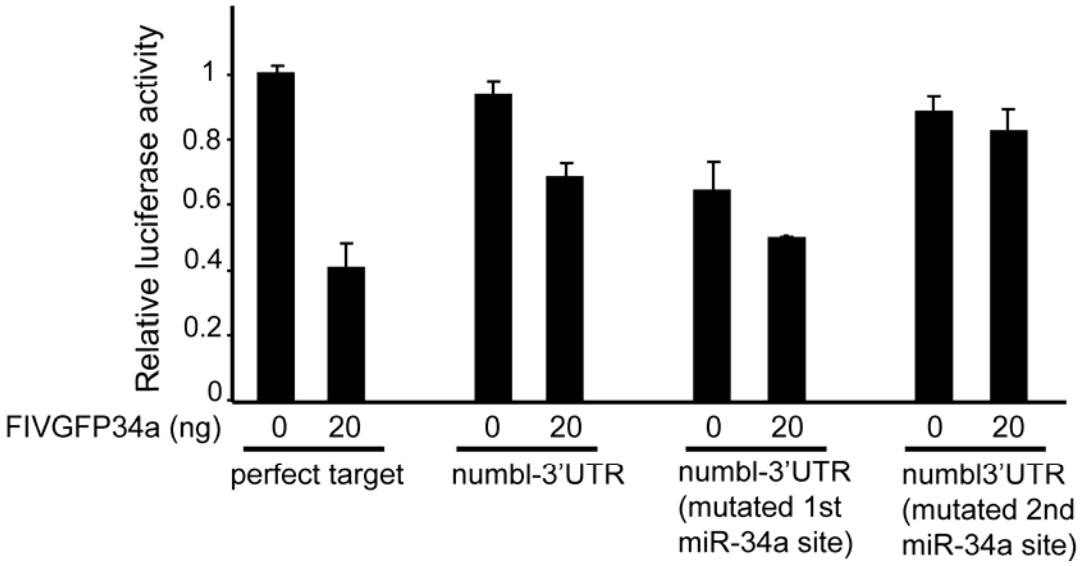

Figure 45. Luciferase assay was used to assess the ability of miR-34a to directly repress the *Numbl* 3'UTR. One-way ANOVA with Holm-Sidak pairwise comparison showed significant differences ($p<0.001$) upon miR-34a delivery to psicheck-34T or psi-check-numblT, but not the numbl target after ablation of either target site.

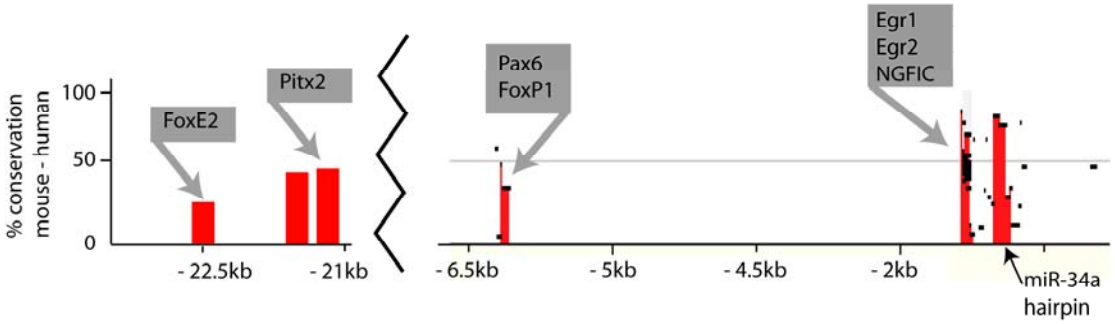

Figure 46. Comparative sequence analysis of the region upstream of miR-34a hairpin and confirmed miR-34a transcription start site in mouse and human reveals several conserved regions that correspond to transcription factor binding site consensus sequences.

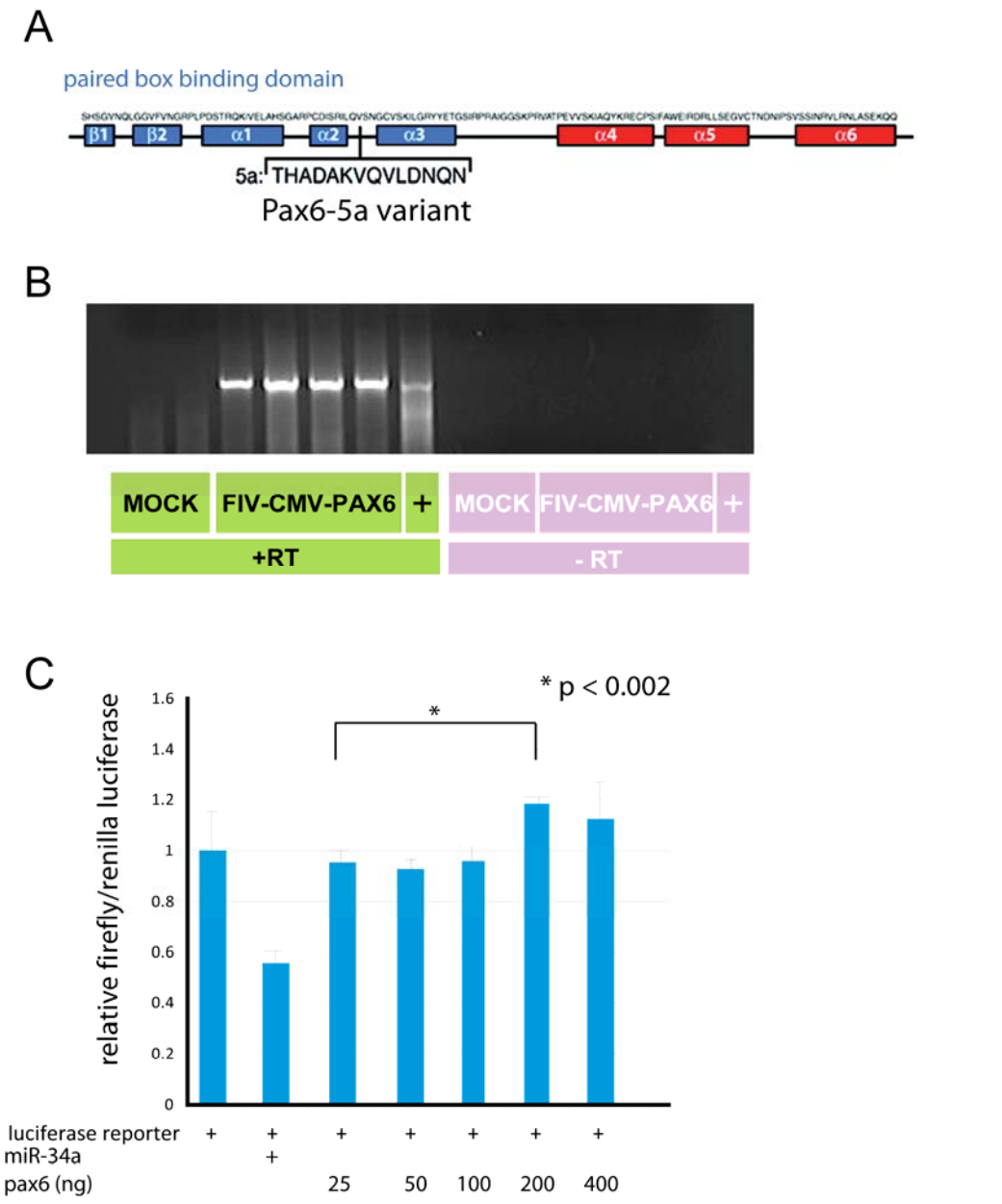

Figure 47. Pax6 may repress miR-34a expression. A) Pax6 has two common isoforms, called Pax6 and Pax6(5a). B) Pax6 expression vector produces Pax6 transcript in HEK-293 cells. RT-PCR was used to detect the mRNA in transfected cells. C) Low dose overexpression of Pax6 in HEK-293 cells had no effect on a luciferase reporter of miR-34a activity. However, high dose Pax6 led to a significant increase in reporter activity.

CHAPTER FOUR. FUTURE DIRECTIONS

4.1. Understanding how mature miRNAs persist after DICER depletion

We and others have observed that for some miRNAs, and some tissues, miRNAs fall readily after Dicer depletion. However, miRNA levels are steady after Dicer removal in some instances.

After Dicer depletion in NPCs followed by several days *in vivo* and two weeks in culture, I found that some mature miRNA levels had not significantly decreased. This result is consistent with others' findings. After mosaic Dicer loss in retina, levels of several miRNAs did not decrease for months. But, the authors comment that this result could reflect an inability to detect small changes in the affected cells in a mixed tissue, including many unaffected cells. More consistent with my results is the finding that removal of Dicer in mature cerebellar Purkinje cell did result in rapid loss of some miRNAs, but others remained steady through the time points tested. Those studies used *in situ* hybridization for miRNA detection, so a mixed population of Dicer-unablated and –ablated cells cannot explain the findings. The *in situ* approach, does, however, introduce the possibility of also detecting the pre-miRNA, which would likely increase in concentration after Dicer removal. In normal tissue, pri- and pre-miRNAs are thought to be short-lived and therefore undetectable in immunohistochemical assays. While some groups have observed loss of sentinel miRNAs by these methods after Dicer loss, neither mature miRNA loss nor the ephemeral nature of pre-miRNAs has been shown to be generalizable to the whole set of miRNAs. Evidence is accumulating that production of individual miRNAs is tightly regulated at multiple processing steps and in a sequence-specific fashion, as discussed in Chapter I. It seems likely, therefore, that elimination of miRNAs is also carefully controlled. Several possible mechanisms would merit testing.

4.1.1. Are mature miRNAs protected from turnover?

Active miRNAs are located within P-bodies. It would be interesting to learn whether miRNAs with more cellular targets, or which are presented with increased levels of cellular targets are longer-lived. This could be tested in several ways.

First, a bio-informatic approach could be used to query if a miRNA with 'predicted' targets correlates with lack of depletion. For this, the available targets for the expressed miRNAs would be correlated to publicly available microarray data, or data the Davidson lab is generating using deep sequencing to determine the entire transcriptome in mouse NPCs. The predicted and present targets would be generated for each miRNA, and this dataset would be compared to the fold knockdown observed for the miRNAs in my study. Of course, all predicted targets may not be regulated by their putative miRNA partner, but it is reasonable to assume that actual target number vary directly with predicted target number for any given miRNA. If the hypothesis is correct, I would expect fold change to vary inversely with the number of NPC-expressed predicted targets.

Second, a simple experiment in a readily transfectable cell line may answer this question. The lifetime of an individual mature miRNA molecule can be tracked by delivery of exogenous, radiolabelled miRNA oligonucleotides, or by a pulse of radiolabel containing media in cell culture. miRNA levels can then be followed by small transcript northern blots (described in the Chapter 3 methods). Several different well-defined endogenous miRNA-target pairs could be used as controls. I would over-express the target or a non-target gene, then track miRNA stability.

More directly, I would look at sub-cellular localization of miRNAs that belong to each set (short-lived and long-lived), combining *in situ* hybridization with TEM for high-resolution inspection of miRNA location. For this, neurospheres would be cut in ultra-thin sections and serial sections stained with P-body markers or miRNA probes.

4.1.2. Are short-lived miRNAs marked for turnover?

The converse could also be true. That is, most miRNAs are depleted, but long-lasting miRNAs are somehow not 'tagged'.

We know that terminal uridylation of mature miRNA leads to degradation. It is interesting to speculate that there may be differential uridylation of the short and long lived species This may also be cell-type specific. One possible approach would be to pull-down the uridylated species using a poly-A probe, and compare qPCR levels of several short- and long-lived miRNA in the pull-down vs. total RNA. In this way, I could quantify the ratio of uridylated/non-uridylated molecules for each miRNA of interest.

4.1.3. Is mRNA turnover a model for miRNA turnover?

Another interesting corollary to these questions is whether miRNA turnover mechanisms are similar to those working to control mRNA levels. mRNA turnover has been extensively studied in yeast (reviewed in [178]) In that system, deadenylation is followed by removal of the 7-G-methyl cap, then 5' to 3' exonucleolyic degradation. A slower 3→5 mechanism also exists. Though some primary miRNA transcripts are known to be capped and polyadenylated, these mechanisms do not seem directly relevant to the short unadorned mature miRNA. However, some of the same stability regulating proteins could be involved. Two factors acting in *trans* to control mRNA stability are AUF1 (a destabilizing force) and the Hu family of proteins (mRNA stabilizers). These factors interact with 50-150 nucleotide sequence elements in mRNAs which are critical for regulation of transcripts called AU-rich elements [179]. Though miRNAs are clearly not long enough to contain full AREs, they could contain the relevant ARE subunits, which are nine nucleotide sequences. Furthermore, there is a neuron-specific Hu family

member, Hu-C, which could be a candidate regulator of miRNA levels in the developing nervous system.

4.1.4. What sequence or structural commonality contributes to miRNA lifespan?

All of the above-proposed mechanisms depend on miRNA interaction with other factors. The substrate for this association could be sequence or structure. Therefore, I propose to consider similarities in these features among the members of the short- and long- lasting miRNA sets.

To discover sequence motifs in common among the members of each set, I would use bio-informatics. Approaches to motif identification are based in complex computer programming, and this aim would benefit from collaboration with bioinformaticists, but several aspects of program function are quite accessible [180]. For example, some programs are designed to look for "words", or defined sets of sequences. In this setting, a query might read: any 7 nucleotide word with as many as 2 non-contiguous mismatches. Word size (nucleotide number) is decided based on the increased likelihood of finding short words by chance, and the decreased likelihood of finding long words at all (and missing their included component parts). Algorithms often employ position weight matrices to describe the strength of evidence for the importance of a certain nucleotide at a given position. In this way, the output distinguishes a degenerate position from a required one.

Furthermore, an analysis of structural motifs might contribute to our understanding of differential processing and the stability of pri- and pre- miRNAs. Structural characteristics of miRNA hairpins are used as features in target miRNA predictions (e.g., the miRWIP algorithm [181], and this approach should be applicable to find commonalities between miRNAs of similar stability.

4.1.5. Is there an alternate Dicing pathway in mammals?

As was discussed in Chapter 2, Dicer is currently the only enzyme known to clip off the loop in pre-miRNA hairpins to release mature miRNA. It is in the Rnase III family of enzymes, like Drosha, which cuts the pre-miRNA out of its primary transcript. The structure of Dicer has been described (reviewed in [182]). However, Dicer, in contrast to Drosha, has the ability to both bind and cleave the RNA substrate, whereas Drosha requires a protein partner capable of RNA binding. In other species, there are multiple Dicer enzymes. Though additional Dicer genes have not been identified in vertebrates, there could be other enzymes not readily identifiable by sequence comparison to Dicer which provide an alternate route from pre-miRNA to mature miRNA.

To search for these proteins, I could take advantage of a new reagent in the Davidson Lab. Ryan Boudreau has developed an expression vector for the RISC-component Argonaute (Ago) in which Ago is tagged with the short peptide FLAG. He calls this vector FLAgo. Because miRNA processing and activity are initiated in the RISC complex, of which Ago is an obligate component, I would expect to also find Dicer alternatives associated with Ago. I would deliver FLAgo to mouse tissues already known to have slow miRNA turnover, for example, the retina. Transgenes can be expressed in the retina by subretinal injection of adenoassociated viral vectors [183, 184]. After confirmation of FLAgo expression by immunostaining, I would use immunoprecipitation to harvest FLAgo and associated proteins. The members of this complex mixture could then be identified by mass spectrometry.

4.1.6. Are miRNAs transferred from other cells?

Exosomes are small membrane bound vesicles that are known to transfer RNA and proteins across short distances between cells. In a recent review, Smalheiser [185] suggests that exosome mediated transfer of RNA and miRNAs may contribute to cell-cell

interaction in the nervous system. Perhaps miRNAs are actively introduced to Dicer-less cells from their neighbors. I could test this hypothesis by expressing an artificial miRNA in the mouse brain from a glial specific expression construct, then testing if the mature miRNA was found in nearby neurons. One experimental design with a simple readout would be to deliver an artificial miRNA capable of silencing GFP (miGFP) in a vector with a red fluorescent reporter. This vector could be delivered to the brain of transgenic mice expressing GFP in neurons. Then tissue sections could be inspected for decreased green fluorescence in red cell neighbors. This experiment could be executed in GFP mice and in GFP;Dicer null mice to look for increased miRNA movement in the context of Dicer loss.

4.2. Interaction of the Notch pathway with miR-34a in mammals?

4.2.1. Which predicted NOTCH pathway targets mediate effects of miR-34a?

Though I have shown repression of several NOTCH pathway proteins, and suggested that repression of these proteins could produce biological changes like those I observed (especially changes in neuron production), I have neither shown causation, nor have I identified which proteins participate *in vivo*. To address these questions of pathway members and epistasis, a possible future direction of this work is to test the effects of miR-34a overexpression in the context of exogenous overexpression of untargetable forms of each of the putative NOTCH pathway targets. I could also take advantage of the Cbf1-GFP reporter mouse developed by Gaiano et al. {Mizutani, 2007 #5713} to monitor NOTCH pathway activity (at least events upstream of DNA binding).

4.2.2. Does the NOTCH pathway regulate miR-34a levels?

I have shown that miR-34a regulates at least some of its predicted targets in the Notch signaling pathway in mouse NPCs. Recent work from the Davidson Lab describes a feedback loop in which the NPC-expressed miR-9 regulates, and it regulated by, the REST complex [77]. The phenomenon of miRNA-target feedback loops has also been described by computational modelling [186]. To test regulation of miR-34a by its targets, I would begin with the NOTCH signaling pathway. I could use bioinformatics and chromatin immunoprecipitation to search for binding sites for the NOTCH effector CBF1 in the predicted miR-34a promoter region.

Also, NOTCH1 and DELTA1 mRNA levels have recently been shown to fluctuate in concert with the cell cycle, falling during S-phase. I would test miR-34a levels during cell cycle phases in NPCs. For this, I would stain intact cells with a nuclear stain, and sort cells by DNA content using flow cytometry. After cells are sorted into G1/0, S, and G2/M phase bins, I would isolate RNA and measure miR-34a levels by q-RTPCR.

4.3. miRNAs may modulate neurodegeneration

Interaction of neurological disease pathways and miRNAs has been demonstrated (reviewed in Barbato *et al.* [187]). Single miRNAs have been identified which are interesting candidates in a few complex neurological diseases. A variant in the SLITRK gene was identified in rare Tourette syndrome patients which interrupts a binding site for the co-expressed miR-189. In midbrain dopaminergic neurons, the cells implicated in Parkinson's disease pathogenesis, miR-133b works in a feedback loop with the transcription factor Pitx3 to control cellular maturation [90]. The miRNA is specifically lost with progression of Parkinson's disease, though a causal relationship of miR-133b to the disease has not been described.

Previous work suggests roles for miRNAs in cerebellar Purkinje cell (PC) maintenance and as modulators of pathogenesis in the spinocerebellar ataxias. Depletion of the miRNA-producing enzyme Dicer in mouse PCs results in late-onset neurodegeneration, with PCs lost between 10 and 13 weeks of age, followed by behavioral changes and premature death [97]. These results suggest that miRNAs are required for cellular homeostasis in the adult mouse cerebellum. Bilen *et al.* [188] found that the disease-causing allele of *Drosophila* ataxin-3 is less toxic in the presence of miR-bantam gain of function, and concordantly, that Dicer ablation (so miRNA depletion) in cell lines increased poly-glutamine induced toxicity. In this case as well, miRNAs seem to protect against cellular dysfunction. The Zoghbi and Orr labs [189] have also investigated this question, beginning with the observation that homozygous transgenic SCA1 mice fare worse than hemizygous littermates, suggesting that mechanisms capable of suppressing transcript levels (like miRNAs) might protect against disease sequelae. In fact, evolutionarily conserved binding sites for miRs 19, 101, and 130 were identified in the 3' untranslated region (UTR) of SCA1, and were shown to be functional: transcript levels vary directly with miR levels in several human cell lines. Importantly, depletion of these miRNAs increased cell death in cultured cells over-expressing expanded SCA1, but not expanded SCA1 with mutated miRNA binding sites. These results are intriguing, and strongly suggest that miRNAs are one factor working to protect cells against the advancement of disease pathogenesis in SCA1. I propose to test the role of miRNAs in neuroprotection by ablating Dicer in PCs in a knock-in mouse model of SCA1. I would time onset of neuropathology (PC dendritic tree morphology, PC number, and astroglial activation) and motor deficit (gait disturbance, spontaneous activity, ability to perform forced running). If differences are present, analysis of differential miRNA expression in the Purkinje cell layer in SCA1 could identify candidate miRNAs which function in neuron maintenance under stress. I would then test the generalizability of these findings

by evaluating the expression levels of these new candidate miRNAs in a variety of neurodegenerative diseases.

Another application of discovering disease regulated miRNAs in the context of dominant gain of function mutations is the hope of harnessing the miRNA promoter and structure as a shuttle for short hairpin RNAs directed against the disease gene. This approach might increase the safety of shRNA use in patients by decreasing the levels and time course of expression. Several lines of research related to the development of disease-regulated RNAi are underway in the Davidson Lab.

4.4. Final Comments

miRNAs, though discovered little more than a decade ago, are now held up as a great source of new promise for biological discovery and therapeutics. These small molecules are surprising, perhaps, for the regulatory power packed into such a short string of nucleic acid sequence comprising the active species. However, the rapidly increasing number of articles describing features of miRNAs seems to tell a story of many diverse functions and mechanisms rather than telling us an answer about "what miRNAs do". I think that more work will show that among the miRNAs were hiding key regulators in many medically relevant and biologically compelling strongs, and that we will continue to stray further from a notion of miRNA function as a cooperative set.

Nevertheless, some themes arise. miRNAs' regulatory roles often work by repression of several genes in the same pathway. This finding underlines the utility of a backward approach to finding the places miRNAs work: by identifying those functionally conserved sequence motifs in targets. I have underscored through several examples above the relevance of bioinformatic contributions to discovery of miRNA functions. I expect many of the next advances to rely heavily on these methods.

miRNAs appear to be modulators, if not critical regulators, in many developmental processes. By attempting to understand miRNA function in development,

I have had occasion to consider the parallels in organ and organismal development. One of the clear values of our reconsideration of regulation in light of miRNAs is the chance to retell the well-described developmental stories, perhaps finding new ways into old problems.

REFERENCES

1. Gato, A. and M.E. Desmond, Why the embryo still matters: CSF and the neuroepithelium as interdependent regulators of embryonic brain growth, morphogenesis and histiogenesis. Dev Biol, 2009.

2. Corbin, J.G., et al., Regulation of neural progenitor cell development in the nervous system. J Neurochem, 2008. **106**(6): p. 2272-87.

3. Poluch, S. and S.L. Juliano, A normal radial glial scaffold is necessary for migration of interneurons during neocortical development. Glia, 2007. **55**(8): p. 822-30.

4. Fujita, S., Analysis of Neuron Differentiation in the Central Nervous System by Tritiated Thymidine Autoradiography. J Comp Neurol, 1964. **122**: p. 311-27.

5. Sidman, R.L., I.L. Miale, and N. Feder, Cell proliferation and migration in the primitive ependymal zone: an autoradiographic study of histogenesis in the nervous system. Exp Neurol, 1959. **1**: p. 322-33.

6. del Rio, J.A. and E. Soriano, Immunocytochemical detection of 5'-bromodeoxyuridine incorporation in the central nervous system of the mouse. Brain Res Dev Brain Res, 1989. **49**(2): p. 311-7.

7. Walsh, C. and C.L. Cepko, Clonally related cortical cells show several migration patterns. Science, 1988. **241**(4871): p. 1342-5.

8. Caviness, V.S., Jr., et al., Cell output, cell cycle duration and neuronal specification: a model of integrated mechanisms of the neocortical proliferative process. Cereb Cortex, 2003. **13**(6): p. 592-8.

9. Gal, J.S., et al., Molecular and morphological heterogeneity of neural precursors in the mouse neocortical proliferative zones. J Neurosci, 2006. **26**(3): p. 1045-56.

10. Noctor, S.C., et al., Cortical neurons arise in symmetric and asymmetric division zones and migrate through specific phases. Nat Neurosci, 2004. **7**(2): p. 136-44.

11. Kowalczyk, T., et al., Intermediate Neuronal Progenitors (Basal Progenitors) Produce Pyramidal-Projection Neurons for All Layers of Cerebral Cortex. Cereb Cortex, 2009.

12. Mizutani, K., et al., Differential Notch signalling distinguishes neural stem cells from intermediate progenitors. Nature, 2007. **449**(7160): p. 351-5.

13. Marin, O. and J.L. Rubenstein, Cell migration in the forebrain. Annu Rev Neurosci, 2003. **26**: p. 441-83.

14. Noctor, S.C., et al., Interference with the development of early generated neocortex results in disruption of radial glia and abnormal formation of neocortical layers. Cereb Cortex, 1999. **9**(2): p. 121-36.

15. Alvarez-Buylla, A. and D.A. Lim, For the long run: maintaining germinal niches in the adult brain. Neuron, 2004. **41**(5): p. 683-6.

16. Guillemot, F., Cellular and molecular control of neurogenesis in the mammalian telencephalon. Curr Opin Cell Biol, 2005. **17**(6): p. 639-47.

17. Itoh, M., et al., Mind bomb is a ubiquitin ligase that is essential for efficient activation of Notch signaling by Delta. Dev Cell, 2003. **4**(1): p. 67-82.

18. Jiang, Y.J., et al., Mutations affecting neurogenesis and brain morphology in the zebrafish, Danio rerio. Development, 1996. **123**: p. 205-16.

19. Taylor, M.K., K. Yeager, and S.J. Morrison, Physiological Notch signaling promotes gliogenesis in the developing peripheral and central nervous systems. Development, 2007. **134**(13): p. 2435-47.

20. Adams, R.J., Metaphase spindles rotate in the neuroepithelium of rat cerebral cortex. J Neurosci, 1996. **16**(23): p. 7610-8.

21. Siller, K.H. and C.Q. Doe, Spindle orientation during asymmetric cell division. Nat Cell Biol, 2009. **11**(4): p. 365-74.

22. Doe, C.Q., Neural stem cells: balancing self-renewal with differentiation. Development, 2008. **135**(9): p. 1575-87.

23. Cappello, S., et al., The Rho-GTPase cdc42 regulates neural progenitor fate at the apical surface. Nat Neurosci, 2006. **9**(9): p. 1099-107.

24. Soriano, E. and J.A. Del Rio, The cells of cajal-retzius: still a mystery one century after. Neuron, 2005. **46**(3): p. 389-94.

25. Chae, T.H. and C.A. Walsh, Genes that control the size of the cerebral cortex. Novartis Found Symp, 2007. **288**: p. 79-90; discussion 91-8.

26. Lewis, J., Neurogenic genes and vertebrate neurogenesis. Curr Opin Neurobiol, 1996. **6**(1): p. 3-10.

27. Johnson, J.E., Numb and Numblike control cell number during vertebrate neurogenesis. Trends Neurosci, 2003. **26**(8): p. 395-6.

28. Wienholds, E., et al., MicroRNA expression in zebrafish embryonic development. Science, 2005 **309**(5732): p. 310-1.

29. Kloosterman, W.P., et al., In situ detection of miRNAs in animal embryos using LNA-modified oligonucleotide probes. Nat Methods, 2006 **3**(1): p. 27-9.

30. Gangaraju, V.K. and H. Lin, MicroRNAs: key regulators of stem cells. Nat Rev Mol Cell Biol, 2009. **10**(2): p. 116-25.

31. Heimberg, A.M., et al., MicroRNAs and the advent of vertebrate morphological complexity. Proc Natl Acad Sci U S A, 2008. **105**(8): p. 2946-50.

32. Zhang, R., Y.Q. Wang, and B. Su, Molecular evolution of a primate-specific microRNA family. Mol Biol Evol, 2008. **25**(7): p. 1493-502.

33. Wienholds, E., et al., The microRNA-producing enzyme Dicer1 is essential for zebrafish development. Nat Genet, 2003 **35**(3): p. 217-8.

34. Wienholds, E. and R.H. Plasterk, MicroRNA function in animal development. FEBS Lett, 2005 **579**(26): p. 5911-22.

35. Krichevsky, A.M., et al., A microRNA array reveals extensive regulation of microRNAs during brain development. Rna, 2003 **9**(10): p. 1274-81.

36. Krichevsky, A.M., et al., Specific microRNAs modulate embryonic stem cell-derived neurogenesis. Stem Cells, 2006 **24**(4): p. 857-64.

37. Gao, F.B., Posttranscriptional control of neuronal development by microRNA networks. Trends Neurosci, 2008. **31**(1): p. 20-6.

38. Hohjoh, H. and T. Fukushima, Expression profile analysis of microRNA (miRNA) in mouse central nervous system using a new miRNA detection system that examines hybridization signals at every step of washing. Gene, 2007. **391**(1-2): p. 39-44.

39. Hohjoh, H. and T. Fukushima, Marked change in microRNA expression during neuronal differentiation of human teratocarcinoma NTera2D1 and mouse embryonal carcinoma P19 cells. Biochem Biophys Res Commun, 2007. **362**(2): p. 360-7.

40. Ozsolak, F., et al., Chromatin structure analyses identify miRNA promoters. Genes Dev, 2008. **22**(22): p. 3172-83.

41. Lee, Y., et al., MicroRNA genes are transcribed by RNA polymerase II. EMBO J, 2004 **23**(20): p. 4051-60.

42. Kim, Y.K. and V.N. Kim, Processing of intronic microRNAs. EMBO J, 2007. **26**(3): p. 775-83.

43. Borchert, G.M., W. Lanier, and B.L. Davidson, RNA polymerase III transcribes human microRNAs. Nat Struct Mol Biol, 2006 **13**(12): p. 1097-101.

44. Mas Monteys, A. and B.L. Davidson, A molecular basis for discordance between intronic miRNAs and their host genes. Submitted.

45. Thomson, J.M., et al., Extensive post-transcriptional regulation of microRNAs and its implications for cancer. Genes Dev, 2006 **20**(16): p. 2202-7.

46. Barbato, C., et al., Dicer expression and localization in post-mitotic neurons. Brain Res, 2007. **1175**: p. 17-27.

47. Han, J., et al., Posttranscriptional crossregulation between Drosha and DGCR8. Cell, 2009. **136**(1): p. 75-84.

48. Viswanathan, S.R., G.Q. Daley, and R.I. Gregory, Selective blockade of microRNA processing by Lin28. Science, 2008. **320**(5872): p. 97-100.

49. Rybak, A., et al., A feedback loop comprising lin-28 and let-7 controls pre-let-7 maturation during neural stem-cell commitment. Nat Cell Biol, 2008. **10**(8): p. 987-93.

50. Kawahara, Y., et al., RNA editing of the microRNA-151 precursor blocks cleavage by the Dicer-TRBP complex. EMBO Rep, 2007.

51. Yang, W., et al., Modulation of microRNA processing and expression through RNA editing by ADAR deaminases. Nat Struct Mol Biol, 2006 **13**(1): p. 13-21.

52. Heo, I., et al., Lin28 mediates the terminal uridylation of let-7 precursor MicroRNA. Mol Cell, 2008. **32**(2): p. 276-84.

53. Dahm, R., M. Kiebler, and P. Macchi, RNA localisation in the nervous system. Semin Cell Dev Biol, 2007. **18**(2): p. 216-23.

54. Hengst, U. and S.R. Jaffrey, Function and translational regulation of mRNA in developing axons. Semin Cell Dev Biol, 2007. **18**(2): p. 209-15.

55. Hengst, U., et al., Functional and selective RNA interference in developing axons and growth cones. J Neurosci, 2006 **26**(21): p. 5727-32.

56. Perkins, D.O., et al., microRNA expression in the prefrontal cortex of individuals with schizophrenia and schizoaffective disorder. Genome Biol, 2007. **8**(2): p. R27.

57. Beveridge, N.J., et al., Dysregulation of miRNA 181b in the temporal cortex in schizophrenia. Hum Mol Genet, 2008. **17**(8): p. 1156-68.

58. Klein, M.E., et al., Homeostatic regulation of MeCP2 expression by a CREB-induced microRNA. Nat Neurosci, 2007. **10**(12): p. 1513-4.

59. Abu-Elneel, K., et al., Heterogeneous dysregulation of microRNAs across the autism spectrum. Neurogenetics, 2008. **9**(3): p. 153-61.

60. Miller, D.T., et al., Microdeletion/duplication at 15q13.2q13.3 among individuals with features of autism and other neuropsychiatirc disorders. J Med Genet, 2008.

61. Talebizadeh Z, B.M., Theodoro MF, Feasibility and relevance of examining lymphoblastoid cell lines to study role of microRNAs in autism. Autism Research, 2008. **1**(4): p. 240-250.

62. Bassell, G.J. and S.T. Warren, Fragile X syndrome: loss of local mRNA regulation alters synaptic development and function. Neuron, 2008. **60**(2): p. 201-14.

63. Castren, M., et al., Altered differentiation of neural stem cells in fragile X syndrome. Proc Natl Acad Sci U S A, 2005. **102**(49): p. 17834-9.

64. Jin, P., et al., Biochemical and genetic interaction between the fragile X mental retardation protein and the microRNA pathway. Nat Neurosci, 2004. **7**(2): p. 113-7.

65. Bolduc, F.V., et al., Excess protein synthesis in Drosophila Fragile X mutants impairs long-term memory. Nature Neuroscience, 2008. **11**(10): p. 1143-1145.

66. Li, Y.J., L. Lin, and P. Jin, The microRNA pathway and fragile X mental retardation protein. Biochimica Et Biophysica Acta-Gene Regulatory Mechanisms, 2008. **1779**(11): p. 702-705.

67. Vasudevan, S. and J.A. Steitz, AU-rich-element-mediated upregulation of translation by FXR1 and Argonaute 2. Cell, 2007. **128**(6): p. 1105-18.

68. Feng, Y., et al., Fragile X mental retardation protein: nucleocytoplasmic shuttling and association with somatodendritic ribosomes. J Neurosci, 1997. **17**(5): p. 1539-47.

69. Stark, K.L., et al., Altered brain microRNA biogenesis contributes to phenotypic deficits in a 22q11-deletion mouse model. Nat Genet, 2008. **40**(6): p. 751-60.

70. Wang, Y., et al., DGCR8 is essential for microRNA biogenesis and silencing of embryonic stem cell self-renewal. Nat Genet, 2007. **39**(3): p. 380-5.

71. Miranda, R.C., et al., Modeling the impact of alcohol on cortical development in a dish: strategies from mapping neural stem cell fate. Methods Mol Biol, 2008. **447**: p. 151-68.

72. Sathyan, P., H.B. Golden, and R.C. Miranda, Competing interactions between micro-RNAs determine neural progenitor survival and proliferation after ethanol exposure: evidence from an ex vivo model of the fetal cerebral cortical neuroepithelium. J Neurosci, 2007. **27**(32): p. 8546-57.

73. Friggi-Grelin, F., L. Lavenant-Staccini, and P. Therond, Control of antagonistic components of the hedgehog signaling pathway by microRNAs in Drosophila. Genetics, 2008. **179**(1): p. 429-39.

74. Ferretti, E., et al., Concerted microRNA control of Hedgehog signalling in cerebellar neuronal progenitor and tumour cells. Embo J, 2008. **27**(19): p. 2616-27.

75. Johnson, R., et al., A microRNA-based gene dysregulation pathway in Huntington's disease. Neurobiol Dis, 2008. **29**(3): p. 438-45.

76. Conaco, C., et al., Reciprocal actions of REST and a microRNA promote neuronal identity. Proc Natl Acad Sci U S A, 2006 **103**(7): p. 2422-7.

77. Packer, A.N., et al., The bifunctional microRNA miR-9/miR-9* regulates REST and CoREST and is downregulated in Huntington's disease. J Neurosci, 2008. **28**(53): p. 14341-6.

78. Nelson, P.T. and J.N. Keller, RNA in brain disease: no longer just "the messenger in the middle". J Neuropathol Exp Neurol, 2007. **66**(6): p. 461-8.

79. Kawahara, Y., et al., Redirection of silencing targets by adenosine-to-inosine editing of miRNAs. Science, 2007. **315**(5815): p. 1137-40.

80. Esquela-Kerscher, A. and F.J. Slack, Oncomirs - microRNAs with a role in cancer. Nat Rev Cancer, 2006 **6**(4): p. 259-69.

81. Schickel, R., et al., MicroRNAs: key players in the immune system, differentiation, tumorigenesis and cell death. Oncogene, 2008. **27**(45): p. 5959-74.

82. Song, L. and R.S. Tuan, MicroRNAs and cell differentiation in mammalian development. Birth Defects Res C Embryo Today, 2006 **78**(2): p. 140-9.

83. Cobb, B.S., et al., T cell lineage choice and differentiation in the absence of the RNase III enzyme Dicer. J Exp Med, 2005. **201**(9): p. 1367-73.

84. Muljo, S.A., et al., Aberrant T cell differentiation in the absence of Dicer. J Exp Med, 2005. **202**(2): p. 261-9.

85. Harfe, B.D., et al., The RNaseIII enzyme Dicer is required for morphogenesis but not patterning of the vertebrate limb. Proc Natl Acad Sci U S A, 2005 **102**(31): p. 10898-903.

86. Giraldez, A.J., et al., MicroRNAs Regulate Brain Morphogenesis in Zebrafish. Science, 2005 **308**(5723): p. 833-838.

87. Bernstein, E., et al., Dicer is essential for mouse development. Nat Genet, 2003 **35**(3): p. 215-7.

88. De Pietri Tonelli, D., et al., miRNAs are essential for survival and differentiation of newborn neurons but not for expansion of neural progenitors during early neurogenesis in the mouse embryonic neocortex. Development, 2008. **135**(23): p. 3911-21.

89. Choi, P.S., et al., Members of the miRNA-200 family regulate olfactory neurogenesis. Neuron, 2008. **57**(1): p. 41-55.

90. Kim, J., et al., A MicroRNA feedback circuit in midbrain dopamine neurons. Science, 2007. **317**(5842): p. 1220-4.

91. Davis, T.H., et al., Conditional loss of Dicer disrupts cellular and tissue morphogenesis in the cortex and hippocampus. J Neurosci, 2008. **28**(17): p. 4322-30.

92. Cuellar, T.L., et al., Dicer loss in striatal neurons produces behavioral and neuroanatomical phenotypes in the absence of neurodegeneration. Proc Natl Acad Sci U S A, 2008. **105**(14): p. 5614-9.

93. Damiani, D., et al., Dicer inactivation leads to progressive functional and structural degeneration of the mouse retina. J Neurosci, 2008. **28**(19): p. 4878-87.

94. Makeyev, E.V., et al., The MicroRNA miR-124 promotes neuronal differentiation by triggering brain-specific alternative pre-mRNA splicing. Mol Cell, 2007. **27**(3): p. 435-48.

95. Rowan, S. and C.L. Cepko, Genetic analysis of the homeodomain transcription factor Chx10 in the retina using a novel multifunctional BAC transgenic mouse reporter. Dev Biol, 2004. **271**(2): p. 388-402.

96. Murchison, E.P., et al., Characterization of Dicer-deficient murine embryonic stem cells. Proc Natl Acad Sci U S A, 2005. **102**(34): p. 12135-40.

97. Schaefer, A., et al., Cerebellar neurodegeneration in the absence of microRNAs. J Exp Med, 2007. **204**(7): p. 1553-8.

98. Zhang, X.M., et al., Highly restricted expression of Cre recombinase in cerebellar Purkinje cells. Genesis, 2004. **40**(1): p. 45-51.

99. Yi, R., et al., Morphogenesis in skin is governed by discrete sets of differentially expressed microRNAs. Nat Genet, 2006 **38**(3): p. 356-62.

100. Kawasaki, H. and K. Taira, Hes1 is a target of microRNA-23 during retinoic-acid-induced neuronal differentiation of NT2 cells. Nature, 2003 **423**(6942): p. 838-42.

101. Lau, P., et al., Identification of dynamically regulated microRNA and mRNA networks in developing oligodendrocytes. J Neurosci, 2008. **28**(45): p. 11720-30.

102. Vo, N., et al., A cAMP-response element binding protein-induced microRNA regulates neuronal morphogenesis. Proc Natl Acad Sci U S A, 2005 **102**(45): p. 16426-31.

103. Schratt, G.M., et al., A brain-specific microRNA regulates dendritic spine development. Nature, 2006 **439**(7074): p. 283-9.

104. Lim, L.P., et al., Microarray analysis shows that some microRNAs downregulate large numbers of target mRNAs. Nature, 2005. **433**(7027): p. 769-73.

105. Yu, J.Y., et al., MicroRNA miR-124 regulates neurite outgrowth during neuronal differentiation. Exp Cell Res, 2008. **314**(14): p. 2618-33.

106. Chang, S., et al., MicroRNAs act sequentially and asymmetrically to control chemosensory laterality in the nematode. Nature, 2004 **430**(7001): p. 785-9.

107. Johnston, R.J. and O. Hobert, A microRNA controlling left/right neuronal asymmetry in Caenorhabditis elegans. Nature, 2003 **426**(6968): p. 845-9.

108. Johnston, R.J., Jr., et al., MicroRNAs acting in a double-negative feedback loop to control a neuronal cell fate decision. Proc Natl Acad Sci U S A, 2005 **102**(35): p. 12449-54.

109. Presutti, C., et al., Non coding RNA and brain. BMC Neurosci, 2006. **7 Suppl 1**: p. S5.

110. Leucht, C., et al., MicroRNA-9 directs late organizer activity of the midbrain-hindbrain boundary. Nat Neurosci, 2008. **11**(6): p. 641-8.

111. Li, Y., et al., MicroRNA-9a ensures the precise specification of sensory organ precursors in Drosophila. Genes Dev, 2006. **20**(20): p. 2793-805.

112. Shibata, M., et al., MicroRNA-9 modulates Cajal-Retzius cell differentiation by suppressing Foxg1 expression in mouse medial pallium. J Neurosci, 2008. **28**(41): p. 10415-21.

113. Visvanathan, J., et al., The microRNA miR-124 antagonizes the anti-neural REST/SCP1 pathway during embryonic CNS development. Genes Dev, 2007. **21**(7): p. 744-9.

114. Hatfield, S.D., et al., Stem cell division is regulated by the microRNA pathway. Nature, 2005 **435**(7044): p. 974-8.

115. Silber, J., et al., miR-124 and miR-137 inhibit proliferation of glioblastoma multiforme cells and induce differentiation of brain tumor stem cells. BMC Med, 2008. **6**: p. 14.

116. Nass, D., et al., MiR-92b and miR-9/9* Are Specifically Expressed in Brain Primary Tumors and Can Be Used to Differentiate Primary from Metastatic Brain Tumors. Brain Pathol, 2008.

117. Gu, J. and V.R. Iyer, PI3K signaling and miRNA expression during the response of quiescent human fibroblasts to distinct proliferative stimuli. Genome Biol, 2006 **7**(5): p. R42.

118. Welch, C., Y. Chen, and R.L. Stallings, MicroRNA-34a functions as a potential tumor suppressor by inducing apoptosis in neuroblastoma cells. Oncogene, 2007

119. Medrano, S. and H. Scrable, Maintaining appearances--the role of p53 in adult neurogenesis. Biochem Biophys Res Commun, 2005. **331**(3): p. 828-33.

120. Medrano, S., et al., Regenerative capacity of neural precursors in the adult mammalian brain is under the control of p53. Neurobiol Aging, 2007.

121. Gil-Perotin, S., et al., Loss of p53 induces changes in the behavior of subventricular zone cells: implication for the genesis of glial tumors. J Neurosci, 2006. **26**(4): p. 1107-16.

122. Berezikov, E., et al., Mammalian mirtron genes. Mol Cell, 2007. **28**(2): p. 328-36.

123. Ruby, J.G., C.H. Jan, and D.P. Bartel, Intronic microRNA precursors that bypass Drosha processing. Nature, 2007. **448**(7149): p. 83-6.

124. Kim, U., et al., Molecular cloning of cDNA for double-stranded RNA adenosine deaminase, a candidate enzyme for nuclear RNA editing. Proc Natl Acad Sci U S A, 1994. **91**(24): p. 11457-61.

125. Shen, Q., et al., The timing of cortical neurogenesis is encoded within lineages of individual progenitor cells. Nat Neurosci, 2006. **9**(6): p. 743-51.

126. Calegari, F., et al., Selective lengthening of the cell cycle in the neurogenic subpopulation of neural progenitor cells during mouse brain development. J Neurosci, 2005. **25**(28): p. 6533-8.

127. Barres, B.A., The mystery and magic of glia: a perspective on their roles in health and disease. Neuron, 2008. **60**(3): p. 430-40.

128. Krishan, A., Rapid DNA content analysis by the propidium iodide-hypotonic citrate method. Methods Cell Biol, 1990. **33**: p. 121-5.

129. Reynolds, B.A. and S. Weiss, Generation of neurons and astrocytes from isolated cells of the adult mammalian central nervous system. Science, 1992 **255(5052)**: p. 1707-1710.

130. Hughes, S.M., et al., Viral-mediated gene transfer to mouse primary neural progenitor cells. Mol Ther, 2002 **5**(1): p. 16-24.

131. Cai, X., C.H. Hagedorn, and B.R. Cullen, Human microRNAs are processed from capped, polyadenylated transcripts that can also function as mRNAs. Rna, 2004 **10**(12): p. 1957-66.

132. Harper, S.Q., et al., Optimization of feline immunodeficiency virus vectors for RNA interference. J Virol, 2006 **80**(19): p. 9371-80.

133. Hammond, S.M., Soaking up small RNAs. Nat Methods, 2007. **4**(9): p. 694-5.

134. Nakamoto, M., et al., Physiological identification of human transcripts translationally regulated by a specific microRNA. Hum Mol Genet, 2005 **14**(24): p. 3813-21.

135. Zeng, Y., X. Cai, and B.R. Cullen, Use of RNA polymerase II to transcribe artificial microRNAs. Methods Enzymol, 2005 **392**: p. 371-80.

136. Xu, S., et al., MicroRNA (miRNA) transcriptome of mouse retina and identification of a sensory organ-specific miRNA cluster. J Biol Chem, 2007. **282**(34): p. 25053-66.

137. Weston, M.D., et al., MicroRNA gene expression in the mouse inner ear. Brain Res, 2006 **1111**(1): p. 95-104.

138. Jensen, K.P., et al., A common polymorphism in serotonin receptor 1B mRNA moderates regulation by miR-96 and associates with aggressive human behaviors. Mol Psychiatry, 2008.

139. Loots, G.G. and I. Ovcharenko, rVISTA 2.0: evolutionary analysis of transcription factor binding sites. Nucleic Acids Res, 2004 **32**(Web Server issue): p. W217-21.

140. Matys, V., et al., TRANSFAC: transcriptional regulation, from patterns to profiles. Nucleic Acids Res, 2003. **31**(1): p. 374-8.

141. Kawasaki, H. and K. Taira, Retraction: Hes1 is a target of microRNA-23 during retinoic-acid-induced neuronal differentiation of NT2 cells. Nature, 2003 **426**(6962): p. 100.

142. Cao, X., S.L. Pfaff, and F.H. Gage, A functional study of miR-124 in the developing neural tube. Genes Dev, 2007 **21**(5): p. 531-6.

143. Mineno, J., et al., The expression profile of microRNAs in mouse embryos. Nucleic Acids Res, 2006. **34**(6): p. 1765-71.

144. Weston, M.D., et al., MicroRNA gene expression in the mouse inner ear. Brain Res, 2006. **1111**(1): p. 95-104.

145. Lagos-Qintana, M., et al., Identification of tissue-specific microRNAs from mouse. Current Biology, 2002 **12**: p. 735-739.

146. Kim, J., et al., Identification of many microRNAs that copurify with polyribosomes in mammalian neurons. Proc Natl Acad Sci U S A, 2004 **101**(1): p. 360-5.

147. Miska, E.A., et al., Microarray analysis of microRNA expression in the developing mammalian brain. Genome Biol, 2004 **5**(9): p. R68.

148. Nelson, P.T., et al., Microarray-based, high-throughput gene expression profiling of microRNAs. Nat Methods, 2004 **1**(2): p. 155-61.

149. Smirnova, L., et al., Regulation of miRNA expression during neural cell specification. Eur J Neurosci, 2005 **21**(6): p. 1469-77.

150. Ciafre, S.A., et al., Extensive modulation of a set of microRNAs in primary glioblastoma. Biochem Biophys Res Commun, 2005. **334**(4): p. 1351-8.

151. Nelson, P.T., et al., RAKE and LNA-ISH reveal microRNA expression and localization in archival human brain. Rna, 2006 **12**(2): p. 187-91.

152. Liang, Y., et al., Characterization of microRNA expression profiles in normal human tissues. BMC Genomics, 2007. **8**: p. 166.

153. Welch, C., Y. Chen, and R.L. Stallings, MicroRNA-34a functions as a potential tumor suppressor by inducing apoptosis in neuroblastoma cells. Oncogene, 2007. **26**(34): p. 5017-22.

154. He, L., et al., A microRNA component of the p53 tumour suppressor network. Nature, 2007. **447**(7148): p. 1130-4.

155. Bommer, G.T., et al., p53-mediated activation of miRNA34 candidate tumor-suppressor genes. Curr Biol, 2007. **17**(15): p. 1298-307.

156. Tazawa, H., et al., Tumor-suppressive miR-34a induces senescence-like growth arrest through modulation of the E2F pathway in human colon cancer cells. Proc Natl Acad Sci U S A, 2007. **104**(39): p. 15472-7.

157. Chang, T.C., et al., Transactivation of miR-34a by p53 broadly influences gene expression and promotes apoptosis. Mol Cell, 2007. **26**(5): p. 745-52.

158. Ason, B., et al., Differences in vertebrate microRNA expression. Proc Natl Acad Sci U S A, 2006. **103**(39): p. 14385-9.

159. Thatcher, E.J., et al., MiRNA expression analysis during normal zebrafish development and following inhibition of the Hedgehog and Notch signaling pathways. Dev Dyn, 2007. **236**(8): p. 2172-80.

160. He, X., L. He, and G.J. Hannon, The guardian's little helper: microRNAs in the p53 tumor suppressor network. Cancer Res, 2007. **67**(23): p. 11099-101.

161. Grimson, A., et al., MicroRNA targeting specificity in mammals: determinants beyond seed pairing. Mol Cell, 2007. **27**(1): p. 91-105.

162. Hanson, I. and V. Van Heyningen, Pax6: more than meets the eye. Trends Genet, 1995. **11**(7): p. 268-72.

163. Amendt, B.A., et al., The molecular basis of Rieger syndrome. Analysis of Pitx2 homeodomain protein activities. J Biol Chem, 1998. **273**(32): p. 20066-72.

164. Amendt, B.A., E.V. Semina, and W.L. Alward, Rieger syndrome: a clinical, molecular, and biochemical analysis. Cell Mol Life Sci, 2000. **57**(11): p. 1652-66.

165. Ebert, M.S., J.R. Neilson, and P.A. Sharp, MicroRNA sponges: competitive inhibitors of small RNAs in mammalian cells. Nat Methods, 2007. **4**(9): p. 721-6.

166. Barad, O., et al., MicroRNA expression detected by oligonucleotide microarrays: system establishment and expression profiling in human tissues. Genome Res, 2004 **14**(12): p. 2486-94.

167. Lund, E., et al., Nuclear export of microRNA precursors. Science, 2004 **303**(5654): p. 95-8.

168. Sempere, L.F., et al., Expression profiling of mammalian microRNAs uncovers a subset of brain-expressed microRNAs with possible roles in murine and human neuronal differentiation. Genome Biol, 2004. **5**(3): p. R13.

169. Lagos-Quintana, M., et al., Identification of novel genes coding for small expressed RNAs. Science, 2001 **294**: p. 853-858.

170. Dostie, J., et al., Numerous microRNPs in neuronal cells containing novel microRNAs. Rna, 2003 **9**(2): p. 180-6.

171. Houbaviy, H.B., M.F. Murray, and P.A. Sharp, Embryonic stem cell-specific MicroRNAs. Dev Cell, 2003 **5**(2): p. 351-8.

172. Luciano, D.J., et al., RNA editing of a miRNA precursor. Rna, 2004 **10**(8): p. 1174-7.

173. Lim, L.P., et al., The microRNAs of Caenorhabditis elegans. Genes Dev, 2003. **17**(8): p. 991-1008.

174. Lai, E.C., et al., Computational identification of Drosophila microRNA genes. Genome Biol, 2003. **4**(7): p. R42.

175. Lai, E.C., C. Wiel, and G.M. Rubin, Complementary miRNA pairs suggest a regulatory role for miRNA:miRNA duplexes. Rna, 2004 **10**(2): p. 171-5.

176. Lagos-Quintana, M., et al., New microRNAs from mouse and human. Rna, 2003 **9**(2): p. 175-9.

177. Liu, C.G., et al., An oligonucleotide microchip for genome-wide microRNA profiling in human and mouse tissues. Proc Natl Acad Sci U S A, 2004. **101**(26): p. 9740-4.

178. Muhlrad, D., C.J. Decker, and R. Parker, Turnover mechanisms of the stable yeast PGK1 mRNA. Mol Cell Biol, 1995. **15**(4): p. 2145-56.

179. Barreau, C., L. Paillard, and H.B. Osborne, AU-rich elements and associated factors: are there unifying principles? Nucleic Acids Res, 2005. **33**(22): p. 7138-50.

180. D'Haeseleer, P., How does DNA sequence motif discovery work? Nat Biotechnol, 2006. **24**(8): p. 959-61.

181. Hammell, M., et al., mirWIP: microRNA target prediction based on microRNA-containing ribonucleoprotein-enriched transcripts. Nat Methods, 2008. **5**(9): p. 813-819.

182. Ji, X., The mechanism of RNase III action: how dicer dices. Curr Top Microbiol Immunol, 2008. **320**: p. 99-116.

183. Hellstrom, M., et al., Cellular tropism and transduction properties of seven adeno-associated viral vector serotypes in adult retina after intravitreal injection. Gene Ther, 2008.

184. Yang, G.S., et al., Virus-mediated transduction of murine retina with adeno-associated virus: effects of viral capsid and genome size. J Virol, 2002. **76**(15): p. 7651-60.

185. Smalheiser, N.R., Exosomal transfer of proteins and RNAs at synapses in the nervous system. Biol Direct, 2007. **2**: p. 35.

186. Zhdanov, V.P., Bistability in gene transcription: interplay of messenger RNA, protein, and nonprotein coding RNA. Biosystems, 2009. **95**(1): p. 75-81.

187. Barbato, C., et al., Thinking about RNA? MicroRNAs in the brain. Mamm Genome, 2008.

188. Bilen, J., et al., MicroRNA pathways modulate polyglutamine-induced neurodegeneration. Mol Cell, 2006 **24**(1): p. 157-63.

189. Lee, Y., et al., miR-19, miR-101 and miR-130 co-regulate ATXN1 levels to potentially modulate SCA1 pathogenesis. Nat Neurosci, 2008. **11**(10): p. 1137-9.